Universidade do Minho
Escola de Medicina

Joana Lima Sá

Dissecting pentraxin-3 role in the modulation of Multiple Sclerosis

Julho de 2019

Joana Lima Sá **Dissecting pentraxin-3 role in the modulation of Multiple Sclerosis**

UMinho | 2019

Universidade do Minho
Escola de Medicina

Joana Lima Sá

Dissecting pentraxin-3 role in the modulation of Multiple Sclerosis

Dissertação de Mestrado
Mestrado em Ciências da Saúde

Trabalho Efetuado sob a orientação da
Professora Doutora Fernanda Cristina Gomes de Sousa Marques
e do
Doutor Agostinho Albérico Rodrigues de Carvalho

Julho de 2019

DIREITOS DE AUTOR E CONDIÇÕES DE UTILIZAÇÃO DO TRABALHO POR TERCEIROS

Acknowledgements

Porque sozinha não teria conseguido...

À Fernanda, por toda a ajuda e apoio, por me ensinar que há sempre soluções para quando as coisas não correm bem. Obrigada por não me deixar desistir.

Ao Agostinho e à Cristina, por todas as sugestões e ajuda. Obrigada por tornarem esta tese possível.

Ao João, por todas as sugestões e por todo o entusiamo mostrado quando discutimos resultados.

À Sofia, por me ter ensinado quase tudo o que sei fazer e por ter sempre uma palavra amiga quando as coisas não correm tão bem. Obrigada pela paciência.

À Marta, por partilhar comigo todos os stresses, mas também por estar lá para festejar todos os sucessos.

À Cláudia, a boss da PTX3. Obrigada por estares sempre disposta a ajudar-me.

À Ângela e à Rita por todas as palavra de apoio e por todas as conversas. Foi um prazer conhecer-vos!

À Inês, Diana, Viana, Helena e Pedro por me ajudarem a manter a sanidade e por todos os momentos que partilhamos. Não teria conseguido sem vocês. São do melhor que Braga me trouxe.

A todos os NERDs pelo ambiente de trabalho e pela ajuda quando necessário.

À Andreia e ao Bruno, obrigada por estarem sempre comigo. São os melhores amigos que podia pedir.

Por fim, às pessoas mais importantes da minha vida, dedico-vos todo este trabalho:

Ao Filipe, por fazeres destes cinco anos algo memorável. Por teres sempre uma palavra de força e um sorriso para mim. Por seres melhor do que eu podia esperar. Que o futuro nos sorria sempre.

Ao Jóni, porque apesar de longe estás sempre perto. Obrigada por seres o melhor irmão e por teres contribuído para me tornar a pessoa que sou hoje. Serás sempre o meu "senisgo".

Por fim, aos meus pais. Porque sem vocês nada disto teria sido possível, um enorme obrigado por todo o amor, apoio e dedicação. Por estarem sempre lá quando eu preciso e por nunca desistirem de mim. Espero deixar-vos sempre orgulhosos.

O trabalho apresentado nesta tese foi realizado no Instituto de Investigação em Ciências da Vida e Saúde (ICVS), Universidade do Minho. O financiamento é proveniente dos fundos da FEDER através do Programa Operacional Fatores de Competitividade – COMPETE, e dos fundos nacionais através da Fundação para a Ciência e Tecnologia sobre POCI-01-0145-FEDER-007038; e sobre o projeto NORTE-01-0145-FEDER-000013 do Programa Operacional Regional do Norte (NORTE 2020), sobre o Acordo de Parceria PORTUGAL 2020, através do Fundo Europeu de Desenvolvimento Regional (FEDER).

STATEMENT OF INTEGRITY

I hereby declare having conducted this academic work with integrity. I confirm that I have not used plagiarism or any form of undue use of information or falsification of results along the process leading to its elaboration.

I further declare that I have fully acknowledged the Code of Ethical Conduct of the University of Minho.

University of Minho, 11th July 2019

Full Name: Joana Lima Sá

Signature: _____

Papel da pentraxina-3 na modulação da Esclerose Múltipla

Resumo

A Esclerose Múltipla (EM) é uma doença inflamatória crónica desmielinizante, caracterizada pela destruição da camada protetora que cobre os axónios, a bainha de mielina, e perda axonal. Geralmente afeta jovens adultos e causa incapacidades a vários níveis, nomeadamente motor, visual e cognitivo. Devido às caraterísticas debilitantes desta doença, existe uma necessidade crescente na descoberta de novos biomarcadores e possíveis alvos terapêuticos. Neste sentido, a pentraxina-3 (PTX3), uma proteína multifuncional envolvida na regulação do recrutamento de leucócitos para os tecidos, resposta inflamatória e manutenção da barreira hematoencefálica, poderá desempenhar um papel importante na patofisiologia desta doença. Para estudarmos esta hipótese, induzimos o modelo animal de EM, o modelo de encefalomielite experimental autoimune (EAE), em murganhos que não expressam PTX3 *(Ptx3$^{-/-}$)* e murganhos selvagens (WT) e avaliamos a evolução da doença nestes animais. Para além disso, avaliamos a expressão de várias citoquinas inflamatórias e também marcadores de astrócitos e microglia no cerebelo destes animais, tanto na fase mais agressiva como na fase crónica da doença. Após esta análise verificamos que os animais *Ptx3*$^{-/-}$ induzidos com EAE não apresentam diferenças significativas em relação aos animais WT, em termos de score clínico e de peso corporal. No entanto, confirmamos que os animais EAE apresentam uma maior expressão de marcadores inflamatórios, como interleucina *(Il) 6*, *Il12*, *Il17* e interferão gamma *(Ifng),* e de alguns marcadores de reatividade de astrócitos e microglia, em comparação com os animais não induzidos. Para além disso, estas diferenças são mais evidentes na fase mais precoce da doença do que na fase crónica. No que diz respeito a diferenças entre genótipos, estas apenas foram observadas na expressão do gene da fibulina-5 *(Fbln5)*, da proteína de ligação ao cálcio *(S100a10)* e do complexo principal de histocompatibilidade 2 *(Mhc2).* Verificámos ainda que os animais *Ptx3*$^{-/-}$ aparentam ter menos lesões no cerebelo do que os animais WT. Para além dos estudos em murganhos, estudámos também o efeito de alterações a nível do gene da *PTX3* em pacientes de EM e controlos saudáveis. Estes pacientes foram genotipados para dois polimorfismos funcionais do gene da *PTX3* e as frequências de haplótipos foram comparados entre grupos. No entanto, nenhum haplótipo estava significativamente relacionado com a suscetibilidade para EM. Medimos também os níveis de PTX3 no soro e verificamos que estes estavam aumentados em pacientes de EM quando comparados com controlos saudáveis, sugerindo um possível papel da PTX3 na patofisiologia de EM.

PALAVRAS-CHAVE: ENCEFALOMIELITE AUTOIMUNE EXPERIMENTAL | ESCLEROSE MÚLTIPLA | NEUROINFLAMAÇÃO | PENTRAXINA-3 | POLIMORFISMOS

Dissecting pentraxin-3 role in the modulation of Multiple Sclerosis

Abstract

Multiple Sclerosis (MS) is a demyelinating chronic inflammatory disease, characterized by degradation of the protective layer that covers the nerves, called the myelin sheath, and axonal loss. It generally affects young adults and causes disabilities at several levels, namely motor, visual and cognitive. Due to the disabling features of this disease, there is an increasing need for the discovery of novel biomarkers and possible therapeutic targets. In this sense, pentraxin-3 (PTX3), a multifunctional protein involved in the regulation of leukocyte recruitment into tissues, inflammatory response and maintenance of the blood brain barrier could play an important role in the pathophysiology of this disease. To study this hypothesis, we induced the widely used MS animal model, the experimental autoimmune encephalomyelitis (EAE), in PTX3-null mice (*Ptx3*$^{-/-}$) and wild-type mice (WT), and assessed the evolution of the disease in these animals. Furthermore, we evaluated the expression of several inflammatory cytokines and also microglial and astrocytic markers, in the cerebellum of these animals, both in the onset and in the chronic phases of disease. After this analysis, we verified that *Ptx3*$^{-/-}$ mice present a similar disease course to WT animals. We confirmed that EAE animals present a higher expression of inflammatory markers, such as interleukin *(Il) 6*, *Il12*, *Il17* and interferon gamma *(Ifng)*, and of some astrocytic and microglial markers in comparison to non-induced controls. Moreover, these differences are more evident in the onset phase than in the chronic phase of disease. Differences between genotypes were only observed in the expression of fibulin-5 *(Fbln5)*, calcium-binding protein *(S100a10)* and major histocompatibility complex class 2 *(Mhc2)* genes. In addition, we observed that *Ptx3*$^{-/-}$ mice seem to present less cerebellum lesions than their WT littermates. Besides this analysis in the animal model, we also studied the effect of genetic variation in the *PTX3* gene in MS patients and healthy controls. These patients were genotyped for two functional single nucleotide polymorphisms (SNPs) of the *PTX3* gene and the haplotype frequencies of the two SNPs were compared between the two groups. However, none of the haplotypes were significantly associated with MS susceptibility. On the other hand, PTX3 serum levels were increased in MS patients when compared to healthy controls, suggesting a possible role of this protein in the pathophysiology of MS.

KEYWORDS: EXPERIMENTAL AUTOIMMUNE ENCEPHALOMYELITIS | MULTIPLE SCLEROSIS | NEUROINFLAMMATION | PENTRAXIN-3 | SINGLE NUCLEOTIDE POLYMORPHISMS

Table of Contents

Abbreviations

A

Amigo2 - Amphoterin-Induced Protein 2

APC – Antigen presenting cell

Atp5b - Adenosine triphosphate synthase subunit beta

B

BBB – Blood brain barrier

BSA – Bovine serum albumin

C

cDNA – Complementary deoxyribonucleic acid

CFA – Complete Freund's adjuvant

CIS – Clinically Isolated Syndrome

CNS – Central Nervous System

CRP – C-reactive protein

CSF – Cerebrospinal Fluid

D

DAMP – Damage-associated molecular pattern

DC – Dendritic cell

DEPC– Diethyl pyrocarbonate

DNA – Deoxyribonucleic acid

E

EAE - Experimental autoimmune encephalomyelitis

EBV – Epstein-barr virus

EDTA - Ethylenediaminetetraacetic acid

ELISA – Enzyme linked immunosorbent assay

F

Fbln5 – Fibulin-5

FGF-2 – Fibroblast growth factor 2

G

GFAP – Glial fibrillary acidic protein

H

H_2O_2 - Hydrogen peroxide

HLA – Human leukocyte antigen

HPR – Horseradish peroxidase

Hspcb - Heat shock protein class beta

I

Iba1 – Allograft inflammatory factor 1

IFN – Interferon

Ig - Immunoglobulin

Il – Interleukin

iNos – Inducible nitric oxide synthase

IRES – Internal ribosomal entry site

J

JC – John Cunningham

L

Lcn2 – Lipocalin-2

LPS - Lipopolysaccharide

M

MBP – Myelin basic protein

$Mgcl_2$ – Magnesium chloride

MHC – Major histocompatibility complex

MOG – Myelin oligodendrocyte glycoprotein

MRI – Magnetic resonance imaging

MS – Multiple Sclerosis

N

NaOH – Sodium hydroxide

NAWM – Normal appearing white matter

O

OCT – Optimal cutting temperature

ON – Optic neuritis

P

PAMP – Pathogen-associated molecular pattern

PBS – Phosphate buffered saline

PCR – Polymerase chain reaction

PFA - Paraformaldehyde

PGK – Phosphoglycerate kinase

PLP – Proteolipid protein

PML – Progressive multifocal leukoencephalopathy

PPMS – Primary-progressive Multiple Sclerosis

PRM – Pattern recognition molecules

PRMS – Progressive-relapsing Multiple Sclerosis

PRR – Pattern recognition receptor

PSGL – P-selectin glycoprotein 1

PTX – Pentraxin

Q

qRT-PCR – quantitative Real time polymerase chain reaction

R

RNA – Ribonucleic acid

RPM – Revolutions per minute RRMS – Relapsing-remitting Multiple Sclerosis

RT – Room temperature

S

S100A10 - S100 Calcium binding protein A10

SAP – Serum amyloid P-component

SNP – Single nucleotide polymorphism

SPMS – Secondary-progressive Multiple Sclerosis

T

TAE – Tris-acetate-EDTA

TGF-β – Transforming growth factor beta

Th – T helper

TLR – Toll-like receptor

TMEV – Theiler's murine encephalomyelitis virus

TNF – Tumour necrosis factor

TSG-6 – Tumour necrosis factor stimulating gene-6

U

UV – Ultraviolet

UVR – Ultraviolet radiation

V

VCAM-1 – Vascular cell-adhesion molecule-1

VEGF – Vascular endothelial growth factor

W

WT – Wild type

Figures Index

Tables Index

1. Introduction

1.1 Multiple Sclerosis: Insights

Multiple Sclerosis (MS) is a chronic inflammatory demyelinating disease of the central nervous system (CNS), where an immune response directed against the myelin sheath that surrounds the axons is developed. This immune response is characterized by chronic inflammation, gliosis and demyelination, which eventually leads to axonal loss and all the related debilitating features (Hauser & Goodin, 2015).

It is estimated that 2.5 million people are affected by this pathology worldwide, being the highest incidence in Europe and North America (Hauser & Goodin, 2015; Mckay, Kwan, Duggan, & Tremlett, 2015). MS affects especially young adults, with a typical age of onset between 20 and 40 years of age (Hauser & Goodin, 2015). In fact, it is the second major cause of neurological disability in this age group, dethroned only by trauma (Dobson & Giovannoni, 2018; Procaccini, De Rosa, Pucino, Formisano, & Matarese, 2015).

Although some mechanisms involved in MS pathology are known, the underlying cause for this disease remains obscure (Dobson & Giovannoni, 2018). In addition, the disease course is extremely variable, ranging from asymptomatic to extremely debilitating phases, with various areas of the CNS susceptible to be affected and with variable aggressiveness (Hauser & Goodin, 2015). This complexity makes it difficult to diagnose and treat MS patients in the initial phases of disease and emphasizes the importance of its study.

Diagnosis of MS requires the presence of clinical signs, but also imagiological and serological evidences (Oh, Vidal-Jordana, & Montalban, 2018). The most common clinical signs correspond to motor and visual deficits that can differ between patients depending on the affected area of the CNS. For instance, a frequently affected area is the cerebellum, originating symptoms such as ataxia and intention tremors (Wilkins, 2017). In addition, magnetic resonance imaging (MRI) is an essential diagnostic tool used in MS, as it allows the immediate visual detection of brain and spinal cord lesions. This technology allows the assessment of the dissemination of lesions both in time and space, a necessary criteria for MS diagnosis (Hauser & Goodin, 2015; Oh et al., 2018). Besides clinical signs and MRI, laboratory tests are also part of the MS diagnostic criteria. In fact, the presence of immunoglobulin G (IgG) oligoclonal bands in the cerebrospinal fluid (CSF) has been shown to be related with MS, and although not specific for this pathology, is still an important component in the process of MS diagnosis (Gelfand, 2014).

In what concerns the clinical course, initially, these patients start by presenting a clinically isolated syndrome (CIS). CIS consists of the first demyelinating event that leads to the appearance of the first

neurological symptoms. Generally, the affected areas in these patients are the optic nerve, brainstem or spinal cord. Moreover, after this first event, some patients develop relapses, and can then be diagnosed with definite MS, but others do not progress (Dobson & Giovannoni, 2018). For the patients who evolve to definite MS, the disease course is variable and although difficult to fully differentiate between subtypes, it has been typically divided in four courses: relapsing-remitting MS (RRMS), primary-progressive MS (PPMS), secondary-progressive MS (SPMS) and progressive/relapsing MS (PRMS) (Hauser & Goodin, 2015; Oh et al., 2018).

The first and most common type is RRMS (Figure 1A), affecting approximately 85% of all MS patients (Hauser & Goodin, 2015). Interestingly, women are three times more prone to develop this subtype than men are. RRMS is characterized by discrete attacks followed by partial or complete recovery (Mckay et al., 2015). Over time, this course of disease is expected to evolve to SPMS (Figure 1C) where there is a steady decline in functional ability regardless of acute attacks (Weissert, 2013). The second most common type is PPMS (Figure 1B), which affects around 10-15% of MS patients. These patients experience a fast disease progression characterized by a stable deterioration in function without the occurrence of occasional attacks. As opposed to RRMS, in PPMS the prevalence of affected females seem to be similar to that of affected males (Mckay et al., 2015). Finally, PRMS (Figure 1D) affects less than 5% of MS patients and is similar to both RRMS and SPMS. This means that these patients present a steady decline in function but also experience occasional attacks during their progressive course (Hauser & Goodin, 2015).

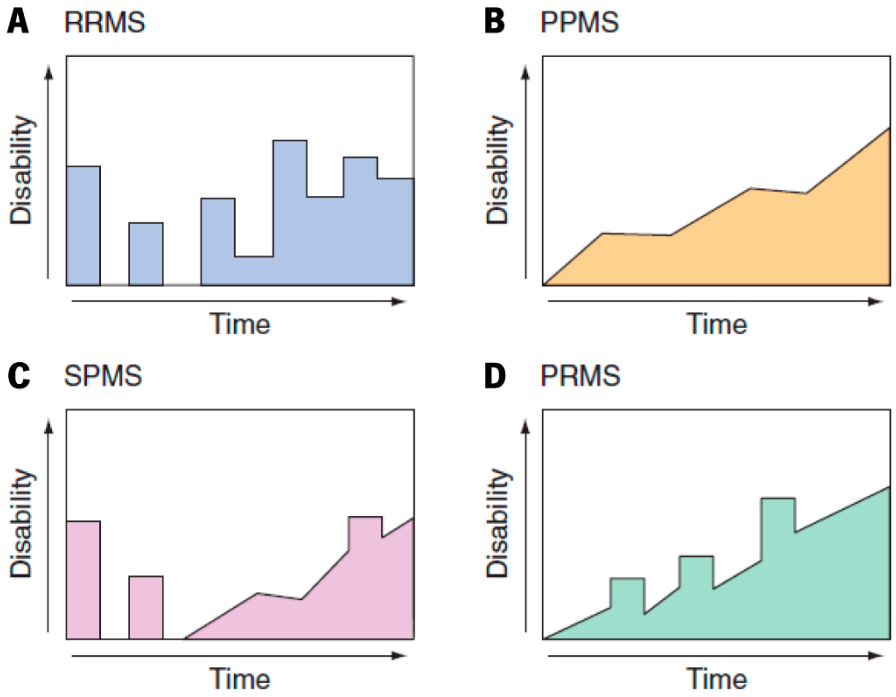

Figure 1. Disease courses of Multiple Sclerosis (MS) patients. (A) Relapsing remitting MS. (B) Primary progressive MS. (C) Secondary progressive MS. (D) Progressive relapsing MS. Reproduced from (Hauser and Goodin, 2015, *Harrison's Principles of Internal Medicine,* p.2664).

Currently, the therapy used in MS is based either on the treatment of acute attacks or on the use of modifying agents that alter the disease course. While the treatment of acute attacks, with the use of glucocorticoids, only provides short-term benefits, the administration of modifying agents seems to offer a long-term approach on disease management (Hauser & Goodin, 2015).

The newly discovered natalizumab, a monotherapy for RRMS patients with high disease activity, appears to be one of the most effective treatments used, because of its unique mechanism of action (Marques et al., 2012). Natalizumab is a recombinant humanized antibody that can bind to $\alpha 4\beta 1$-integrin present on the surface of leukocytes and block their binding to vascular cell adhesion molecule-1 (VCAM-1), present on the surface of endothelial cells. This is important because this interaction is essential for leukocyte transmigration across the blood brain barrier (BBB). By inhibiting this interaction, natalizumab stops the transmigration of leukocytes into the brain, preventing the formation of new lesions (Hutchinson, 2007; Steinman, 2012). However, as this drug stops the migration of these immune cells into the brain parenchyma, the CNS becomes immunosuppressed, which allows pathogens to propagate. This is what happens with progressive multifocal leukoencephalopathy (PML), one of the side effects of natalizumab in some patients (Hutchinson, 2007). PML is a rare demyelinating disorder of CNS, caused by a reactivation of John Cunningham (JC) virus. This virus generally infects children, originating asymptomatic

primary infections. After this, the virus remains inactive only to be activated when patients present a supressed immune system (Fayyaz & Jaffery, 2018). Because of this association between natalizumab and PML, only a restricted number of patients are indicated for natalizumab treatment (Hauser & Goodin, 2015). Moreover, even those that start natalizumab treatment need to be controlled for the JC virus levels and discontinuation of this drug is strongly recommended upon the first signs or symptoms and/or MRI findings suggestive of PML. For the patients susceptible of developing this side effect, the treatment approaches are mostly immunomodulatory drugs that are not as effective as natalizumab and include interferon beta-1a (IFNβ-1a), interferon beta-1b (IFNβ-1b), glatiramer acetate and mitoxantrone. Unfortunately, about two thirds of the patients treated with these drugs eventually develop relapses and disease progression (Hutchinson, 2007).

Taking all this into account, we conclude that the treatment approaches available today are yet to be the ideal ones. Therefore, it is important to continue the search for new therapies that are both effective and safe, in order to provide a better care for these patients.

1.1.1 Aetiology of Multiple Sclerosis

Even though the exact cause of MS remains undiscovered, it is thought to be multifactorial and, in fact, some factors have already been related with a higher predisposition for its development.

First, genetic predisposition for MS development has been described and this predisposition is believed to be polygenic. However, the strongest genetic association, so far, is the one located on the human leukocyte antigen (HLA) complex. Actually, for subjects with the class II allele HLA-DBR1*15:01, the risk of MS increases approximately three-fold in the majority of populations (Hedström, 2018; Mouhieddine et al., 2015). This association of MS risk with the HLA complex indicates that this pathology is possibly an antigen-specific autoimmune disease (Hauser & Goodin, 2015). Moreover, other genes related with the regulation of immune functions have been identified as risk enhancers for MS, in genome-wide association studies (Hauser & Goodin, 2015; Hedström, 2018). Amongst them are the genes for interleukin-17 (IL17) receptor and IL2 receptor (Hauser & Goodin, 2015). Furthermore, given the polygenic nature of this disease, it is believed that in the future the analysis of single nucleotide polymorphisms (SNPs) of several immune-related molecules will be important to allow an earlier treatment of MS (Hemmer, Kerschensteiner, & Korn, 2015).

Besides genetic predisposition, viral infections and, in particular, those caused by Epstein-Barr virus (EBV), have also been reported to increase the risk for MS development. EBV is a herpes virus that infects around 90% of the population and is found in 99% of the MS population (Mouhieddine et al., 2015).

Although the causal role is still not understood, it is proposed that the increased amount of EBV antigens in these patients can overstimulate the immune system, triggering a cascade of events that ultimately leads to MS (Nejati et al., 2016).

Another factor that seems to be related with MS is the vitamin D levels. Indeed, there is a large amount of studies on sun exposure/vitamin D, provoked by epidemiologic observations of a latitude-dependent differences in MS incidence and prevalence. Considering that we depend on ultraviolet radiation (UVR) to convert vitamin D to an active metabolite, it is difficult to distinguish the effect of UVR from that of vitamin D and to safely affirm which are the pathways affecting the risk of MS development. But both these exposures have been related to a decreased risk for this disease (Lucas, Byrne, Correale, Ilschner, & Hart, 2015).

Finally, cigarette smoking is another factor that seems to increase the predisposition for MS and this effect seems to be more pronounced in men than in women (Zhang et al., 2016). Remarkably, the lung has been identified as a critical site for activation of pathogenic T lymphocytes necessary for autoimmune activation in MS (Hauser & Goodin, 2015). Moreover, cigarette smoke contains a high amount of harmful substances such as free radicals, which have been related with neural tissue damage, and cyanide, shown to produce demyelinating CNS lesions (Hedström, 2018).

1.1.2 Multiple Sclerosis: Symptoms

As referred previously, MS is a highly heterogeneous disease. As a result, the symptoms presented by its patients are highly variable as well (Figure 2). They can be so insignificant that the patient ignores them, or they can rapidly evolve to severe loss of function, varying between motor, cognitive and even emotional manifestations (Hauser & Goodin, 2015).

When the spinal cord is affected, the symptoms can be either motor or autonomic. Regarding the first, up to 89% of patients are affected by weakness (Gelfand, 2014) , which may manifest as loss of strength or speed, as fatigue or as altered gait. Spasticity, especially in the legs, also affects around 30% of MS patients and once again, can vary between subtle or severe spasms (Hauser & Goodin, 2015). Autonomic symptoms manifest as bladder, bowel and sexual dysfunction (Luzzio & Dangond, 2018). Bladder dysfunction is one of the most common manifestations, being present in more than 90% of the patients. It is generally characterized as increased urinary frequency and incontinence. In contrast, bowel dysfunction is less common and the most frequent complaint is constipation. Finally, sexual dysfunction presents as loss of libido, erectile dysfunction in men and reduced vaginal lubrication in women (Gelfand, 2014; Hauser & Goodin, 2015).

Another frequently affected area is the cerebellum. When this occurs, patients present symptoms as ataxia that manifests as a lack of coordination, tremors and dysarthria (scanning speech) (Parmar et al., 2018; Tornes, Conway, & Sheremata, 2014).

Visual symptoms are also common in these patients and consist in optic neuritis (ON), visual blurring and diplopia (double vision). ON is expected to affect approximately half of the MS population at some point in their disease course (Gelfand, 2014) and is presented as a decreased visual acuity, blurring or decreased colour perception in the middle of the field of vision (Hauser & Goodin, 2015).

Although motor symptoms are the focus in the study of MS, cognitive dysfunction also seems to be an important part of this pathology. Surprisingly, 40-70% of MS population experience cognitive deficits (Gelfand, 2014) being the most common manifestations, memory loss, attention deficits and dysfunction on performing executive functions (Sokolov, Grivaz, & Bove, 2018).

Finally, some patients also experience depression that can be attributed to frontotemporal lesions or to the morbid condition itself (Gelfand, 2014; Hauser & Goodin, 2015).

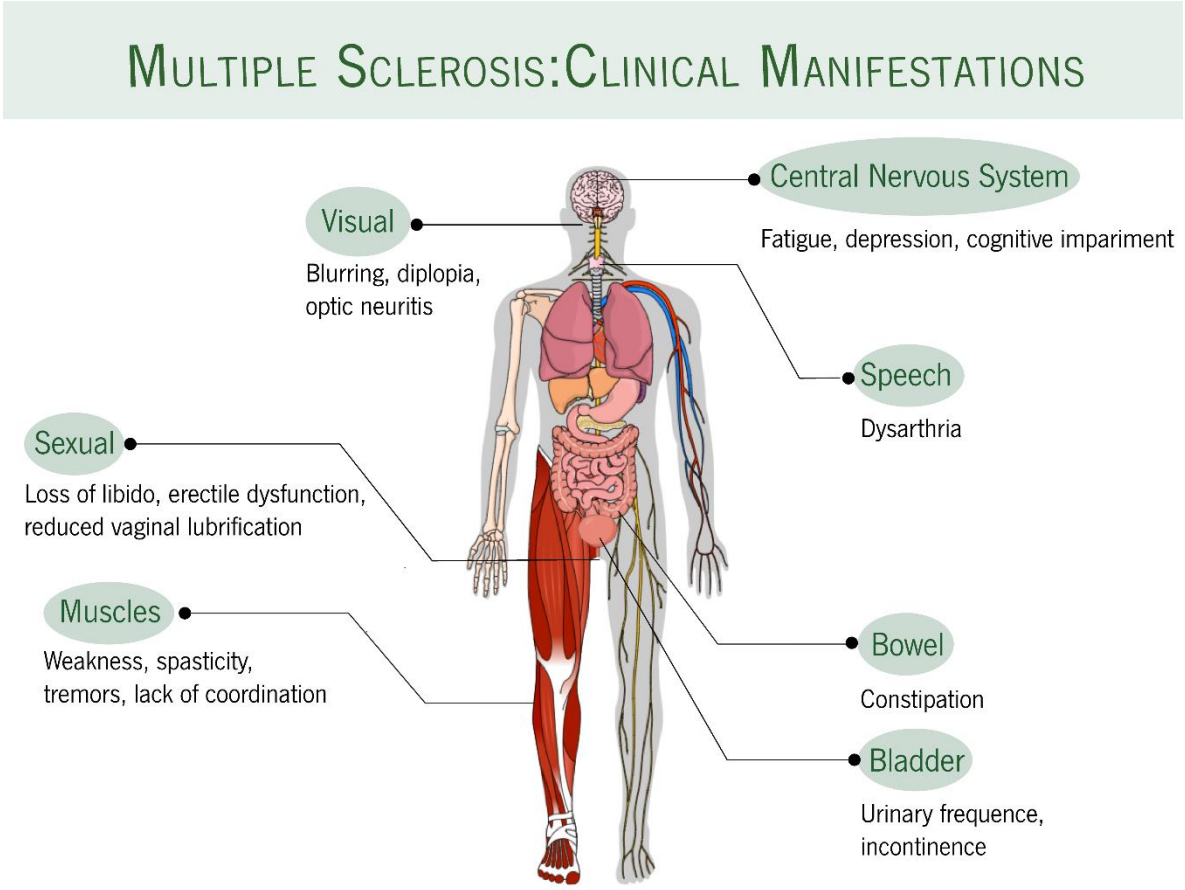

Figure 2. Schematic representation of Multiple Sclerosis (MS) clinical manifestations. MS patients can experience a wide variety of symptoms, ranging from visual manifestations to digestive and urinary symptoms.

1.2 Multiple Sclerosis animal models

MS is a debilitating disease with a high incidence and prevalence. This emphasizes the importance of studying the pathways involved in its pathogenesis and of developing new treatments to improve the quality of life of its patients. In this sense, the development of animal models that simulate this pathological state is one of the biggest achievements in scientific research.

Although none of the existing models can mimic exactly what happens in MS due to the high heterogeneity of symptoms and disease courses, they are still important to understand the basic biology of the disease and to discover molecules with diagnostic and therapeutic potential (Miller, Fyffe-Maricich, & Caprariello, 2017; Robinson, Harp, Noronha, & Miller, 2014). At the moment, the most used animal models of MS are viral, toxic and immunological models.

Given the fact that viral infections are considered a risk factor for MS, some models of viral mediated demyelination have been developed. The most widely used is Theiler's murine encephalomyelitis virus (TMEV), used to assess axonal damage and the demyelination process. In this model, animals are inoculated with the TMEV virus through an intracerebral injection (Lassmann & Bradl, 2017). This virus infects macrophages/microglia lineage cells, oligodendrocytes and astrocytes and always originates a chronic-progressive disease phenotype in susceptible mice (Procaccini et al., 2015). The immune system orchestrates a response against TMEV infected cells, which eventually leads to their death, together with the normal occurring lysis of infected cells. The death of oligodendrocytes, which produce myelin, and the occurring immune response eventually lead to the characteristic demyelination patterns observed in MS (Miller et al., 2017; Procaccini et al., 2015).

Toxin induced models are especially used to better understand the remyelination process since in this model, the location and timing of the demyelination and remyelination processes can be controlled. Initially, the animals are inoculated with specific demyelinating toxins that can be either injected directly in the area of interest (focal toxins) or supplemented in the rodent chow (systemic toxins) (Miller et al., 2017). Focal toxins, such as lysolecithin, are generally used to induce lesions in the spinal cord, corpus callosum, optic nerve and caudal cerebellar peduncle. In this case, the demyelination is thought to be caused by lysolecithin toxic detergent effect and not by an immune mediated response. Nevertheless, after injection and demyelination, infiltration of T-cells and other immune mediators is observed, which may indicate the initiation of an immunological repair response (Miller et al., 2017; Procaccini et al., 2015). In young animals, complete remyelination is observed in 5-6 weeks post-injection, demonstrating the importance of this model in the study of this process (Procaccini et al., 2015).

Systemic toxins, such as cuprizone, can be used to induce demyelination without the direct injection of the toxin into the CNS. Cuprizone is a copper chelating agent that is supplemented in the rodent chow (Lassmann & Bradl, 2017; Miller et al., 2017; Procaccini et al., 2015). The accepted mechanism of action for cuprizone is that by chelating copper, this agent causes apoptosis of oligodendrocytes through metabolic failure. This oligodendrocyte death on its turn causes demyelination through oxidative injury mechanisms (Lassmann & Bradl, 2017). The areas that are frequently affected in this model are the corpus callosum, hippocampus, cerebellar peduncles, cerebellum, striatum and cerebral cortex (Miller et al., 2017). When cuprizone is removed from the animals diet, new oligodendrocytes begin to be generated and when mature they begin to form new myelin sheaths, allowing the study of the remyelination process (Procaccini et al., 2015). Unfortunately, the exact mechanism by which cuprizone acts and why only oligodendrocytes are affected is not fully comprehended (Miller et al., 2017).

Taken together all this data, we can verify that both toxic and viral-mediated models are useful when trying to understand the demyelination and remyelination processes, but, unfortunately, none of them seems to truly reflect human MS disease (Procaccini et al., 2015).

Despite the variability of models available, the experimental autoimmune encephalomyelitis (EAE) model continues to be the model of choice, due to its high similarity to MS pathophysiology. Because of this resemblance, EAE is used to study the pathogenic process of MS development, CNS inflammation, demyelination, cell trafficking and tolerance induction (Constantinescu, Farooqi, O'Brien, & Gran, 2011). This model was first described by *Stuart and Krikorian*, in 1928, after they observed that repeated inoculation of "nerve substance" led to development of paralytic disease (Stuart & Krikorian, 1928). Afterwards, based on their work, *Rivers et al. (1933),* showed that injection of rabbit brain emulsions in monkeys lead to an inflammatory reaction and CNS demyelination in primates (Rivers, Sprunt, & Berry, 1933). EAE has been used ever since those discoveries.

This model can be induced either passively, through the transfer of pathogenic, myelin-reactive CD4+ T-cells produced in donor animals into the recipient animals, or actively (Constantinescu et al., 2011).

In "active" EAE, the demyelinating disease is generated by immunization of the animals with a specific self-antigen, component of the myelin layer, namely myelin basic protein (MBP), myelin oligodendrocyte glycoprotein (MOG) or proteolipid protein (PLP) (Robinson et al., 2014). Interestingly, depending on the genetic background of the mice used, specific peptides give rise to different disease phenotypes, broadening even more the possibilities for EAE use (Miller et al., 2017). For example, immunization of SJL/J mice with $PLP_{139-151}$ gives rise to a relapsing-remitting phenotype while immunization of C57Bl/6 with MOG_{35-55} originates a more chronic progressive disease course (Procaccini et al., 2015).

Besides the myelin-associated peptides, these animals are also injected with complete Freund's adjuvant (CFA) and Pertussis Toxin, which potentiate the humoral immune response and enhance disease onset and severity (Freund & McDermott, 1942; Munoz, Bernard, & Mackay, 1984).

The pathophysiology of EAE is similar to the one established for MS, despite the obvious fact that no external immunization occurs in MS. In EAE, CFA, containing bacterial components, initiates the activation of the innate immune system. This activation leads to a sensitization against the myelin peptide present in the emulsion and consequently the formation of autoreactive T-cells. These T-cells differentiate and release cytokines that activate both adaptive and innate neighbouring cells. Eventually, all these components are able to migrate to the CNS where they can directly attack the myelin layer, leading ultimately to axonal loss (Constantinescu et al., 2011; Miller et al., 2017).

Given the fact that only C57Bl/6 mice will be used in the context of this thesis, that is the model we will be focusing from now on.

As already mentioned, when inducing EAE in C57Bl/6 mice with the myelin peptide MOG_{35-55}, the animals present a chronic disease course with the absence of remission (Procaccini et al., 2015). As a result, it is used mainly to model later stages of disease (Miller et al., 2017). This type of EAE is characterized by multifocal areas of inflammatory infiltrates composed especially of macrophages and CD4+ T-cells and by demyelination in the spinal cord and cerebellum (Constantinescu et al., 2011).

In EAE, the disease is generally induced in female animals at 9-13 weeks of age, because, as it happens in humans, females show a higher susceptibility to develop EAE (Butterfield et al., 1999). These animals experience a predictable clinical course, with symptoms first appearing at 9-14 days after immunization. Mice present motor deficits that start as tail paralysis and ascend through the hind limbs until the front limbs are also affected. These mobility deficits are usually assessed using a 5-point scale, where 1 corresponds to limp tail and 5 corresponds to dead/moribund animals. Generally, these mice reach maximum scores of 3.0-3.5, characterized by hind limb paralysis (Kipp et al., 2012; Miller et al., 2017; Procaccini et al., 2015).

A great advantage of inducing EAE in the C57Bl/6 mice is the fact that the majority of genetically modified strains are created in this background. This allows the broadening of the study of MS to specific gene alterations (Kuerten et al., 2007). However, EAE induction in this mice strain also entails some limitations, such as the impossibility of studying the physiology of MS relapses and the difficulty in studying remyelination (Ransohoff, 2012). Since our aim is to study the role of pentraxin (PTX) 3 in MS and because this protein belongs to the innate immune arm of the immune system, we will explore next the role of the innate immune system in MS.

1.3 The role of innate immunity in Multiple Sclerosis pathophysiology

The innate immune system is the first line of defence of our body against pathogens, providing a fast and effective response against pathogens, although not very specific (Owen, Punt, & Stranford, 2013). The cellular and humoral mechanisms that compose the innate immune system are encoded in the germline and include the complement system and various cellular types that possess specific receptors present in their cell membranes, known as the pattern recognition receptors (PRRs) (Owen et al., 2013). More specifically, the humoral arm comprises the complement system and fluid-phase pattern recognition molecules (PRM), such as pentraxins (Inforzato et al., 2013), while the cellular arm is composed by cell-associated PRMs that are located in the different cellular compartments, such as Toll-like receptors (TLRs) (Bottazzi, Doni, Garlanda, & Mantovani, 2010). These cells and molecules first recognize the pathogenic invader and then activate T and B cells, members of the adaptive immune system, initiating the cascade of events that in normal conditions leads to the resolution of the infection (Gandhi, Laroni, & Weiner, 2010).

The focus in the study of MS pathophysiology has mainly been the role of the adaptive immune system. In fact, the proposed onset mechanism (Figure 3) states that myelin-specific auto-reactive T-cells are primed in the periphery by myelin peptides (Gandhi et al., 2010) and then, can differentiate into T helper (Th) 1 and Th17 subtypes and produce their signature inflammatory cytokines. In addition, activated T-cells gain the ability of crossing the BBB by upregulating integrins. When in the CNS they can encounter their associated myelin antigen, such as MBP, PLP or MOG (Steinman, 2001). These peptides are presented by antigen presenting cells (APCs) that express major histocompatibility complex (MHC) class II molecules. CD8+ T-cells also become activated by recognizing peptides presented by MHC class I molecules (Hemmer et al., 2015). Upon interaction with the antigen, T-cells start producing cytokines and chemokines that activate other immune cells and propagate the inflammatory response directed at myelin (Constantinescu et al., 2011). Consequently, these cells and their mediators start to attack the myelin sheath surrounding the axons (Hemmer, Archelos, & Hartung, 2002; Yadav, Mindur, Ito, & Dhib-Jalbut, 2015). With demyelination, there is a reduction in trophic support for axons, redistribution of ion channels and destabilization of action potentials with consequent axonal degeneration, originating neurological deficits (Hauser & Goodin, 2015).

Currently, however, there is also a rising interest in understanding the role of the innate immune system in the evolution of MS. It is known that besides playing an autonomous role, this system can also influence the adaptive branch by expressing cytokines and other small molecules that interact with T and B cells, further activating them (Gandhi et al., 2010).

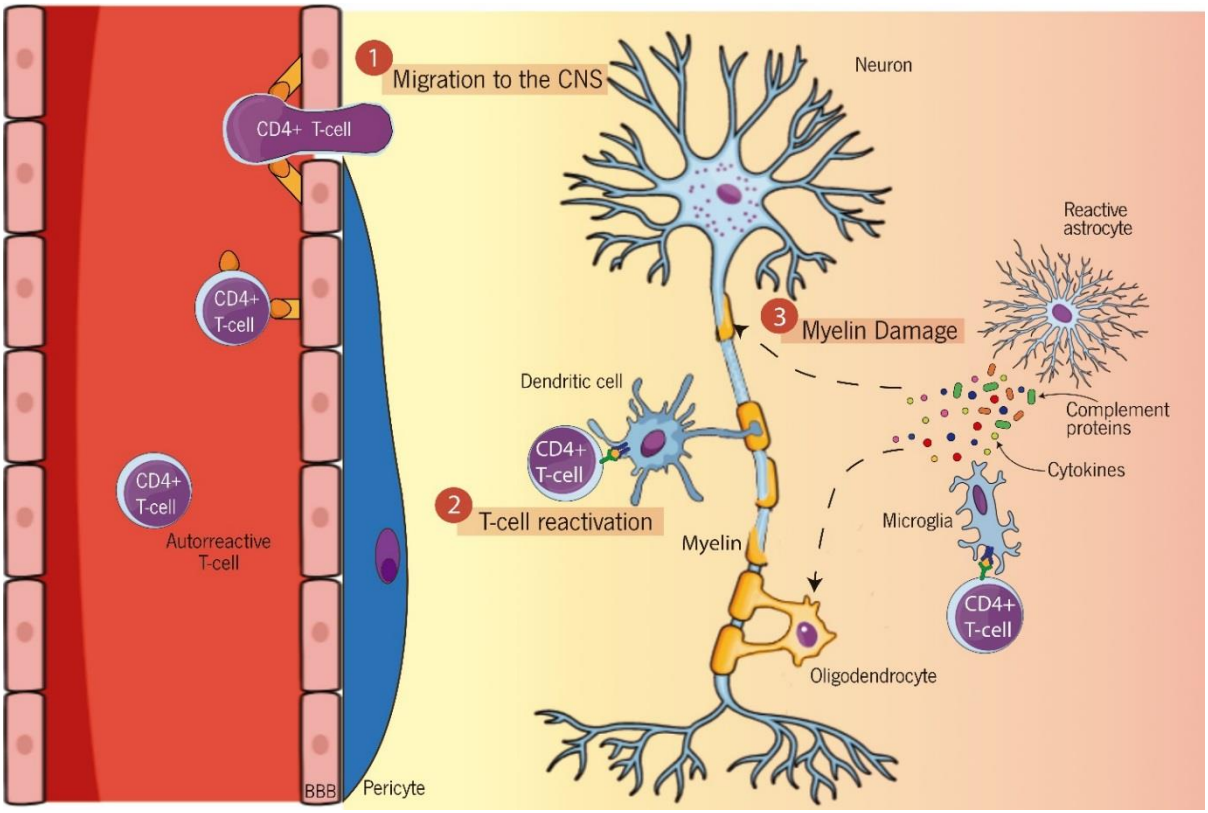

Figure 3. An overview of the proposed mechanism for Multiple Sclerosis (MS) development. Initially, autoreactive CD4+ T cells gain the ability to migrate to the CNS by an overexpression of adhesion molecules. When inside the CNS, these cells are reactivated by interaction with APCs, such as dendritic cells. Upon reactivation, T-cells interact with other immune components and initiate the release of inflammatory mediators, namely cytokines. Reactive astrocytes and microglial cells also start to produce cytokines and complement protein. This increased inflammatory response will act on the myelin layer and on oligodendrocytes causing, eventually, myelin damage.

TLRs are molecules expressed on the cell surface that recognize molecular patterns specific of pathogens, the pathogen associated molecular patterns (PAMPs) and of damaged self-molecules, the damage associated molecular patterns (DAMPs) (Owen et al., 2013). The interaction between TLRs and the respective PAMPs/DAMPs, initiates innate and adaptive immune responses through the induction of cytokines, chemokines and the production of costimulatory molecules (Hernández-Pedro, Espinosa-Ramirez, De La Cruz, Pineda, & Sotelo, 2013; Saresella et al., 2014). Interestingly, it was shown that depending on the molecules induced, TLRs can play different roles in MS. In fact, it is reported that in the EAE model, TLR3 stimulation has a protective effect, while TLR stimulation upon the release of pro-inflammatory mediators increases disease severity (Saresella et al., 2014).

The complement system, a major component of innate immunity, has also been described in the context of MS. This system becomes activated during neuroinflammation and is responsible for cell-lysis,

chemotaxis, opsonisation and stimulation of immune cells (Lindblom et al., 2016). In MS, it was demonstrated that CSF levels of complement component 3 (C3) and soluble complement receptor 2 (sCR2) are increased in MS patients, with C3 levels correlating with clinical disability (Aeinehband et al., 2015; Lindblom et al., 2016). Moreover, several complement components are present in active MS lesions and persist until later stages of disease. In addition, complement markers were co-localized with active astrocytes and microglia, as well as with areas of myelin degeneration and damaged axons. All of this supports the role of the complement system in maintaining progressive inflammation and in contributing to myelin and axonal damage along with microglia activation during the course of MS (Ingram et al., 2014). On the other hand, in the EAE model, it was shown that complement component 5 (C5) could play a neuroprotective effect, through the regulation of the inflammatory response and inhibition of oligodendrocyte apoptosis (Niculescu et al., 2004). Due to the controversial information available, we could assume a dual role for the complement system in the pathogenesis of MS. Consequently, more studies are needed in order to better understand the functions of this system in MS initiation and progression.

Several innate cell types also seem to play a role in MS pathophysiology, however, macrophages and microglia appear to be the biggest contributors to MS pathogenesis (Hemmer et al., 2015). These cells can be observed near MS lesions and are responsible for the degradation of the myelin sheath and later for debris clearance. Also, they are important antigen presenting cells, along with dendritic cells, meaning that after engulfing myelin peptides they can present them to adaptive immune cells and further activate the immune response against myelin (Chu et al., 2018; Gandhi et al., 2010). Interestingly, it was observed that during the acute phase of disease, macrophages and microglia present a M1 phenotype, more associated with a pro-inflammatory role. During this phase it is proposed that these cells induce demyelination and neuronal death in the CNS, through the release of pro-inflammatory cytokines, such as IL-6 (Chu et al., 2018). In contrast, during a more chronic phase of disease, M2 microglia/macrophages are the predominant cell types in the CNS and are responsible for an anti-inflammatory activity that mediates tissue repair. This anti-inflammatory activity is characterized by the release of cytokines, such as IL-4, IL-10 and transforming growth factor-beta (TGF-β) (Chu et al., 2018). Although the exact mechanism that mediates this shift is not well understood, it is believed that the M1 phenotype may be induced by the release of pro-inflammatory cytokines, such as interferon-gamma (IFN-γ), IL-1 and tumour necrosis factor-alpha (TNF-α), by myelin reactive T cells (Yadav et al., 2015). These cytokines, on their turn, can induce the release of other inflammation mediators, such as PTX3 (Ummenthum et al., 2016).

Surprisingly, groups of activated microglia, usually present in preactive lesions, have been observed in normal appearing white matter (NAWM). These preactive lesions precede BBB damage and leukocyte infiltration and are believed to be the earliest stage of MS lesions (Ummenthum et al., 2016; Yadav et al., 2015). This indicates the existence of an endogenous factor in the CNS which probably initiates the cascade of events that leads to MS, but also a role for the innate immune cells in this event (Yadav et al., 2015). Indeed, whether the activation of the immune system is a cause or consequence of the disease is a matter of debate.

Besides macrophages and microglia, neutrophils also seem to be somewhat related to MS. These cells can be activated by a variety of pro-inflammatory cytokines such as TNFα, IFN-γ and IL-6 and have been shown to be increased in patients with RRMS. Although their exact role is still not known, it is believed that this increase is related with a reduction in apoptosis, induction of inflammatory response and oxidative burst that eventually leads to demyelination (Hernández-Pedro et al., 2013).

Taking all this into account, it appears that the innate immune system plays a role in both initiation and progression of MS (Hernández-Pedro et al., 2013). Although many of the mechanisms involved are still unknown, we expect that the continuous efforts to uncover these mechanisms will provide new insights on all the players involved in MS pathogenesis. Herein, we are particularly interested in studying the role of a class of proteins, PTXs, which are involved in the humoral arm of the innate immune response. In this case, we aim to study the role of PTX3, a protein that is rapidly produced and released by several cell types, in particular by mononuclear phagocytes, dendritic cells (DCs), fibroblasts and endothelial cells in response to primary inflammatory signals (e.g, TLR engagement, TNFα, IL-1β) and that we will describe in more detail in the next section.

1.4 The pentraxins protein family

PTXs are a superfamily of serum proteins, members of the humoral branch of innate immunity, responsible for regulating innate responses and inflammation (Rajkovic, Denes, Allan, & Pinteaux, 2016). These acute-phase proteins are conserved throughout evolution, from arachnids to humans (Deban et al., 2009) and have the ability to recognize an extensive range of exogenous substances, but also damaged self-molecules, by acting as PRRs (Mantovani, Garlanda, & Doni, 2008). They have a cyclic multimeric structure and are characterized by the presence of a 200 amino acid PTX domain in their carboxyl-terminal, with an eight amino acid long conserved PTX signature (Clos, 2013; Deban et al., 2009).

Due to their structure, PTXs can play a wide variety of functions, being involved in the activation of the complement cascade, host defence against pathogens, clearance of damaged cells and macrophage polarization (Clos, 2013).

The PTXs family is subdivided in two structural classes, depending on the size of their primary structure: the short PTXs (25 kDa) and the long PTXs (40-50 kDa) (Goodman et al., 1996; Rajkovic et al., 2016). Regarding the first class, the main acute-phase responders in human and mouse are C reactive protein (CRP) and serum amyloid P component (SAP), respectively (Deban et al., 2009). In fact, CRP was the first PTX to be described (Tillett & Jr., 1930). These proteins are barely detectable in the plasma of healthy individuals, but upon inflammatory stimuli, especially by IL-6, their liver production increases rapidly, being classified as a positive acute phase protein (Mantovani et al., 2008). After being released from the liver, they can bind to a wide variety of pathogens namely fungi, bacteria and yeasts, and promote their phagocytosis and clearance (Deban et al., 2009).

PTX3 is the prototype for the long PTXs. However, other molecules belong to this family, namely neuronal PTXs 1 (NP1) and 2 (NP2) and PTX4. The molecules from this group are similar to the short PTXs in the C-terminal region, however, they have a longer N-terminal domain, hence their name (Clos, 2013; Goodman et al., 1996). On the other hand, unlike short PTXs that are produced in the liver, long PTXs are produced locally at the site of inflammation by a wide variety of cell types, for instance macrophages and microglia, myeloid DCs and astrocytes. These cells produce PTX3, upon induction by a variety of inflammatory signals, such as TNF-α, IL-1β or TLR engagement (Deban et al., 2009; Mantovani et al., 2008; Ummenthum et al., 2016). PTX3 is also present in a "ready-to-use" form in neutrophil granules, being rapidly released upon inflammatory stimuli (Deban et al., 2009; Mantovani et al., 2008).

Considering that this thesis is based on the immunoregulatory role of PTX3 in MS, we will now focus only on this protein.

1.4.1 PTX3 major functions

PTX3 is an acute-phase protein, member of the PTXs superfamily of proteins. It was discovered by *Brevario et al.*, in 1992, after screening a cDNA library of IL-1β-inducible genes. This protein has been shown to be highly conserved from mouse to man, as opposed to CRP and SAP, which emphasizes the translational power of the study of this molecule using mice models (Introna et al., 2014). Similar to the short PTXs, PTX3 plasmatic levels are very low in physiological conditions but increase rapidly under

inflammatory stimuli. The same is observed in the CNS, as it is not detected in the normal brain, but increases under neuropathological conditions (Rajkovic et al., 2016).

The study of PTX3 functional capabilities has continued since its discovery and its multifunctionality continues to be demonstrated nowadays. Actually, its various functions can be attributed, in part, to its structure, which allows interactions with several different ligands (Figure 4), a feature shared by long and short PTXs (Clos, 2013).

One of the best described ligands of PTX3 is complement component 1q (C1q). This interaction can induce either the activation or inhibition of the classical complement cascade, depending on the way that C1q is presented. PTX3 can also interact with factor H, regulating the alternative pathway of complement activation. Besides controlling the initiation of the complement pathway, PTX3 also seems to be relevant in mediating the complement system response to apoptotic cells. It does this by controlling both the deposition of complement mediators and their clearance (Deban et al., 2009; Mantovani et al., 2008).

PTX3 has also been reported to play a role in regulating angiogenesis and blood vessel repair through its interaction with fibroblast growth factor-2 (FGF2). The interaction between PTX3 and FGF2 blocks the binding of the latter to its receptors, inhibiting its bioactivity and consequently blocking angiogenesis (Presta, Camozzi, Salvatori, & Rusnati, 2007). PTX3 also binds collagen and fibrinogen, regulating platelet aggregation and directly binds platelets blocking their pro-inflammatory actions (Presta, Foglio, Churruca Schuind, & Ronca, 2018).

Another ligand of PTX3 is TNF stimulating gene-6 (TSG-6), involved in the assembly of extracellular matrix. For example, PTX3 induces the formation of a hyaluronan-rich matrix that is necessary for a successful ovulation and fertilization, thus playing a role in fertility. Indeed, studies show that female mice lacking the *Ptx3* gene are subfertile (Salustri et al., 2004; Varani et al., 2002). TSG-6 is also the main regulator of PTX3/FGF2 interaction. In response to inflammatory stimuli, TSG-6 is produced at neovascularization sites and binds to PTX3, releasing its blockage to FGF2, allowing this growth factor to perform its role in angiogenesis (Presta et al., 2018).

An interesting function of PTX3 is the fact that it is also responsible for the regulation of leukocyte recruitment into tissues, through interaction with P-selectin. Upon inflammatory stimuli, endothelial cells start to express P-selectin in their surface. This protein binds to P-selectin glycoprotein 1 (PSGL-1), expressed by leukocytes and mediates their binding and rolling on endothelial cells, a mechanism necessary for leukocyte crossing into the tissues. When there is an excessive recruitment of leukocytes, locally released PTX3 selectively binds P-selectin and acts as a negative feedback mediator, inhibiting the recruitment of more leukocytes and slowing down the pro-inflammatory response (Deban et al., 2010).

PTX3 also seems to play a role in BBB maintenance, which could be relevant in MS. Studies show that during the acute phase of stroke, vascular endothelial growth factor (VEGF) downregulates the levels of some BBB components, breaking its integrity. On the other hand, astrocyte-derived PTX3 can counteract this effect possibly by interacting with VEGF and blocking its activity (Shindo et al., 2016).

Interestingly, specific SNPs of the *PTX3* gene have already been shown to play a role in susceptibility to invasive aspergillosis (Cunha et al., 2014) and in the modulation of female fertility (May et al., 2010), however there is no information regarding their role in the modulation of MS. Therefore, it is important to continue the study of this protein in different pathological contexts in order to unravel more functions and to further acknowledge its biological importance. Additionally, due to all the referred immunoregulatory roles of PTX3, we hypothesize that it could be a potential therapy target for MS. Firstly, due to its role in inhibiting leukocyte recruitment into the CNS, a similar role to natalizumab, but also because of its functions on maintaining BBB integrity and in regulating phagocytosis and tissue repair.

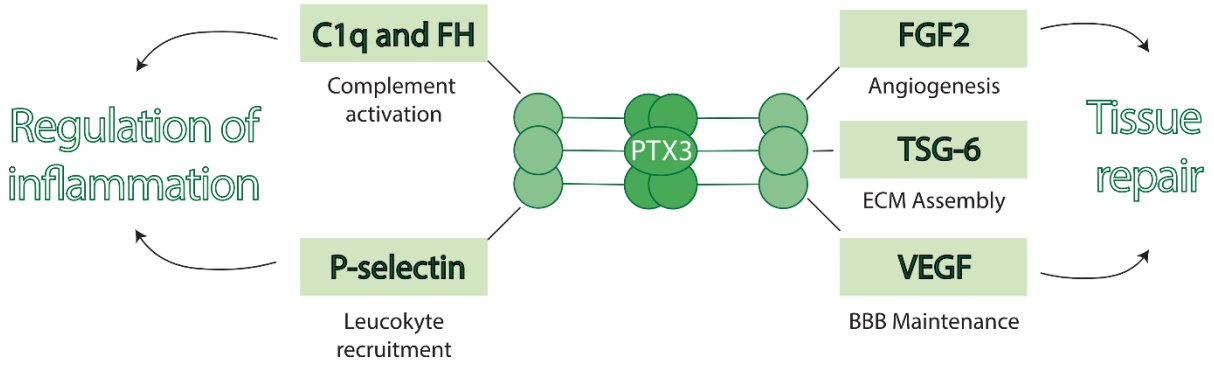

Figure 4. PTX3 as a multifunctional protein. PTX3 plays several roles in the regulation of immunity. Besides the recognition of several pathogens, PTX3 helps in their elimination through the activation of the complement system. In addition, by regulating leukocyte recruitment it seems to regulate the inflammatory response. Furthermore, this molecule is important in tissue repair, through the regulation of angiogenesis, extracellular matrix (ECM) assembly and BBB maintenance. Adapted from *Rajkovic, I. et al, Journal of Neuroimmunology, 2016*.

1.4.2 PTX3 in the Central Nervous System

Although the majority of studies concerning PTX3 focus on its peripheral effect, this protein also appears to play an important role in the CNS. In fact, it is not expressed in the CNS under normal conditions but its levels increase rapidly upon inflammatory or neurotoxic stimuli (Fornai et al., 2015). Besides, it has been shown that PTX3 can be induced in the murine brain through lipopolysaccharide (LPS) or IL-1β injection, being astrocytes its major producers (Polentarutti et al., 2000). It can also be produced by microglia, being capable of modulating its phagocytic activity (Jeon, Lee, Lee, & Suk, 2010).

The fact that this protein is produced in the CNS upon pro-inflammatory stimuli supports the idea that it plays a role during CNS infections/inflammation. Indeed, this protein has already been associated with several pathological conditions of the CNS, where it could be playing a dual role in both conferring neuroprotection but also promoting neuroinflammation (Rajkovic et al., 2016). As already reported, astrocyte-derived PTX3 can reduce BBB damage, by interacting with VEGF, during the active phase of stroke (Shindo et al., 2016) and it also seems to play a protective role in seizure induced neurodegeneration, as mice lacking PTX3 presented increased levels of neurodegeneration (Ravizza et al., 2001). Also, increased levels of PTX3 were found in the CSF of patients with anti-NMDAR encephalitis, an inflammatory disease of the CNS, indicating that PTX3 does in fact reflect underlying neuroinflammatory disorders (Liu et al., 2018). Moreover, PTX3 was found up-regulated in an animal model of prion disease, a chronic neurodegenerative disease of the CNS (Cunningham, Wilcockson, Boche, & Perry, 2005). However, the exact role of PTX3 on the pathophysiology of this disease is still not understood.

Besides being a major player in disease conditions, PTX3 also presents a more fundamental role. Interestingly, it seems to play an important part even during the period of brain development where it has been reported has promoting synaptogenesis (Fossati et al., 2019). Once again, this supports the idea that PTX3 is an important modulator of several pathways, even in the CNS and that it could be playing an important role in the modulation of MS, as we will explore next.

1.4.3 PTX3 and Multiple Sclerosis

PTX3 has already been described in the context of MS. Of interest, it has been shown that PTX3 is increased in the plasma of MS patients, during the relapse phase but not during remission. Moreover, in the relapse phase, increased levels of this protein were correlated with increased disease disability (Wang et al., 2013). In addition, an increased *Ptx3* mRNA expression was observed in the spinal cord of EAE rats and it was maximal during the active phase of disease (Agnello et al., 2000). Then, although still detectable, its expression decreased until the end of the experiment (Agnello et al., 2000). Taken together, this data indicates a possible role of PTX3 as a biomarker of inflammatory activity in MS.

Finally, PTX3 was also detected in active MS lesions of post-mortem brain slices of patients. Its location in these samples correlated with that of activated microglia and macrophages, suggesting a possible role in phagocytosis and tissue repair, after lesion formation. Surprisingly, in the same study it is stated that the lack of *Ptx3* gene does not alter EAE disease progression in mice (Ummenthum et al., 2016).

Considering all this, it seems that PTX3 could in fact be playing a role in MS. Nevertheless, there is still much to be learned regarding the real mechanisms played by this protein in MS pathogenesis. With this thesis, we expect to contribute to uncover some of these functions and to better understand the importance of PTX3 in the context of MS.

2. Research Objectives

It is clear that MS is a complex disease with many of the players involved in its pathophysiology still undiscovered. In this thesis, we propose that PTX3 could be a modulator of MS due to its immunoregulatory role in inhibiting leukocyte recruitment into the CNS and in regulating the inflammatory response and tissue repair. In this sense, we intend to study its impact in this disease, focusing on the analysis of the cerebellum, a structure known to be affected in MS patients and EAE animals. Therefore, using the EAE mice model, we propose to:

1 - Assess the effects of *Ptx3* ablation on disease course and cerebellar demyelination and inflammatory patterns of EAE induced mice.

Then, taking into consideration the importance of the study of immune-related gene polymorphisms in the context of MS, as well as the lack of information regarding the influence of *PTX3* gene SNPs on MS development, we intend to:

2 - Evaluate the influence of *PTX3* SNPs and protein serum levels on MS susceptibility.

3. Materials and Methods

3.1 Ethical Statement

All animals procedures were conducted after consent from the Portuguese National Authority for Animal Experimentation, *Direção Geral de Veterinária* (ID:DGAV9458). Animals were handled and kept in accordance with European regulations on animal care and experimentation (EU Directive 2010/63/EU) and the 3R's principles were followed. Housed animals were maintained under a standard controlled environment (22-24°C; 55% humidity; 12 hours light/dark cycles; fed with regular rodent's chow and tap water *ad libitum)*. Animals were housed 5 per box, with regular paper as environmental enrichment.

3.2 Animals

The experiments were conducted using PTX3-null (*Ptx3*$^{-/-}$) female mice and the respective wild type (WT) littermate controls, on a C57Bl/6 background, at 10 weeks of age. These mice were obtained from heterozygous mattings, which in their turn were obtained from the breeding of WT mice with *Ptx3*$^{-/-}$ mice where an internal ribossome entry site (IRES)-lacZ cassette followed by the phosphoglycerate kinase 1 (PGK)-neomycin resistance gene was integrated in exon 1 of the *Ptx3* gene (Figure 5) (Garlanda et al., 2002).

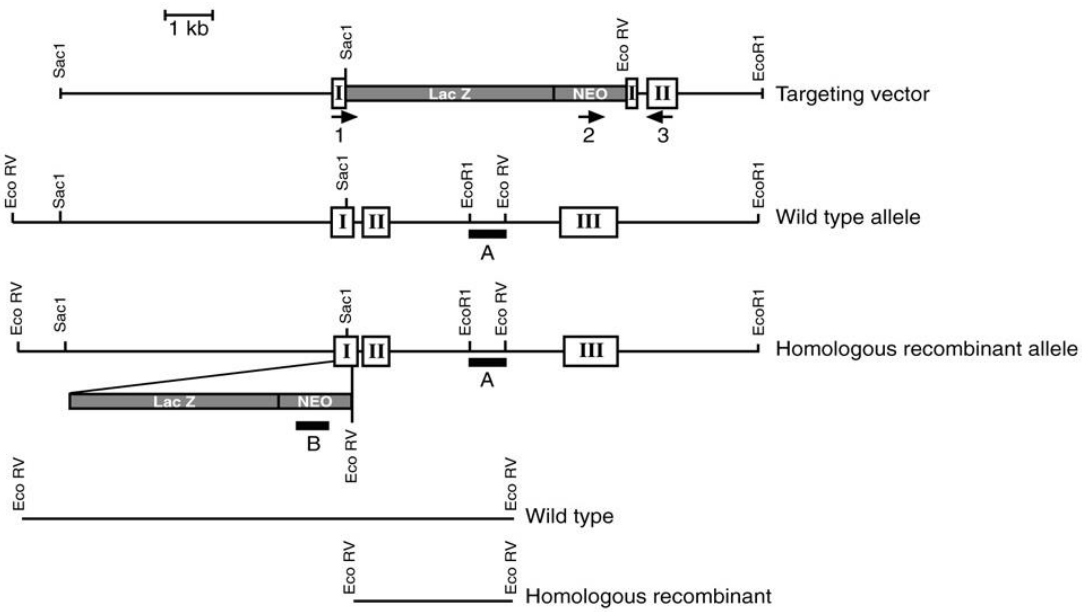

Figure 5. Generation of *Ptx3*$^{-/-}$ mice. An IRES-lacZ cassette followed by the PGK-neomycin resistance gene was integrated in exon 1 of the *Ptx3* gene. Reproduced from *Garlanda et al, Nature, 2002*.

3.3 Genotyping *Ptx3*$^{-/-}$ mice

Tissue samples were acquired from the female mice toes, at postnatal days 5-6 and DNA extraction was performed in order to genotype the animals. For this, samples were placed in an eppendorf tube and 300 µl of NaOH (50 mM) were added to each tube. They were then placed in a thermo-block at 98°C for 50 minutes. After heating, samples were vortexed for around 15 seconds. Then, 30 µl of Tris solution (1 M, pH = 8) were added, to maintain the pH of the solution (around 8.0) and they were centrifuged for 6 minutes at 14,000 rpm. Finally, the supernatant was removed and transferred to a new eppendorf tube.

Next, the DNA of interest was amplified by polymerase chain reaction (PCR). The PCR mix was prepared with 2.2 µl of H_2O, 6 µl of Supreme NZYTaq II 2x Green Master Mix (NZYTech, Lisbon, Portugal) and 0.6 µl of each primer (10 µM) for each reaction. Then, 10 µl of mix and 2 µl of DNA were distributed to each PCR tube. The primers DNA sequence and cycling programs can be observed in Table 1 and Table 2, respectively.

Table 1. Primers' sequence for genotyping *Ptx3*$^{-/-}$ animals and WT littermates.

Genotype	Primer	Primer sequence (5' → 3')
WT	*QI18*	TCCTCGGTGGGATGAAGTCCA
	QI17	AGCAATGCACCTCCCTGCGAT
Ptx3$^{-/-}$	*QI17*	AGCAATGCACCTCCCTGCGAT
	PGK	CTGCTCTTTACTGAAGGCTC

Table 2. Cycling program used in the genotyping of *Ptx3*$^{-/-}$ animals and WT littermates.

Reaction Step	Temperature (ºC)	Time (seconds)	Number of cycles
Initiation	95	300	1
Denaturation	94	30	
Annealing	55	30	30
Extension	72	20	
Final Extension	72	300	1
Arrest	4	∞	

The DNA fragments were visualized in a 1.5% agarose gel, in TAE buffer. Green Safe (NZYTech) was added to the gel to allow the visualization the DNA bands. Results were observed under ultraviolet (UV) light and analysed using the UV transilluminator, Gel Doc™ EZ Imager (Bio-Rad Laboratories, Hercules, CA, USA). From those animals only *Ptx3*$^{-/-}$ and WT animals were selected.

3.4 Experimental Autoimmune Encephalomyelitis Induction

EAE was induced in both *Ptx3*$^{-/-}$ and WT female mice, when they reached 10 weeks of age. For this, a commercially available kit was used, Hooke Kit™ MOG_{35-55}/CFA Emulsion PTX (EK-2110, Hooke Laboratories, MA, USA). Non-induced mice were injected with Hooke Kit™ CFA Emulsion PTX (CK-2110, Hooke Laboratories). Briefly, on day 0, animals were restrained and injected subcutaneously, in the upper and lower back with 100 µl of emulsion per site. Approximately 2 hours later, animals were injected intraperitoneally, with 100 µl of Pertussis Toxin (200 ng/µL) and once again 24h later (Figure 6).

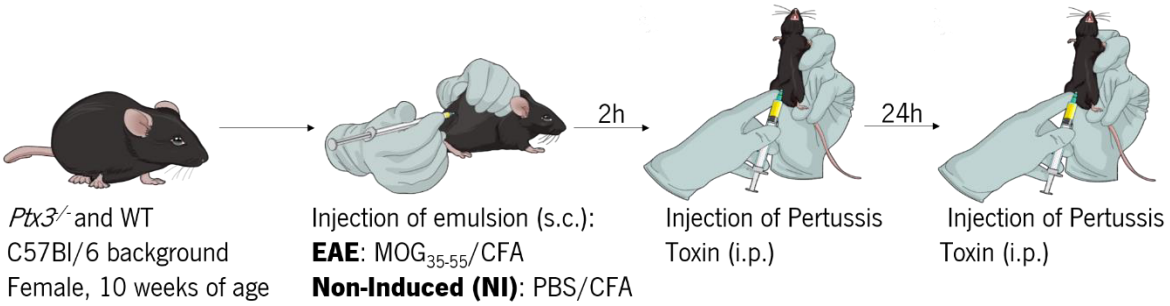

Figure 6. Schematic representation of the EAE induction protocol.

Weight and motor signs of EAE were assessed daily, in a blind manner regarding the animals' genotype. Motor deficits were scored taking into consideration the characteristics described in Table 3. WT littermate animals served as controls, as well as non-induced animals.

Table 3. Clinical score system used to evaluate disease progression in EAE mice.

Score	Description
0	No changes in motor functions compared to non-induced mice.
0.5	Tip of tail is limp.
1	Limp tail. When picked up by the base of the tail, the whole tail drapes over finger.
1.5	When the mouse is dropped on a wire rack, at least one hind limb falls through consistently.
2	Limp tail and weakness of hind limbs. Mouse presents a wobbly walk.
2.5	Limp tail and dragging of hind limbs. Mouse trips on hind feet.
3	Limp tail and paralysis of hind limbs.
3.5	When placed on its side, the mouse is unable to right itself.
4	Limp tail, paralysis of hind limbs and partial front limb paralysis.
4.5	Complete hind limb and front limb paralysis. Mouse is not alert.
5	Dead or moribund state.

3.5 Tissue samples collection and storage

In one experiment animals were sacrificed at the onset phase (peak of disease, day 17) and in another experiment a different cohort of animals were sacrificed in the chronic phase of the disease (day 28). For this, animals were first anesthetized with an intraperitoneal injection of ketamine hydrochloride (150 mg/kg, Imalgene® 1000) and medetomidine hydrochloride (0.3 mg/kg, Dorben®). The effects of anaesthesia were confirmed by toe pinch. When under deep anaesthesia, CSF samples were acquired from the cisterna magna and blood samples were collected from the inferior vena cava. After, mice were transcardially perfused with 0.9% saline solution. The brains were removed from the skull and the spinal cord was also isolated. For RNA extraction, the cerebellum was macrodissected under a conventional light Stereomicroscope (Olympus, Hamburg, Germany) and for the sectioning of this brain region, brains were preserved in optimal cutting temperature (OCT) (Sakura Finetek, Netherlands).

A piece of the tail was also collected in order to extract DNA and confirm the animals' genotype.

3.6 Lesioned area assessment

Brains collected at sacrifice were sectioned at 20 µm, using a Leica CM1950 cryostat (Leica Biosystems, Wetzlar, Germany) and cerebellum sections were selected to assess demyelination, using the Luxol Fast Blue staining protocol. First, slides were fixated in 95% ethanol for 15 minutes and then incubated in 0.5% Luxol Fast Blue MBS (TCS Biosciences, Buckingham, UK) solution, overnight, at 55-56°C. After this, they were rinsed thoroughly with 95% ethanol and also with tap water. Slides were then incubated in 0.05% Lithium Carbonate solution (Sigma Aldrich, MO, USA) for 10 minutes to allow differentiation and then transferred to dH_2O and counterstained with haematoxylin. Finally, sections were let to air dry and mounted with Entellan® mounting medium (Merck Millipore, MA, USA).

The quantification of lesioned areas was performed using an Olympus BX51 Stereology microscope (Olympus) and the Visiopharm Integrator System software v.2.12.3.0 (Visiopharm, Hoersholm, Denmark). The white matter area was outlined using a 4x objective and the lesioned areas using a 10x objective. From each animal, 8 representative sections of the whole cerebellum were evaluated and the percentage of lesioned area was calculated in comparison to that of the total white matter per animal.

3.7 Astrocyte morphology reconstruction

Cerebellum sections, obtained as described above, were selected to assess astrocytic structure in the white matter and for this, immunofluorescence for glial fibrillary acidic protein positive ($GFAP^+$) cells was performed. Briefly, slides were fixated in paraformaldehyde (PFA) 4% for 30 minutes at room

temperature (RT). Then, an antigen retrieval step was performed and for this, slides were placed in a pre-heated citrate buffer for 20 minutes, at the lowest temperature in a microwave. This step was followed by permeabilization in phosphate buffered saline (PBS)-Triton 0.3% for 10 minutes. Then, slides were once again washed and incubated in blocking solution (Fetal Bovine Serum (FBS) 10% in PBS-Triton 0.3%) for 30 minutes in humid chamber. After, slides were incubated with rabbit anti-mouse GFAP polyclonal antibody (1:200 in blocking solution; DAKO, Agilent, CA, USA) overnight in humid chamber. Slides were then washed in PBS-Triton 0.3% and incubated with donkey anti-rabbit 594 antibody (1:500 in PBS-Triton 0.3%; Life Technologies, CA, USA) for 2 hours in humid chamber. This step was followed by another washing step with PBS-Triton 0.3%. Finally, in order to stain the cell nucleus, slides were incubated with DAPI (1:200; Invitrogen, CA, USA) for 10 min and after another washing step, they were mounted with Immumount (ThermoFisher Scientific, MA, USA). In order to perform the 3D reconstruction of astrocytes in these slides, the Z-Stack of confocal images was obtained using an Olympus FV1000 Confocal microscope (Olympus). Then, 6 astrocytes were reconstructed per animal, using the Simple Neurite Tracer plugin of the Fiji-ImageJ software and their total process length and sholl analysis were performed, as previously described (Tavares et al., 2017).

3.8 Gene Expression Analysis

3.8.1 RNA Extraction

To extract RNA from the cerebellum samples, 1 mL of TRIzol (Invitrogen) was added to the tubes containing the samples. Then, using a 1 mL syringe and a 20G needle, tissue was mechanically disrupted. Afterwards, samples were incubated for 5 minutes, at RT to allow the complete dissociation of the nucleoprotein complex. Next, 200 µl of chloroform were added to all samples, mixed vigorously and incubated for 3 minutes at RT. Samples were then centrifuged at 8,000 rpm for 15 minutes at 4°C. After this, 3 distinct phases were obtained - an upper colourless aqueous phase that contained the RNA, an interphase, containing the DNA and a lower red phenol-chloroform phase that contained proteins.

The upper phase was carefully removed and placed in a new eppendorf tube. Then, 500 µl of isopropanol were added to the tube containing the RNA and incubated at RT for 10 minutes. Samples were then centrifuged at 9,000 rpm for 10 minutes at 4°C, allowing an RNA precipitate to form.

The supernatant was discarded and the pellet was washed in 40 µl of 75% ethanol and centrifuged at 5,000 rpm for 7 minutes at 4°C. Again, the supernatant was discarded and the pellet was left to air dry. Finally, it was ressuspended in 20 µl of RNAse free water.

The RNA sample obtained was quantified using the Nanodrop® ND-1000 Spectrophotometer (ThermoFisher Scientific), diluted to a final concentration of approximately 1,000 ng/µl and stored at -80°C for further use.

3.8.2 DNAse Treatment

DNAse treatment allows the elimination of contaminant genomic DNA from the samples. This is an important step because if the genomic DNA is not eliminated it can be amplified along with complementary DNA (cDNA) during quantitative Real Time-PCR (qRT-PCR), leading to false positive results.

For that, we added to an RNAse free tube, 1 µl of buffer with $MgCl_2$, 4 µl of DNAse I (ThermoFisher Scientific), 4 µl of RNA and 1 µl DEPC-treated water. Samples were incubated at 37°C for 30 minutes. Then, DNAse activity was inhibited to avoid cDNA degradation and for this 1 µl of EDTA (50 mM) was added to the samples and they were incubated for 10 minutes at 65°C. At the end, samples were quantified again using the Nanodrop® ND-1000 Spectrophotometer (ThermoFisher Scientific).

3.8.3 cDNA synthesis

Synthesis of cDNA consists in the reverse transcription of an RNA template into a molecule of cDNA, through the use of a reverse transcriptase. The cDNA can then be used as a template for qRT-PCR, allowing us to analyse gene expression levels in a specific tissue.

The iScript™ cDNA Synthesis Kit (Bio-Rad Laboratories) was used in the synthesis process. For that, for each sample, 4 µl of iScript Reaction Mix (5x) (which contains buffers, dNTPs and primers that allow the optimization of the reverse transcriptase activity) were mixed with 1 µl of iScript Reverse Transcriptase, 1 µg of RNA and finally, nuclease-free water, until a final volume of 20 µl. The PCR tubes were placed in a thermocycler. The cycling program is presented in Table 4. Samples were stored at -20°C until use for qRT-PCR.

Table 4. Cycling program used for the synthesis of cDNA.

Reaction Step	Temperature (ºC)	Time (minutes)
Priming	25	5
Reverse Transcription	46	20
RT Inactivation	95	1
Hold	4	∞

3.8.4 qRT-PCR Reaction

In order to evaluate the expression of the genes of interest a qRT-PCR reaction was performed. For the analysis of the cDNA obtained from animals sacrificed in the onset phase of disease, the 5x HOT FIREPol EvaGreen® qPCR Mix Plus (ROX) (Solis Biodyne, Tartu, Estonia) was used. First, for a reaction volume of 20 µl, 14 µl of H_2O, 4 µl of 5x HOT FIREPol EvaGreen® qPCR Mix and 0.5 µl of each primer (reverse and forward) were mixed in an eppendorf tube. This mix was made for each gene of interest, using the corresponding primers. Then, 19 µl of the mix were distributed to each well of a 96-well plate and 1 µl of the cDNA samples was added. The qRT-PCR reaction was performed in an Applied Biosystems 7500 Fast qPCR thermocycler (Applied Biosystems, CA, USA) and the data obtained was analysed with the 7500 Software v2.3 (Applied Biosystems). The cycling program used in this assessment is presented in Table 5.

Table 5. Cycling program used in the qRT-PCR reaction for the analysis of samples obtained in the onset phase of disease.

	Reaction Step	Temperature (ºC)	Time (seconds)	Number of cycles
5x HOT FIREPol EvaGreen® qPCR Mix	Initiation	95	900	1
	Denaturation	95	15	1
	Annealing	Primer Specific (See table 7)	20	39
	Extension	72	30	1
	Melting Curve	95	15	1
		60	60	
		95	30	
		60	15	

For the analysis of cDNA obtained from animals sacrificed in the chronic phase of disease, the SsoFast™ EvaGreen® supermix (Bio-Rad Laboratories) was used. Briefly, for a reaction volume of 10 µl, 3 µl of H_2O, 5 µl of SsoFast™ EvaGreen® supermix and 0.5 µl of each primer (reverse and forward) were mixed in an eppendorf tube. Again, this mix was made for each gene of interest, using the corresponding primers. Then, 9 µl of the mix were distributed to each well of a 96-well plate and 1 µl of the cDNA samples was added. The qRT-PCR reaction was performed in a CFX 96TM real-time system instrument (Bio-Rad Laboratories). The cycling program used in this assessment is presented in Table 6.

Table 6. Cycling program used in the qRT-PCR reaction for the analysis of samples obtained in the chronic phase of disease.

	Reaction Step	Temperature (ºC)	Time (seconds)	Number of cycles
SsoFast™ EvaGreen® supermix	Initiation	95	60	1
	Denaturation	95	15	
	Annealing	Primer Specific (See table 7)	20	39
	Extension	72	20	
	Melting Curve	65 - 95	5	1

All melting curves exhibited a sharp peak at the expected temperature. The reference genes, used as internal standard for the normalization of the expression levels of the genes of interest, were adenosine triphosphate synthase subunit beta (Atp5b) and Heat Shock Protein class beta (Hspcb). The primers DNA sequence are presented in Table 7.

Table 7. List of genes that were amplified by qRT-PCR, respective primer DNA sequence, annealing temperature and GenBank™ accession number.

Gene Symbol	Primers (5' → 3')		Annealing Temperature (ºC)	GenBank™ accession number
Atp5b	Forward	GGCCAAGATGTCCTGCTGTT	60	NM_016774.3
	Reverse	GCTGGTAGCCTACAGCAGAAGG		
Fbln5	Forward	CTTCAGATGCAAGCAACAA	60	NM_001361987.1
	Reverse	AGGCAGTGTCAGAGGCCTTA		
Gfap	Forward	AAACCGCATCACCATTCCTG	60	NM_001131020.1
	Reverse	TCTGGTGAGCCTGTATTGGG		
Hspcb	Forward	GCTGGCTGAGGACAAGGAGA	60	NM_008302.3
	Reverse	CGTCGGTTAGTGGAATCTTCATG		
Iba1	Forward	GAAGCGAATGCTGGAGAAAC	60	NM_001361501.1
	Reverse	CTCATACATCAGAATCATTCTC		
Ifng	Forward	ACTGGCAAAAGGATGGTGAC	58	NM_008337.3
	Reverse	TGAGCTCATTGAATGCTTGG		

Table 7. List of genes that were amplified by qRT-PCR, respective primer DNA sequence, annealing temperature and GenBank™ accession number (continued).

Gene Symbol		Primers (5' → 3')	Annealing Temperature (ºC)	GenBank™ accession number
Il4	Forward	GTCACAGGAGAAGGGACGCCAT	58	NM_021283.2
	Reverse	AGCCTTACAGACGAGCTCACTC		
Il6	Forward	CCGGAGAGGAGACTTCACAG	59	NM_031168.2
	Reverse	TCCACGATTTCCCAGAGAAC		
Il12 (p35)	Forward	GTGTCTTAGCCAGTCCCGAA	59	NM_008351.3
	Reverse	TTCAAGTCCTCATAGATGCTACCA		
Il17a	Forward	GGACTCTCCACCGCAATGAA	58	NM_010552.3
	Reverse	CATGTGGTGGTCCAGCTTTC		
iNos	Forward	CTCGGAGGTTCACCTCACTGT	59	NM_010927.4
	Reverse	GCTGGAAGCCACTGACACTT		
Lcn2	Forward	CCAGTTCGCCATGGTATTTT	58	NM_008491.1
	Reverse	GGTGGGGACAGAGAAGATGA		
Mhc2	Forward	GAG CAT CCC AGC CTG AAG A	60	NM_207105.3
	Reverse	CGA TGC CGC TCA ACA TCT T		
S100a10	Forward	CCTCTGGCTGTGGACAAAAT	60	NM_009112.2
	Reverse	CTGCTCACAAGAAGCAGTGG		

3.9 Patient Population

For the human studies, DNA and serum samples from MS patients were obtained from the small existent MS biobank (in collaboration with Dr. João Cerqueira at Hospital of Braga), containing currently 182 samples from MS patients and controls. Samples were obtained from patients admitted for lumbar puncture in the Hospital of Braga. These patients were diagnosed with either RRMS, PPMS or CIS, according to the McDonald 2010 criteria (dissemination in space and time). Of the CIS patients, some progressed to MS since sample collection. Controls were healthy individuals of similar age and gender as cases. The studies with human serum and DNA were approved by the ethical committee of Hospital of Braga and all patients signed an informed consent. The anonymity of all participants and the confidentiality of the information are protected according to the Portuguese law and EU directives. The

demographic information of the patients and healthy controls used for the ELISA assessment are presented in Table 8 and of those used for PTX3 SNP genotyping are presented in Table 9.

Table 8. Demographic data of healthy controls and patients whose serum samples were used in the ELISA.

Variables	Healthy Controls (n = 40)	MS Patients (n = 66)
Age – no (%)		
≤40 years	25 (62.5)	41 (62.1)
>40 years	15 (37.5)	25 (37.9)
Gender – no (%)		
Female	28 (70)	47 (72.5)
Male	12 (30)	19 (27.5)
MS Type – no (%)		
CIS	-	5 (7.6)
RRMS	-	51 (77.3)
PPMS	-	10 (15.1)

Table 9. Demographic data of healthy controls and patients whose DNA samples were used for SNP genotyping.

Variables	Healthy Controls (n = 215)	MS Patients (n = 48)
Age – no (%)		
≤40 years	90 (41.9)	29 (60.4)
>40 years	56 (26.0)	19 (39.6)
Gender – no (%)		
Female	89 (41.4)	35 (72.9)
Male	57 (26.5)	13 (27.1)
MS Type – no (%)		
CIS	-	5 (10.4)
RRMS	-	35 (72.9)
PPMS	-	8 (16.7)
Demographic data not available	69 (32.1)	

3.10 Patient Genotyping

SNPs in the *PTX3* gene with minor allele frequencies ≥0.05 were selected as previously described (Cunha et al., 2014). For the patient genotyping of the rs2305619 and rs3816527 SNPs, a commercial kit, KASpar Assay, was used (LCG Genomics, Hertfordshire, UK). Initially, all components were thoroughly vortexed. Then, the genotyping mix, which contained 5 µl of 2 x KASP Master mix and 0.14 µl of the KASP Assay mix, was prepared for each sample. After preparation, 5 µl of this genotyping mix were distributed to each well of a qPCR-compatible 96-well plate along with 5 µl of each DNA (1.25 ng/µl) sample. Non-template control (NTC) wells were also present, to control for contaminations. The cycling program is represented in Table 10. Bi-allelic discrimination was performed in an Applied Biosystems 7500 Fast qPCR thermocycler (Applied Biosystems) and the thermal cycle was completed by an end-

point fluorescence reading at 25°C for 1 minute. The data obtained was analysed with the 7500 Software v2.3 (Applied Biosystems).

Table 10. Cycling program used in the KASP reaction.

Reaction Step	Temperature (°C)	Time (seconds)	Number of cycles
Activation	94	900	1
Denaturation	94	20	10 (-0.6°C/cycle)
Annealing/Elongation	61-55	60	
Denaturation	94	20	26
Annealing/Elongation	55	60	
Post-PCR read	94	20	3
	57	60	

3.11 PTX3 serum levels quantification

PTX3 in human serum samples was quantified by enzyme linked immunosorbent assay (ELISA) using the Human PTX3/TSG-14 DuoSet ELISA (R&D Systems, MN, USA), according to the manufacturer's instructions. Firstly, the capture antibody was diluted to the working concentration using PBS and then, 100 µl were used per well to coat a 96-well microplate. The plate was sealed and left to incubate overnight at RT. After, each well was washed three times using a squirt bottle with Tween 20 0.05% in PBS, pH 7.2-7.4. The plate was blocked by adding 300 µl of 1% bovine serum albumin (BSA, Sigma-Aldrich) in PBS to each well and let to incubate for 1h at RT. The washing step was repeated and then 100 µl of the standards or sample (undiluted) were added to each well and let to incubate, at RT for 2 hours. Again, the washing steps were repeated and 100 µl of 1:40 streptavidin-horseradish peroxidase (HRP) were added. The plate was sealed and incubated for 20 minutes at RT and once again, it was washed three times with the same washing solution. After, 100 µl of 1x eBioscience™ TMB Solution (ThermoFisher Scientific), were added to each well and incubated at RT for 20 min. Finally, 50 µl of stop solution (H_2SO_4, 2 N) were added and the plate gently tapped to ensure thorough mixing.

The optical density of each well was determined using a microplate reader set to 450 nm.

3.12 Statistical Analysis

Results were analysed using the GraphPad Prism® software v.6.01 (GraphPad Software, San Diego, CA, USA) and IBM SPSS Statistics v.25 (IBM Corp., Armonk, NY, USA). Statistical significance was

considered for $p < 0.05$. For the animal experiments, where clinical score/weight were evaluated a repeated measures (RM) two-way ANOVA was used to compare between groups and their evolution through time. For the assessment of gene expression and astrocytic structure, a two-way ANOVA was used to compare between Non-Induced WT/*Ptx3*$^{-/-}$ and EAE WT/*Ptx3*$^{-/-}$. Differences between groups were determined by Bonferroni's multiple comparison test post hoc analysis. To compare disease measurements (first clinical score (higher than 0), maximum score, day of appearance of first symptoms and day of score 3) and the percentage of lesioned area between WT and *Ptx3*$^{-/-}$ mice, a t-test for independent samples was used. To assess the association between *PTX3* genetic variants and MS susceptibility, a case-control study was performed by using the Chi-Squared test.

The normality assumptions were evaluated for all datasets. All data is presented as mean ± Standard Error of Mean (SEM) and as an average of all experiments. Effect size was calculated using the Cohen's d or $\eta^2_{partial}$.

4. Results

4.1 *Ptx3* is expressed in WT mice cerebellum under pathological conditions

In order to understand if *Ptx3* is expressed during EAE disease course, we decided to analyse the expression of this gene in the cerebellum of EAE animals. Firstly, we confirmed that this gene is not expressed in *Ptx3*$^{-/-}$ mice, as expected. Then, we observed that this gene is also not expressed in WT mice under normal conditions, confirming the role of PTX3 as an acute phase protein (Figure 7). The results from the two-way ANOVA analysis are presented in Table 11.

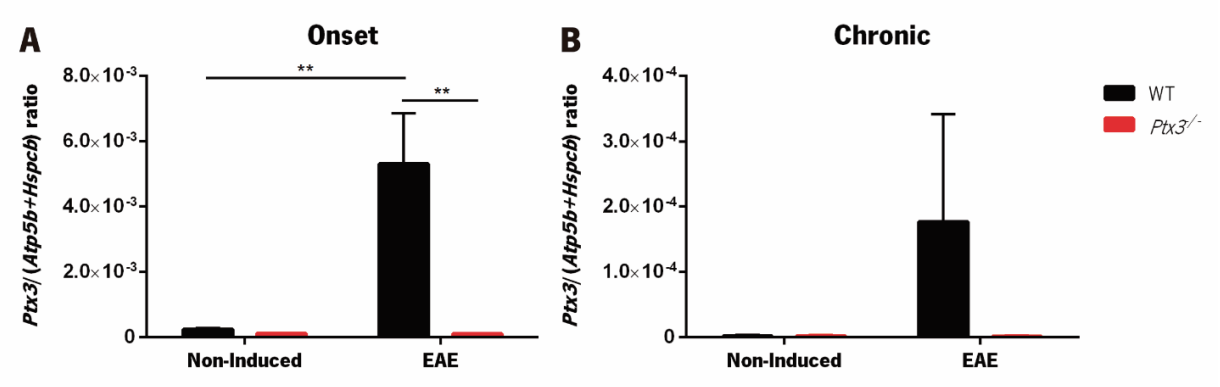

Figure 7. *Ptx3* is only expressed in EAE WT mice. During both the onset (A) and chronic (B) phases of disease, *Ptx3* is only expressed in WT EAE mice, confirming that the knockout of this gene in these mice is effective. Besides, *Ptx3* in not expressed in WT mice under normal conditions, supporting the activation of this molecule only under pathological conditions. (Onset: $n_{\text{Non-Induced WT}} = 7$, $n_{\text{Non-Induced } Ptx3^{-/-}} = 6$, $n_{\text{EAE WT}} = 7$, $n_{\text{EAE } Ptx3^{-/-}} = 6$. Chronic: $n_{\text{Non-Induced WT}} = 6$, $n_{\text{Non-Induced } Ptx3^{-/-}} = 6$, $n_{\text{EAE WT}} = 6$, $n_{\text{EAE } Ptx3^{-/-}} = 5$). Data presented as mean ± SEM. ** $p < 0.01$).

Table 11. Results from the two-way ANOVA analysis used for the comparison of *Ptx3* gene expression between *Ptx3*$^{-/-}$ and WT mice.

			Mean ± SEM	Disease Factor	Genotype Factor	Interaction
Onset	WT	Non-Induced	2.4e-4 ± 3.8e-5	$F_{(1,22)} = 8.900$, $p = 0.007$, $\eta^2_{\text{partial}} = 0.174$	$F_{(1,22)} = 9.892$, $p = 0.005$, $\eta^2_{\text{partial}} = 0.193$	$F_{(1,22)} = 8.951$, $p = 0.007$, $\eta^2_{\text{partial}} = 0.175$
		EAE	5.3e-3 ± 1.6e-3			
	Ptx3$^{-/-}$	Non-Induced	1.2e-4 ± 2.2e-5			
		EAE	1.1e-4 ± 2.1e-5			
Chronic	WT	Non-Induced	1.7e-6 ± 1.7e-6	$F_{(1,19)} = 1.013$, $p = 0.327$, $\eta^2_{\text{partial}} = 0.046$	$F_{(1,19)} = 1.023$, $p = 0.325$, $\eta^2_{\text{partial}} = 0.046$	$F_{(1,19)} = 1.023$, $p = 0.325$, $\eta^2_{\text{partial}} = 0.046$
		EAE	1.8e-4 ± 1.6e-4			
	Ptx3$^{-/-}$	Non-Induced	1.7e-6 ± 1.7e-6			
		EAE	1.3e-6 ± 9.3e-7			

4.2 PTX3 does not affect disease clinical score in mice

After EAE induction, the animals were observed daily in order to assess motor deficits and weight variations. In order to better understand the potential role of PTX3 in a more active phase of disease a cohort of animals was induced with EAE, and these animals were sacrificed in the onset phase of disease, which corresponded to day 17 after immunization. In this experiment, mice started developing symptoms at around day 12 (Figure 8A), around the same time as weight loss started (Figure 8B). In another experiment, animals induced with EAE were let to reach the chronic phase of disease, in order to understand the impact of this protein in later stages of EAE. In this case, both WT and *Ptx3*$^{-/-}$ mice developed a chronic disease course, as expected, with symptoms first appearing around day 13 (Figure 8C), again correlating with the start of weight loss (Figure 8D). Then, both groups reached the peak of disease at day 17 and were sacrificed at day 28, when the chronic phase was already installed.

Two *Ptx3*$^{-/-}$ and one WT mice from the onset experiment and two *Ptx3*$^{-/-}$ mice from the chronic experiment did not develop EAE symptoms and were, therefore, excluded from the data analysis.

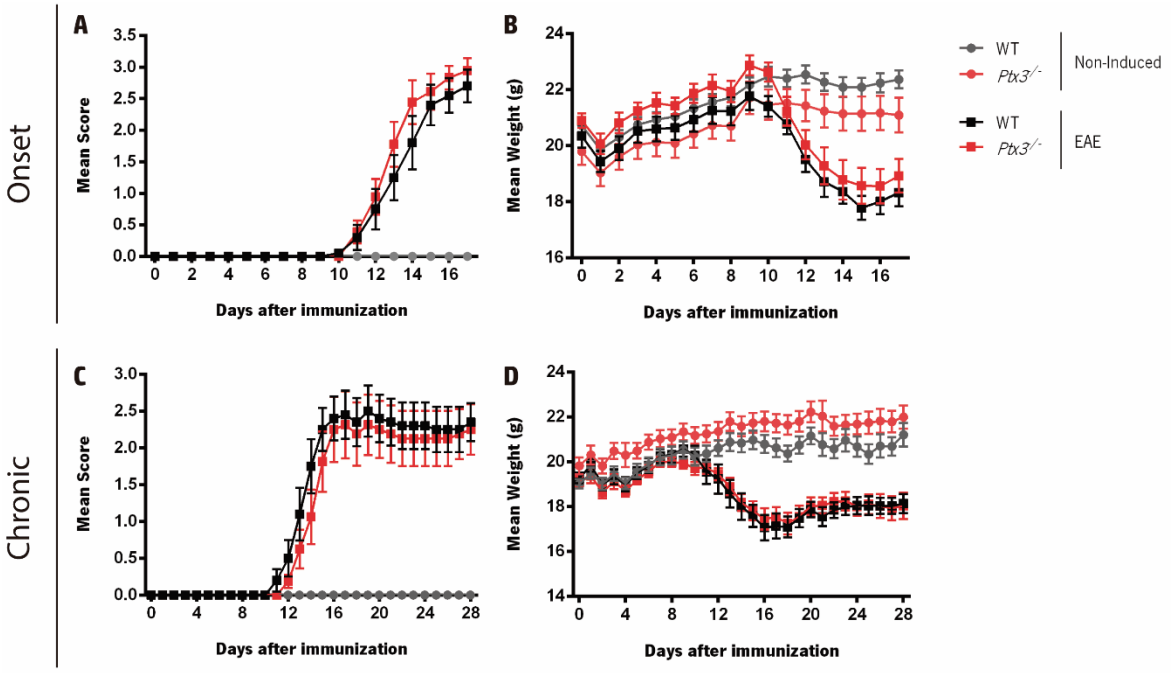

Figure 8. Disease course of MOG_{35-55} induced WT and *Ptx3*$^{-/-}$ mice. (A) EAE WT and *Ptx3*$^{-/-}$ mice presented a similar disease course with symptoms first appearing at around day 12 in both groups. Animals were sacrificed at the onset phase of disease, which corresponded to day 17 after immunization. (B) Animals started to lose weight from the appearance of clinical symptoms (C) Another cohort of animals were let to reach the chronic phase of disease. In this case, EAE WT and *Ptx3*$^{-/-}$ mice also presented a similar disease course, with symptoms first appearing at day 13. After the onset of disease at day 17 in both groups, the animals presented a chronic disease course, until sacrifice, which occurred at day 28. (D) Both groups of animals started to lose weight from the moment

of appearance of clinical symptoms. (A and B: $n_{Non\text{-}Induced\ WT}$=11; $n_{Non\text{-}Induced\ Ptx3^{-/-}}$=10; $n_{EAE\ WT}$=10; $n_{EAE\ Ptx3^{-/-}}$=9; C and D: $n_{Non\text{-}Induced\ WT}$=10; $n_{Non\text{-}Induced\ Ptx3^{-/-}}$=10; $n_{EAE\ WT}$=10; $n_{EAE\ Ptx3^{-/-}}$=8. Data presented as mean ± SEM).

No differences were found between genotypes in what concerns clinical score or weight. The data from the RM two way ANOVA performed to analyse score is presented in Table 12 and the one performed to analyse weight is presented in Table 13.

Table 12. Results from the RM two-way ANOVA analysis used for the comparison of clinical score evolution between *Ptx3*$^{-/-}$ and WT mice.

			Mean ± SEM	Disease Factor	Genotype Factor	Interaction
Onset	WT	Non-Induced	0 ± 0	$F_{(1, 36)}$ = 111,076, p < 0.0001, $\eta^2_{partial}$ = 0.755	$F_{(1, 36)}$ = 0.771, p = 0.386, $\eta^2_{partial}$ = 0.021	$F_{(1, 36)}$ = 0.771, p = 0.386, $\eta^2_{partial}$ = 0.021
		EAE	0.69 ± 0.13			
	Ptx3$^{-/-}$	Non-Induced	0 ± 0			
		EAE	0.82 ± 0.11			
Chronic	WT	Non-Induced	0 ± 0	$F_{(1, 34)}$ = 91.031, p < 0.0001, $\eta^2_{partial}$ = 0.728	$F_{(1, 34)}$ = 0.339, p = 0.564, $\eta^2_{partial}$ = 0.010	$F_{(1, 34)}$ = 0.339, p = 0.564, $\eta^2_{partial}$ = 0.010
		EAE	1.21 ± 0.19			
	Ptx3$^{-/-}$	Non-Induced	0 ± 0			
		EAE	1.07 ± 0.21			

Table 13. Results from the RM two-way ANOVA analysis used for the comparison of weight variation between *Ptx3*$^{-/-}$ and WT mice.

			Mean ± SEM	Disease Factor	Genotype Factor	Interaction
Onset	WT	Non-Induced	21.65 ± 0.31	$F_{(1, 36)}$ = 4.185, p = 0.048, $\eta^2_{partial}$ = 0.104	$F_{(1, 36)}$ = 0.06, p = 0.808, $\eta^2_{partial}$ = 0.002	$F_{(1, 36)}$ = 4.188, p = 0.048, $\eta^2_{partial}$ = 0.104
		EAE	19.95 ± 0.44			
	Ptx3$^{-/-}$	Non-Induced	20.70 ± 0.59			
		EAE	20.70 ± 0.46			
Chronic	WT	Non-Induced	20.39 ± 0.39	$F_{(1, 34)}$ = 41.722, p < 0.001, $\eta^2_{partial}$ = 0.551	$F_{(1, 34)}$ = 1.692, p = 0.202, $\eta^2_{partial}$ = 0.047	$F_{(1, 34)}$ = 2.051, p = 0.161, $\eta^2_{partial}$ = 0.057
		EAE	18.61 ± 0.41			
	Ptx3$^{-/-}$	Non-Induced	21.36 ± 0.44			
		EAE	18.56 ± 0.36			

Subsequent analysis of specific measurements, namely first clinical score (higher than 0), maximum score, day of appearance of first symptoms and day of score 3, displayed no difference between genotypes, in either of the experiments (Table 14).

Table 14. EAE progression in WT and *Ptx3*$^{-/-}$ mice when sacrificed in the chronic and onset phase.

	Group	1st Clinical Score ± SEM (n)	Maximum Score ± SEM (n)	Day of First Symptoms ± SEM (n)	Day of score 3 ± SEM (n)	Disease Incidence (%)
Onset	WT	0.6 ± 0.1 (10)	2.6 ± 0.29 (10)	12.5 ± 0.54 (10)	14.7 ± 0.67 (6)	10/11 (91%)
	Ptx3$^{-/-}$	0.8 ± 0.14 (9)	2.8 ± 0.19 (9)	12.1 ± 0.45 (9)	14.0 ± 0.22 (7)	9/11 (82%)
	t test value	$t_{(17)} = 1.352$	$t_{(17)} = 0.666$	$t_{(17)} = 0.542$	$t_{(11)} = 1.015$	
	p value	$p = 0.194$	$p = 0.515$	$p = 0.595$	$p = 0.332$	
	Cohen's *d*	$d = 0.615$	$d = 0.309$	$d = 0.252$	$d = 0.547$	
Chronic	WT	0.9 ± 0.2 (10)	2.9 ± 0.21 (10)	12.8 ± 0.44 (10)	15.3 ± 0.53 (8)	10/10 (100%)
	Ptx3$^{-/-}$	0.5 ± 0.0 (8)	2.5 ± 0.39 (8)	13.9 ± 0.88 (8)	15.8 ± 0.40 (6)	8/10 (80%)
	t test value	$t_{(16)} = 1.697$	$t_{(16)} = 0.958$	$t_{(16)} = 1.166$	$t_{(12)} = 0.8298$	
	p value	$p = 0.109$	$p = 0.352$	$p = 0.261$	$p = 0.423$	
	Cohen's *d*	$d = 0.854$	$d = 0.441$	$d = 0.537$	$d = 0.460$	

4.3 Lesioned area pattern of the cerebellum of *Ptx3*$^{-/-}$ mice

Considering that in MS, both patients and its animal model present inflammatory infiltrates in several brain areas, we proposed to evaluate the levels of these lesioned sites in the cerebellum of the EAE mice, using the Luxol Fast Blue staining protocol. The analysis was performed on 4 animals per group, except for the *Ptx3*$^{-/-}$ group, in the chronic phase, were 1 animal was eliminated from the analysis as it did not present lesions. Representative sections of the cerebellum of non-induced and EAE mice are presented in Figure 9A. In order to obtain the percentage of lesioned area, the sum of all lesions was multiplied by 100 and divided by the total white matter per animal. Interestingly, we observed that *Ptx3*$^{-/-}$ mice seem to present a lower percentage of lesions when compared to WT mice in both the onset and chronic phases of disease. However these differences are not statistically significant neither in the onset (WT = 8.213 ± 2.325, *Ptx3*$^{-/-}$ = 3.960 ± 0.8379, $t_{(6)} = 1.721$, $p = 0.1361$, Cohen's $d = 1.22$) (Figure 9B) nor in the chronic phases (WT= 2.035 ± 0.2633, *Ptx3*$^{-/-}$ = 1.273 ± 0.2223, $t_{(5)} = 2.099$, $p = 0.0899$, Cohen's $d = 1.65$) of disease (Figure 9C). Moreover, it can be observed that in the onset phase there is a higher percentage of lesions in both groups than in the chronic phase.

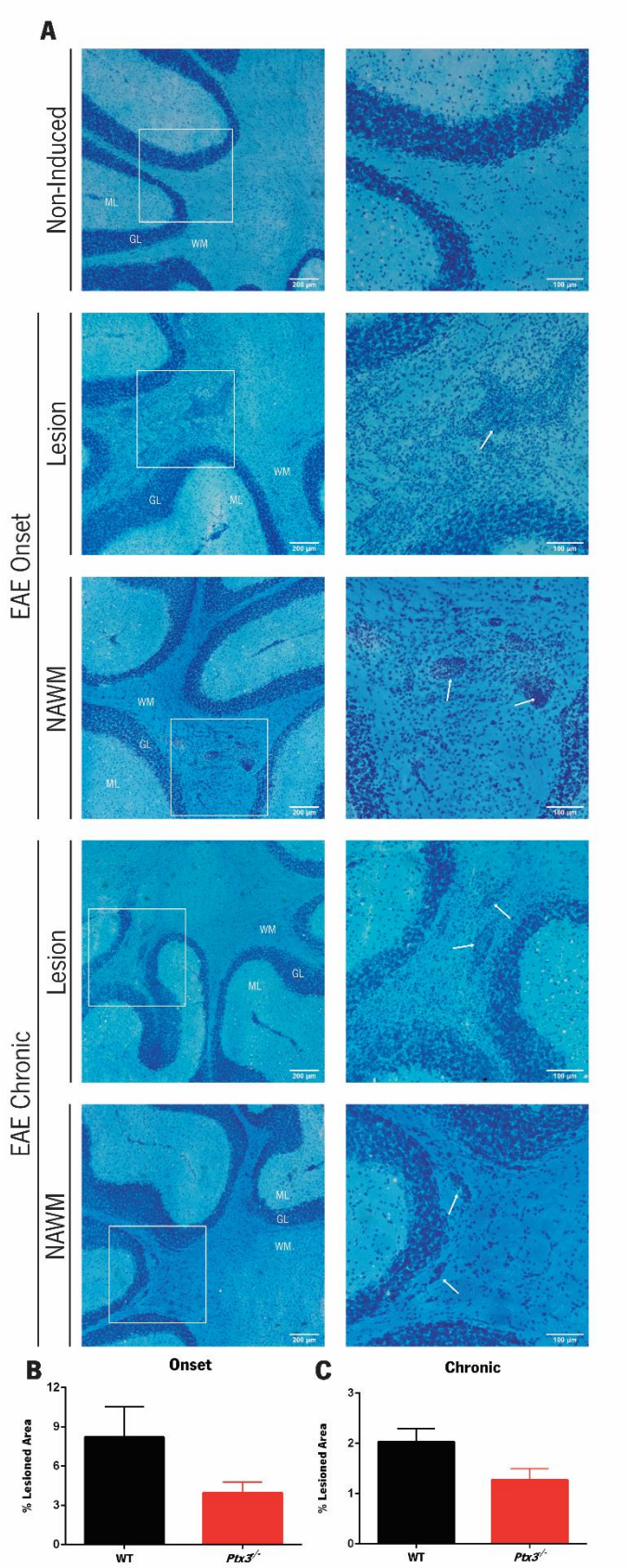

Figure 9. Evaluation of the percentage of lesioned area in the cerebellum of EAE mice. (A) The cerebellum of EAE animals presents inflammatory infiltrates that are not observed in the cerebellum of healthy animals. These infiltrates, or lesions (arrows), are characterized as areas that have a higher cell density and a

lighter blue background and can be observed through staining with Luxol Fast Blue, a dye that marks myelin. (ML – Molecular layer, GL – Granular layer, WM – White Matter; Left panel: Images acquired with the 4x objective, bar = 200 μm, Right panel: Images acquired with the 10x objective, bar = 100 μm) (B) Although not statistically significant, in the onset phase, *Ptx3*$^{-/-}$ mice seem to have a lower percentage of lesioned area when compared to WT mice ($n_{Onset\ WT}$ = 4, $n_{Onset\ Ptx3^{-/-}}$ = 4) (C) Accordingly, in the chronic phase, *Ptx3*$^{-/-}$ mice present a lower percentage of lesions in the cerebellum when compared to WT mice. Furthermore, in this phase both groups of animals' present lower percentages of lesions than in the onset phase. $n_{Chronic\ WT}$ = 4, $n_{Chronic\ Ptx3^{-/-}}$ = 3. Data presented as mean ± SEM.

4.4 Inflammatory cytokine expression varies during disease course

Considering the fact that *Ptx3*$^{-/-}$ mice have a tendency for a lower percentage of inflammatory infiltrates when compared to WT littermate controls, we tried to further understand this effect at a molecular level. For this, we proceed to the analysis of the expression of inflammatory molecules in the cerebellum of these animals both in the onset and in chronic phases of disease. No major statistically significant differences were observed, in the expression levels of the different immune mediators between the two genotypes in either phase of disease. Interestingly, however, in the onset phase of disease, we observed an increased expression of *Il6* (Figure 10A) and *Il17a* (Figure 10B), which are involved in the Th17 response, in EAE mice when compared to non-induced controls. In addition, in EAE mice we also observed increased levels of *Il12(p35)* (Figure 10C) and interferon-gamma *(Ifng)* (Figure 10D), which are important mediators of the Th1 response. This increased expression of *Il6* (Figure 10F) and *Il17a* (Figure 10G), in EAE animals when compared to non-induced controls, remained present in the chronic phase disease. On the other hand, the expression of *Il4* does not seem to be affected by either genotype or phase of disease (Figure 10E and J). The results from the two-way ANOVA test are presented in Table 15.

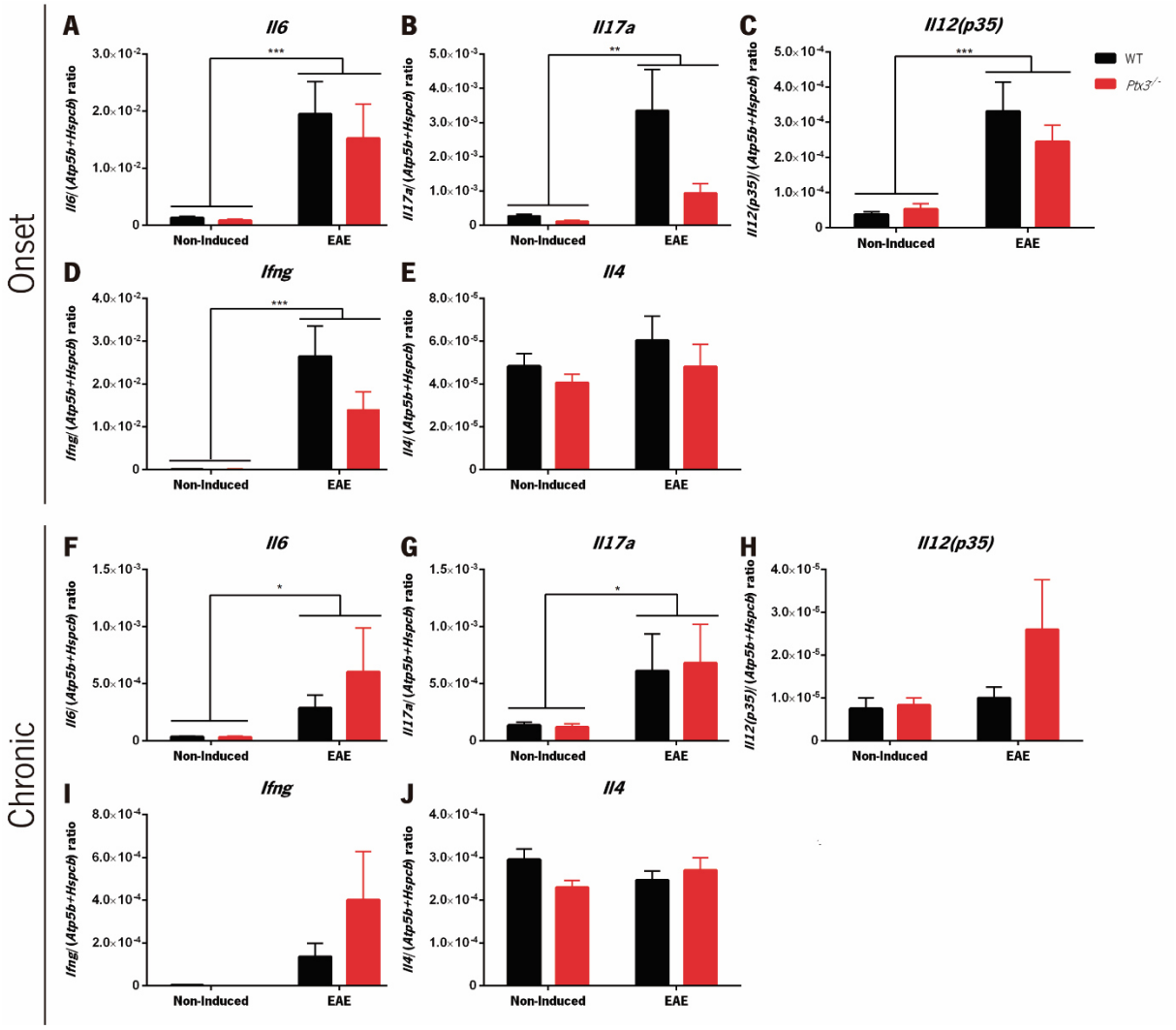

Figure 10. Expression levels of inflammatory cytokines in the cerebellum of EAE mice. During the onset phase of disease, both *Il6* (A) and *Il17a* (B) are increased in EAE mice when compared to non-induced animals. These molecules are also increased in the chronic phase (F and G, respectively). Furthermore, *Il12(p35)* (C) and *Ifng* (D) have an increased expression in EAE animals when compared to non-induced controls, in the onset phase of disease. *Il4* seems to maintain stable levels of expression between genotypes and does not present different expression levels between EAE and control animals, in either time point (E and J). (Onset: $n_{\text{Non-Induced WT}} = 7$, except for *Il12*, where one animal did not present detectable levels; $n_{\text{Non-Induced } Ptx3^{-/-}} = 6$; $n_{\text{EAE WT}} = 7$, except for *Il4* where one animal did not present detectable levels; $n_{\text{EAE } Ptx3^{-/-}} = 6$. Chronic: $n_{\text{Non-Induced WT}} = 6$, except for *Il12* where two animals did not present detectable levels; $n_{\text{Non-Induced } Ptx3^{-/-}} = 6$; $n_{\text{EAE WT}} = 6$; $n_{\text{EAE } Ptx3^{-/-}} = 5$. Data presented as mean ± SEM. * $p < 0.05$, ** $p < 0.01$, *** $p < 0.001$).

Table 15. Results from the two-way ANOVA analysis used for the comparison of cytokine gene expression in the cerebellum, between *Ptx3*$^{-/-}$ and WT mice.

				Mean ± SEM	Disease Factor	Genotype Factor	Interaction
Onset	*Il6*	WT	Non-Induced	1.31e3 ± 2.58e-4	$F_{(1,22)}$ = 15.52, p = 0.0007, $\eta^2_{partial}$ = 0.404	$F_{(1,22)}$ = 0.327, p = 0.5735, $\eta^2_{partial}$ = 0.009	$F_{(1,22)}$ = 0.214, p = 0.6482, $\eta^2_{partial}$ = 0.006
			EAE	1.95e-2 ± 5.67e-3			
		Ptx3$^{-/-}$	Non-Induced	8.60e-4 ± 2.08e-4			
			EAE	1.52e-2 ± 5.98e-3			
	Il17a	WT	Non-Induced	2.74e-4 ± 4.81e-5	$F_{(1,22)}$ = 3.755, p = 0.007, $\eta^2_{partial}$ = 0.228	$F_{(1,22)}$ = 3.755, p = 0.066, $\eta^2_{partial}$ = 0.098	$F_{(1,22)}$ = 2.911, p = 0.102, $\eta^2_{partial}$ = 0.076
			EAE	3.35e-3 ± 1.19e-3			
		Ptx3$^{-/-}$	Non-Induced	1.21e-4 ± 2.62e-5			
			EAE	9.46e-4 ± 2.71e-4			
	Il12 (p35)	WT	Non-Induced	3.8e-5 ± 7.9e-6	$F_{(1,21)}$ = 21.29, p = 0.0001, $\eta^2_{partial}$ = 0.48	$F_{(1,21)}$ = 0.459, p = 0.506, $\eta^2_{partial}$ = 0.010	$F_{(1,21)}$ = 0.928, p = 0.346, $\eta^2_{partial}$ = 0.021
			EAE	3.3e-4 ± 8.3e-5			
		Ptx3$^{-/-}$	Non-Induced	5.3e-5 ± 1.6e-5			
			EAE	2.5e-4 ± 4.7e-5			
	Ifng	WT	Non-Induced	4.52e-5 ± 2.61e-5	$F_{(1,22)}$ = 22.17, p = 0.0001, $\eta^2_{partial}$ = 0.447	$F_{(1,22)}$ = 2.072, p = 0.164, $\eta^2_{partial}$ = 0.042	$F_{(1,22)}$ = 2.123, p = 0.159, $\eta^2_{partial}$ = 0.043
			EAE	2.65e-2 ± 7.10e-3			
		Ptx3$^{-/-}$	EAE	1.20e-4 ± 3.87e-5			
			Non-Induced	1.41e-2 ± 4.07e-2			
	Il4	WT	Non-Induced	4.84e-5 ± 5.84e-6	$F_{(1,21)}$ = 1.351, p = 0.258, $\eta^2_{partial}$ = 0.057	$F_{(1,21)}$ = 1.441, p = 0.243, $\eta^2_{partial}$ = 0.061	$F_{(1,19)}$ = 0.074, p = 0.788, $\eta^2_{partial}$ = 0.003
			EAE	6.04e-5 ± 1.15e-5			
		Ptx3$^{-/-}$	Non-Induced	4.06e-5 ± 3.96e-6			
			EAE	4.81e-5 ± 1.05e-5			
Chronic	*Il6*	WT	Non-Induced	3.5e-5 ± 6.19e-6	$F_{(1,19)}$ = 5.609, p = 0.027, $\eta^2_{partial}$ = 0.217	$F_{(1,19)}$ = 0.821, p = 0.376, $\eta^2_{partial}$ = 0.032	$F_{(1,19)}$ = 0.838, p = 0.371, $\eta^2_{partial}$ = 0.032
			EAE	2.88e-4 ± .13e-4			
		Ptx3$^{-/-}$	Non-Induced	3.33e-5 ± .67e-6			
			EAE	6.06e-4 ± .82e-4			
	Il17a	WT	Non-Induced	1.4e-4 ± 2.7e-5	$F_{(1,19)}$ = 5.356, p = 0.032, $\eta^2_{partial}$ = 0.22	$F_{(1,19)}$ = 0.013, p = 0.909, $\eta^2_{partial}$ = 0.0006	$F_{(1,19)}$ = 0.036, p = 0.8512 $\eta^2_{partial}$ = 0.001
			EAE	6.1e-4 ± 3.2e-4			
		Ptx3$^{-/-}$	Non-Induced	1.2e-4 ± 2.8e-5			
			EAE	6.8e-4 ± 3.4e-4			

Table 15. Results from the two-way ANOVA analysis used for the comparison of cytokine gene expression in the cerebellum, between *Ptx3*$^{-/-}$ and WT mice (continued).

				Mean ± SEM	Disease Factor	Genotype Factor	Interaction
Chronic	*Il12 (p35)*	WT	Non-Induced	7.5e-6 ± 2.5e-6	$F_{(1,17)}$ = 2.867, p = 0.109, $\eta^2_{partial}$ = 0.123	$F_{(1,17)}$ = 1.998, p = 0.176, $\eta^2_{partial}$ = 0.086	$F_{(1,17)}$ = 1.622, p = 0.220, $\eta^2_{partial}$ = 0.069
			EAE	1.0e-5 ± 2.6e-6			
		Ptx3$^{-/-}$	Non-Induced	8.3e-6 ± 1.7e-6			
			EAE	2.6e-5 ± 1.2e-5			
	Ifng	WT	Non-Induced	1.0e-5 ± 0	$F_{(1,10)}$ = 1.331 p = 0.276, $\eta^2_{partial}$ = 0.102	$F_{(1,10)}$ = 0.310, p = 0.590, $\eta^2_{partial}$ = 0.024	$F_{(1,10)}$ = 0.361 p = 0.561, $\eta^2_{partial}$ = 0.028
			EAE	1.4e-4 ± 6.1e-5			
		Ptx3$^{-/-}$	Non-Induced	0 ± 0			
			EAE	4.0e-4 ± 2.3e-4			
	Il4	WT	Non-Induced	2.95e-4 ± 2.5e-5	$F_{(1,19)}$ = 0.033, p = 0.857, $\eta^2_{partial}$ = 0.0014	$F_{(1,19)}$ = 0.834, p = 0.373, $\eta^2_{partial}$ = 0.035	$F_{(1,19)}$ = 3.750, p = 0.068, $\eta^2_{partial}$ = 0.157
			EAE	2.47e-4 ± 2.1e-5			
		Ptx3$^{-/-}$	Non-Induced	2.3e-4 ± 1.63e-5			
			EAE	2.7e-4 ± 2.88e-5			

4.5 Assessment of astrocytic activation in *Ptx3*$^{-/-}$ mice

Considering the importance of astrocytes in the context of MS and their role in PTX3 production, we proposed to evaluate the morphology of these cells and the expression of astrocytic markers in *Ptx3*$^{-/-}$ mice. To assess astrocytic morphology, we stained cerebellum slices of mice sacrificed at the onset and chronic phases of disease, for GFAP^{+} cells and acquired the Z-stack of confocal images of the cerebellum of these animals. Then, we proceeded to the 3D reconstruction of astrocytes, using the Fiji-ImageJ software. Six astrocytes were reconstructed per animal in non-induced mice and per region in EAE mice. The length and complexity of these astrocytes were compared between groups. Representative images of these regions and examples of reconstructed astrocytes are presented in Figure 11A.

After reconstruction, we observed that in the onset phase, astrocytes of EAE animals presented a higher process length than those of non-induced mice, in both the normal appearing white matter and in lesion sites (Figure 11B). Furthermore, in this phase, the morphology of these cells, as assessed by sholl analysis, indicates a higher astrocytic complexity of EAE *Ptx3*$^{-/-}$ mice when compared to non-induced *Ptx3*$^{-/-}$ mice and to non-induced WT mice (Figure 11C). On the other hand, we did not find any differences in the total length of astrocytic processes, nor between genotypes neither between EAE and control animals, in the chronic phase of disease (Figure 11D). Also in this phase, astrocytes of non-induced and EAE

animals appear to have a similar morphology (Figure 11E). Moreover, no differences were found between genotypes in none of the assessments, in either phase of disease. The results from the two-way ANOVA test for total process length and sholl analysis can be observed in Table 16 and Table 17, respectively.

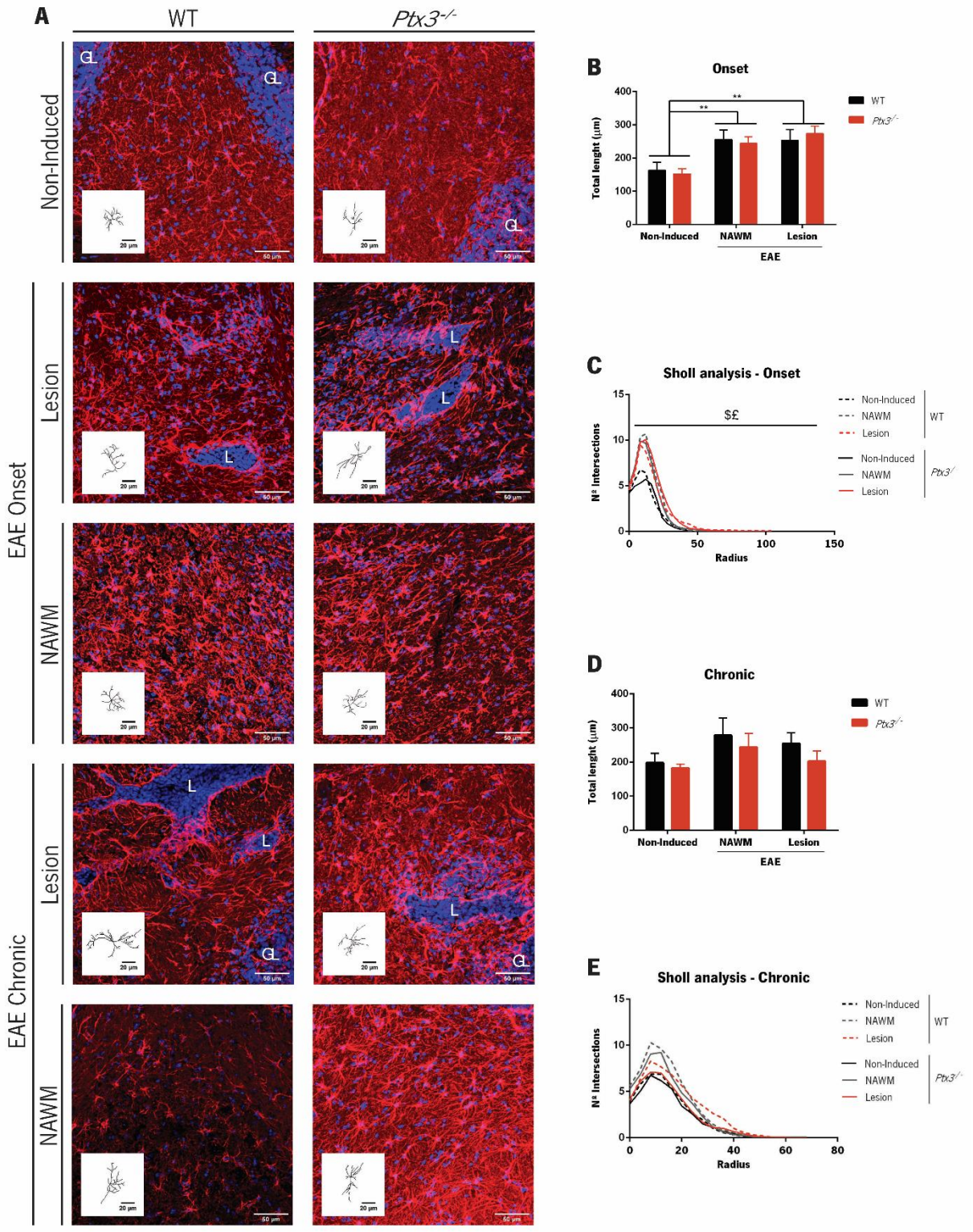

Figure 11. GFAP⁺ cells immunofluorescence staining and astrocyte morphological analysis. (A) Representative Z-stack images of the white matter of the cerebellum of EAE and non-induced mice were obtained

with the confocal microscope. (Images acquired with the 40x objective, bar – 50 µm, WM – White Matter, GL – Granular layer, L – Lesion, NAWM – Normal Appearing White Matter). Three images were captured per region and two astrocytes were reconstructed from each image. Examples of reconstructed astrocytes are shown in the left inferior corner of each image (Bar – 20 µm) (B) The total process length of the reconstructed astrocytes, is higher in EAE animals than in non-induced controls in the onset phase of disease. (C) Furthermore, the morphology of these astrocytes appears to be more complex in EAE *Ptx3*$^{-/-}$ mice than in non-induced *Ptx3*$^{-/-}$ and WT mice. (D) On the other hand, in the chronic phase of disease, the total process length of astrocytes is similar between genotypes and is not altered by disease state. (E) In addition, in this phase, the morphology of these cells is also similar between genotypes and disease states. (Onset: $n_{\text{Non-Induced WT}} = 4$, $n_{\text{Non-Induced } Ptx3^{-/-}} = 3$, $n_{\text{EAE WT NAWM}} = 4$, $n_{\text{EAE WT Lesion}} = 4$, $n_{\text{EAE } Ptx3^{-/-} \text{ NAWM}} = 4$, $n_{\text{EAE } Ptx3^{-/-} \text{ Lesion}} = 4$; Chronic: $n_{\text{Non-Induced WT}} = 4$, $n_{\text{Non-Induced } Ptx3^{-/-}} = 4$, $n_{\text{EAE WT NAWM}} = 4$, $n_{\text{EAE WT Lesion}} = 4$, $n_{\text{EAE } Ptx3^{-/-} \text{ NAWM}} = 3$, $n_{\text{EAE } Ptx3^{-/-} \text{ Lesion}} = 3$. From each of these groups, 6 astrocytes were reconstructed per animal). Data presented as mean ± SEM for the length analysis and as only mean for the sholl analysis. ** $p < 0.01$. $ $p < 0.05$ for non-induced *Ptx3*$^{-/-}$ vs Lesion *Ptx3*$^{-/-}$, £ $p < 0.05$ for non-induced WT vs Lesion *Ptx3*$^{-/-}$.

Table 16. Results from the two-way ANOVA analysis used for the comparison of total process length of reconstructed astrocytes in the cerebellum, between *Ptx3*$^{-/-}$ and WT mice.

			Mean ± SEM	Region Factor	Genotype Factor	Interaction
Onset	WT	Non-Induced	162.92 ± 25.08	$F_{(2, 17)} = 9.491$, $p = 0.0017$, $\eta^2_{\text{partial}} = 0.520$	$F_{(1, 17)} = 0.0001$, $p = 0.991$, $\eta^2_{\text{partial}} = 0.000003$	$F_{(2, 17)} = 0.262$, $p = 0.773$, $\eta^2_{\text{partial}} = 0.014$
		NAWM	255.48 ± 29.33			
		Lesion	252.88 ± 32.59			
	Ptx3$^{-/-}$	Non-Induced	152.48 ± 14.99			
		NAWM	244.25 ± 19.92			
		Lesion	273.835 ± 22.34			
Chronic	WT	Non-Induced	198.06 ± 27.81	$F_{(2, 16)} = 2.186$ $p = 0.145$, $\eta^2_{\text{partial}} = 0.195$	$F_{(1, 16)} = 1.496$, $p = 0.239$, $\eta^2_{\text{partial}} = 0.067$	$F_{(2, 16)} = 0.141$ $p = 0.870$, $\eta^2_{\text{partial}} = 0.013$
		NAWM	278.60 ± 50.11			
		Lesion	254.612 ± 31.35			
	Ptx3$^{-/-}$	Non-Induced	182.00 ± 12.37			
		NAWM	243.35 ± 41.30			
		Lesion	202.533 ± 29.71			

Table 17. Results from the two-way ANOVA analysis used for the comparison of astrocytic complexity (sholl analysis) in the cerebellum, between Ptx3$^{-/-}$ and WT mice.

			Mean ± SEM	Radius Factor	Group Factor	Interaction
Onset	WT	Non-Induced	1.27 ± 0.42	$F_{(26, 442)} = 281.4$, $p < 0.0001$, $\eta^2_{partial} = 0.851$	$F_{(5, 17)} = 4.418$, $p = 0.0092$, $\eta^2_{partial} = 0.014$	$F_{(130, 442)} = 2.656$, $p < 0.0001$, $\eta^2_{partial} = 0.040$
		NAWM	1.98 ± 0.66			
		Lesion	1.96 ± 0.56			
	Ptx3$^{-/-}$	Non-Induced	1.193 ± 0.39			
		NAWM	1.89 ± 0.61			
		Lesion	2.16 ± 0.64			
Chronic	WT	Non-Induced	2.21 ± 0.61	$F_{(17, 272)} = 164.8$, $p < 0.0001$, $\eta^2_{partial} = 0.820$	$F_{(5, 16)} = 1.485$, $p = 0.249$, $\eta^2_{partial} = 0.019$	$F_{(85, 272)} = 1.145$, $p = 0.210$, $\eta^2_{partial} = 0.029$
		NAWM	3.17 ± 0.87			
		Lesion	2.96 ± 0.69			
	Ptx3$^{-/-}$	Non-Induced	2.05 ± 0.56			
		NAWM	2.81 ± 0.78			
		Lesion	2.35 ± 0.62			

Although no major differences were found in astrocytic morphology, we still wanted to understand the impact of *Ptx3* ablation in these cells at a more molecular level. In this sense, we decided to evaluate the expression of some astrocytic markers in the cerebellum of these animals. In fact, the expression of *Gfap*, a pan-reactive marker (Liddelow et al., 2017), was found increased in EAE mice when compared to non-induced controls in both phases of disease (Figure 12A and F). On the other hand, lipocalin-2 *(Lcn2)*, which is also a pan-reactive marker (Liddelow et al., 2017), was only found to be significantly increased in EAE mice in the onset phase (Figure 12D). Of interest, we observed an increased expression of fibulin-5 *(Fbln5)*, which is an A1 marker (Liddelow et al., 2017) in EAE animals when compared to non-induced controls, in both phases of disease (Figure 12B and G). Moreover, in the chronic phase, this gene was increased in EAE *Ptx3*$^{-/-}$ mice when compared to EAE WT animals (Figure 12G). On what concerns the expression of Amphoterin-Induced Protein 2 *(Amigo2),* another A1 marker (Liddelow et al., 2017) no differences were found in its expression between genotypes or between disease states, in either phase of disease (Figure 12E and J). S100 Calcium Binding Protein A10 *(S100a10)*, an A2 marker (Liddelow et al., 2017), had a decreased expression in *Ptx3*$^{-/-}$ mice when compared to WT mice in both non-induced and in EAE animals, in the onset phase of disease (Figure 12C). But, in the chronic phase this gene was overexpressed in EAE mice when compared to non-induced mice (Figure 12H). Finally,

Ptx3, which is also an A2 marker (Liddelow et al., 2017) was found significantly increased in EAE WT mice in the onset phase of disease (Figure 7A). In the chronic phase, although not statistically significant, this gene was only expressed in EAE WT (Figure 7B) mice as well. The results from the two-way ANOVA test are presented in Table 18.

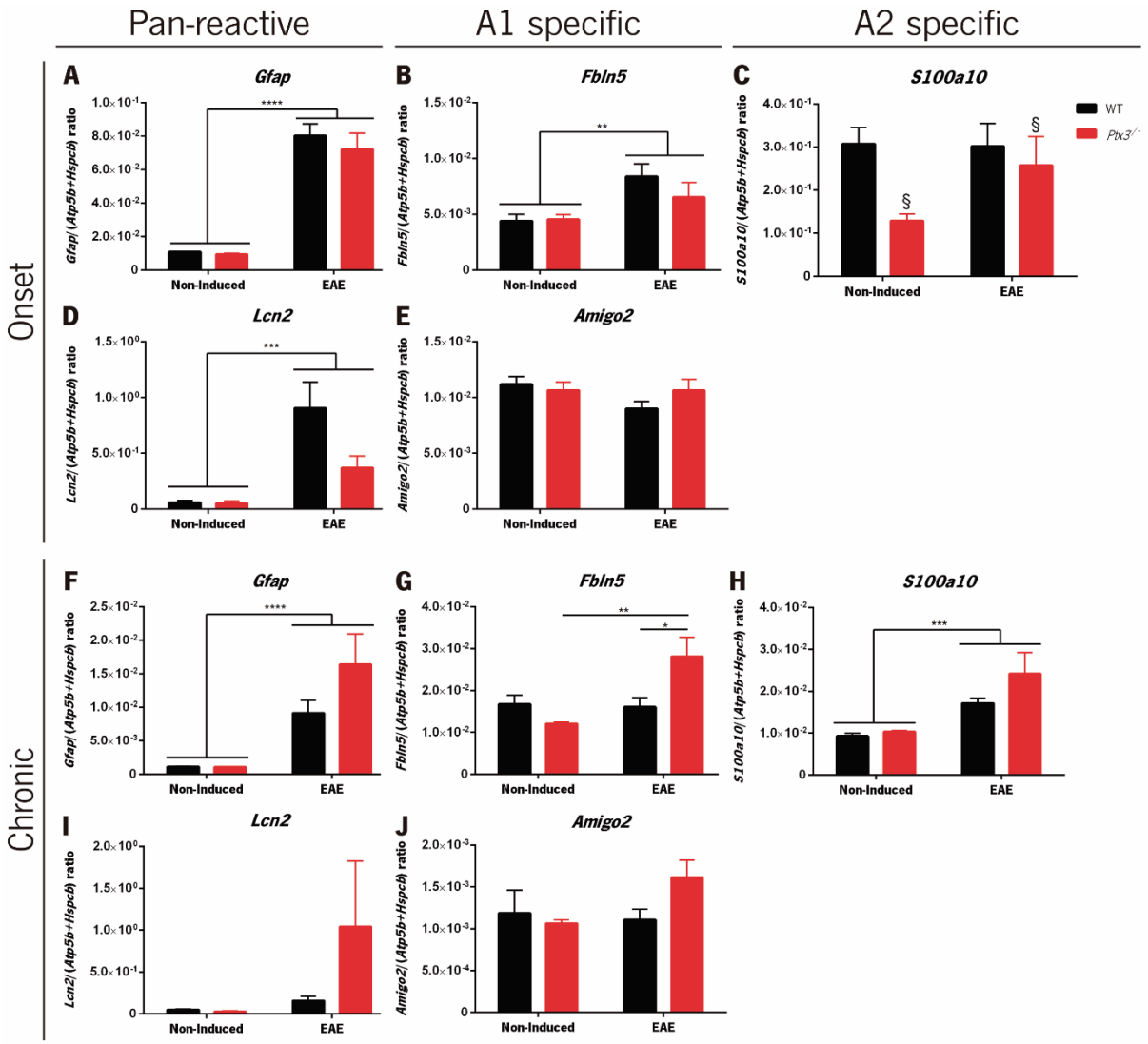

Figure 12. Expression levels of astrocytic markers in the cerebellum of EAE mice. During the onset phase of disease, pan reactive astrocytic markers *Gfap* (A) and *Lcn2* (D) and A1 marker *Fbln5* (B), are overexpressed in EAE animals. In addition, the expression of *S100a10* (C), an A2 marker, is decreased in *Ptx3*$^{-/-}$ mice when compared to WT animals. In the chronic phase, only *Gfap* (F), *Fbln5* (G) and *S100a10* (H) were overexpressed, again in the EAE animals when compared to non-induced controls. Interestingly, in this phase, EAE *Ptx3*$^{-/-}$ mice presented a higher expression of *Fbln5* (G) than EAE WT mice. In what regards the expression of A1 marker, *Amigo2,* no differences were found neither between genotypes nor between disease states, in either phase (E and J). (Onset: $n_{\text{Non-Induced WT}} = 7$; $n_{\text{Non-Induced } Ptx3^{-/-}} = 6$; $n_{\text{EAE WT}} = 7$; $n_{\text{EAE } Ptx3^{-/-}} = 6$. Chronic: $n_{\text{Non-Induced WT}} = 6$, $n_{\text{Non-Induced } Ptx3^{-/-}} = 6$; $n_{\text{EAE WT}} = 6$;

$n_{EAE\ Ptx3^{-/-}}$ = 5. Data presented as mean ± SEM. * $p < 0.05$, ** $p < 0.01$, *** $p < 0.001$, **** $p < 0.0001$. § $p < 0.05$ for *Ptx3*$^{-/-}$ Non-Induced/EAE vs WT Non-Induced/EAE animals).

Table 18. Results from the two-way ANOVA analysis used for the comparison of astrocytic gene expression in the cerebellum, between *Ptx3*$^{-/-}$ and WT mice.

				Mean ± SEM	Disease Factor	Genotype Factor	Interaction
Onset	*Gfap*	WT	Non-Induced	1.1e-2 ± 3.3e-4	$F_{(1,22)}$ = 124.9, $p < 0.0001$, $\eta^2_{partial}$ = 0.835	$F_{(1,22)}$ = 0.666, p = 0.423, $\eta^2_{partial}$ = 0.0044	$F_{(1,22)}$ = 0.332, p = 0.570, $\eta^2_{partial}$ = 0.0022
			EAE	8.0e-2 ± 7.0e-3			
		Ptx3$^{-/-}$	Non-Induced	9.5e-3 ± 5.3e-4			
			EAE	7.2e-2 ± 9.8e3			
	Lcn2	WT	Non-Induced	5.99e-2 ± 1.83e-2	$F_{(1,22)}$ = 17.91, p = 0.0003, $\eta^2_{partial}$ = 0.367	$F_{(1,22)}$ = 3.911, p = 0.061, $\eta^2_{partial}$ = 0.080	$F_{(1,22)}$ = 3.668, p = 0.069, $\eta^2_{partial}$ = 0.075
			EAE	9.05e-1 ± 2.34e-1			
		Ptx3$^{-/-}$	Non-Induced	5.14e-2 ± 2.13e-2			
			EAE	3.70e-1 ± 1.08e-1			
	Fbln5	WT	Non-Induced	4.43e-3 ± 5.87e-4	$F_{(1,22)}$ = 9.874, p = 0.0047, $\eta^2_{partial}$ = 0.288	$F_{(1,22)}$ = 0.8331, p = 0.371, $\eta^2_{partial}$ = 0.024	$F_{(1,22)}$ = 1.064, p = 0.313, $\eta^2_{partial}$ = 0.031
			EAE	8.40e-3 ± 1.15e-3			
		Ptx3$^{-/-}$	Non-Induced	4.54e-3 ± 4.57e-4			
			EAE	6.55e-3 ± 1.32e-3			
	Amigo2	WT	Non-Induced	1.1e-2 ± 6.9e-4	$F_{(1,22)}$ = 2.007, p = 0.171, $\eta^2_{partial}$ = 0.075	$F_{(1,22)}$ = 0.513, p = 0.481, $\eta^2_{partial}$ = 0.019	$F_{(1,22)}$ = 2.042, p = 0.167, $\eta^2_{partial}$ = 0.076
			EAE	9.0e-3 ± 6.6e-4			
		Ptx3$^{-/-}$	Non-Induced	1.1e-2 ± 7.3e-4			
			EAE	1.1e-2 ± 9.9e-4			
	S100a10	WT	Non-Induced	3.07e-1 ± 3.80e-2	$F_{(1,22)}$ = 1.650, p = 0.212, $\eta^2_{partial}$ = 0.054	$F_{(1,22)}$ = 5.454, p = 0.029, $\eta^2_{partial}$ = 0.177	$F_{(1,22)}$ = 1.961, p = 0.175, $\eta^2_{partial}$ = 0.064
			EAE	3.02e-1 ± 5.32e-2			
		Ptx3$^{-/-}$	Non-Induced	1.29e-1 ± 1.58e-2			
			EAE	2.57e-1 ± 6.73e-2			
Chronic	*Gfap*	WT	Non-Induced	1.14e-3 ± 7.17e-5	$F_{(1,19)}$ = 28.03, $p < 0.0001$, $\eta^2_{partial}$ = 0.552	$F_{(1,19)}$ =2.696, p = 0.117, $\eta^2_{partial}$ = 0.053	$F_{(1,19)}$ = 2.809, p = 0.110, $\eta^2_{partial}$ = 0.053
			EAE	9.12e-3 ± 1.94e-3			
		Ptx3$^{-/-}$	Non-Induced	1.06e-3 ± 7.77e-5			
			EAE	1.64e-2 ± 4.55e-3			

Table 18. Results from the two-way ANOVA analysis used for the comparison of astrocytic gene expression in the cerebellum, between *Ptx3*$^{-/-}$ and WT mice (continued).

				Mean ± SEM	Disease Factor	Genotype Factor	Interaction
Chronic	*Lcn2*	WT	Non-Induced	5.0e-2 ± 9.4e-3	$F_{(1,19)}$ = 2.760, p = 0.113, $\eta^2_{partial}$ = 0.112	$F_{(1,19)}$ = 1.637, p = 0.216, $\eta^2_{partial}$ = 0.066	$F_{(1,19)}$ = 1.815, p = 0.194, $\eta^2_{partial}$ = 0.074
			EAE	1.6e-1 ± 5.3e-2			
		Ptx3$^{-/-}$	Non-Induced	2.7e-2 ± 1.0e-2			
			EAE	1.0 ± 7.8e-1			
	Fbln5	WT	Non-Induced	1.7e-2 ± 2.1e-3	$F_{(1,19)}$ = 8.866, p = 0.0077, $\eta^2_{partial}$ = 0.229	$F_{(1,19)}$ = 1.998, p = 0.174, $\eta^2_{partial}$ = 0.052	$F_{(1,19)}$ = 10.51, p = 0.0043, $\eta^2_{partial}$ = 0.271
			EAE	1.6e-2 ± 2.2e-3			
		Ptx3$^{-/-}$	Non-Induced	1.2e-2 ± 4.6e-4			
			EAE	2.8e-2 ± 4.7e-3			
	Amigo2	WT	Non-Induced	1.2e-3 ± 2.7e-4	$F_{(1,19)}$ = 1.666, p = 0.212, $\eta^2_{partial}$ = 0.069	$F_{(1,19)}$ = 1.107, p = 0.306, $\eta^2_{partial}$ = 0.046	$F_{(1,19)}$ = 2.971, p = 0.101, $\eta^2_{partial}$ = 0.122
			EAE	1.1e-3 ± 1.3e-4			
		Ptx3$^{-/-}$	Non-Induced	1.1e-3 ± 4.3e-5			
			EAE	1.6e-3 ± 2.0e-4			
	S100a10	WT	Non-Induced	9.3e-3 ± 6.6e-4	$F_{(1,19)}$ = 22.35, p = 0.0001, $\eta^2_{partial}$ = 0.499	$F_{(1,19)}$ = 3.110, p = 0.094, $\eta^2_{partial}$ = 0.069	$F_{(1,19)}$ = 1.767, p = 0.1995, $\eta^2_{partial}$ = 0.0395
			EAE	1.7e-2 ± 1.3e-3			
		Ptx3$^{-/-}$	Non-Induced	1.0e-2 ± 3.1e-4			
			EAE	2.4e-2 ± 5.0e-3			

4.6 Microglial markers are increased in EAE mice

Interestingly, PTX3 is expressed by macrophages and has been described as being specific of M2 macrophages (Pucci et al., 2014; Sun, Tian, Xian, Xie, & Yang, 2015). In addition, microglia can also produce PTX3 in the CNS. For that reason, herein we also analysed the impact of PTX3 in the microglial profile of EAE induced mice. For this, we assessed the expression levels some of microglial markers through qRT-PCR. Interestingly, we found an increased expression of allograft inflammatory factor 1 *(Iba1),* a pan-microglial marker (Figure 13A) and of M1 specific markers, inducible nitric oxide synthase *(iNos)* (Figure 13B) and major histocompatibility complex class 2 *(Mhc2)* (Figure 13C) (Orihuela, Mcpherson, & Harry, 2016), in EAE animals when compared to non-induced controls, in the onset phase of disease. However, in the chronic phase, we only found increased levels of *Iba1* (Figure 13D) and *Mhc2* (Figure 13F) between these groups. Of interest, in the onset phase, *Ptx3*$^{-/-}$ EAE animals presented a

decreased expression of *Mhc2* gene when compared to WT EAE animals. The results from the two-way ANOVA test are presented in Table 19.

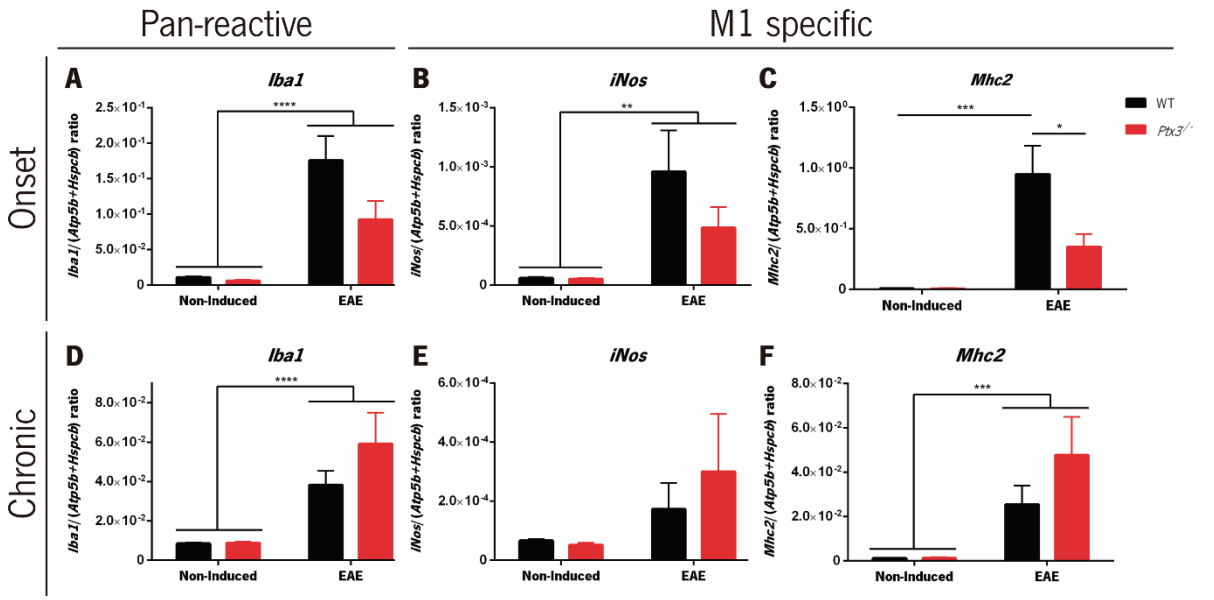

Figure 13. Expression levels of microglia markers in the cerebellum of EAE mice. During the onset phase of disease, pan-reactive microglial specific gene *Iba1* (A) and M1 microglial marker *iNos* (B) are overexpressed in EAE animals compared non-induced controls. Also in this phase, *Mhc2* (C) presents lower expression levels in EAE *Ptx3*$^{-/-}$ mice in comparison to EAE WT animals. In the chronic phase, only *Iba1* (D) and *Mhc2* (F) are overexpressed in EAE animals. (Onset: $n_{\text{Non-Induced WT}} = 7$; $n_{\text{Non-Induced } Ptx3^{-/-}} = 6$; $n_{\text{EAE WT}} = 7$; $n_{\text{EAE } Ptx3^{-/-}} = 6$. Chronic: $n_{\text{Non-Induced WT}} = 6$, $n_{\text{Non-Induced } Ptx3^{-/-}} = 6$; $n_{\text{EAE WT}} = 6$; $n_{\text{EAE } Ptx3^{-/-}} = 5$. Data presented as mean ± SEM. * $p < 0.05$, ** $p < 0.01$, *** $p < 0.001$, **** $p < 0.0001$).

Table 19. Results from the two-way ANOVA analysis used for the comparison of microglial gene expression in the cerebellum, between *Ptx3*$^{-/-}$ and WT mice.

				Mean ± SEM	Disease Factor	Genotype Factor	Interaction
Onset	*Iba1*	WT	Non-Induced	1.09e-2 ± 1.38e-3	$F_{(1,22)} = 31.71$, $p < 0.0001$, $\eta^2_{partial} = 0.508$	$F_{(1,22)} = 3.870$, $p = 0.062$, $\eta^2_{partial} = 0.062$	$F_{(1,22)} = 3.122$, $p = 0.0911$, $\eta^2_{partial} = 0.050$
			EAE	1.76e-1 ± 3.45e-2			
		Ptx3$^{-/-}$	Non-Induced	6.41e-3 ± 8.88e-4			
			EAE	9.26e-2 ± 2.61e-2			
	iNos	WT	Non-Induced	5.9e-5 ± 1.1e-5	$F_{(1,22)} = 10.56$, $p = 0.0037$, $\eta^2_{partial} = 0.295$	$F_{(1,22)} = 1.376$, $p = 0.253$, $\eta^2_{partial} = 0.038$	$F_{(1,22)} = 1.291$, $p = 0.268$, $\eta^2_{partial} = 0.036$
			EAE	9.6e-4 ± 3.5e-4			
		Ptx3$^{-/-}$	Non-Induced	5.1e-5 ± 6.5e-6			
			EAE	4.9e-4 ± 1.7e-4			

Table 19. Results from the two-way ANOVA analysis used for the comparison of microglial gene expression in the cerebellum, between *Ptx3*$^{-/-}$ and WT mice (continued).

				Mean ± SEM	Disease Factor	Genotype Factor	Interaction
Onset	*Mhc2*	WT	Non-Induced	1.1e-2 ± 1.1e-3	$F_{(1,22)}$ = 22.40, p = 0.0001, $\eta^2_{partial}$ = 0.401	$F_{(1,22)}$ = 4.869, p = 0.038, $\eta^2_{partial}$ = 0.087	$F_{(1,22)}$ = 4.775, p = 0.0398, $\eta^2_{partial}$ = 0.086
			EAE	9.5e-1 ± 2.3e-1			
		Ptx3$^{-/-}$	Non-Induced	8.0e-3 ± 2.0e-3			
			EAE	3.5e-1 ± 1.0e-1			
Chronic	*Iba1*	WT	Non-Induced	8.5e-3 ± 5.7e-4	$F_{(1,19)}$ = 26.02, p < 0.0001, $\eta^2_{partial}$ = 0.550	$F_{(1,19)}$ = 1.842, p = 0.191, $\eta^2_{partial}$ = 0.039	$F_{(1,19)}$ = 1.703, p = 0.208, $\eta^2_{partial}$ = 0.036
			EAE	3.8e-2 ± 7.2e-3			
		Ptx3$^{-/-}$	Non-Induced	8.9e-3 ± 5.6e-4			
			EAE	5.9e-2 ± 1.6e-2			
	iNos	WT	Non-Induced	6.7e-5 ± 5.6e-6	$F_{(1,19)}$ = 3.407, p = 0.081, $\eta^2_{partial}$ = 0.148	$F_{(1,19)}$ = 0.337, p = 0.568, $\eta^2_{partial}$ = 0.015	$F_{(1,19)}$ = 0.543, p = 0.470, $\eta^2_{partial}$ = 0.024
			EAE	1.7e-4 ± 8.9e-5			
		Ptx3$^{-/-}$	Non-Induced	5.2e-5 ± 7.9e-6			
			EAE	3.0e-4 ± 2.0e-4			
	Mhc2	WT	Non-Induced	1.3e-3 ± 1.5e-4	$F_{(1,19)}$ = 16.71, p = 0.0006, $\eta^2_{partial}$ = 0.4396	$F_{(1,19)}$ = 1.682, p = 0.210, $\eta^2_{partial}$ = 0.044	$F_{(1,19)}$ = 1.650, p = 0.215, $\eta^2_{partial}$ = 0.043
			EAE	2.5e-2 ± 8.5e-3			
		Ptx3$^{-/-}$	Non-Induced	1.4e-3 ± 2.5e-4			
			EAE	4.8e-2 ± 1.7e-2			

4.7 Multiple Sclerosis patients have increased circulating levels of PTX3

Taking into consideration that PTX3 serum levels have been reported as being increased in some pathologies, including MS (Wang et al., 2013), we quantified the levels of circulating PTX3 in MS patients, using ELISA. The levels of PTX3 in the serum of MS patients were compared to those of age and gender matched healthy controls. Of all analysed samples, six MS patients and one control were excluded from the analysis because they presented a high coefficient of variability between replicates. Moreover, two control samples were excluded because they presented a lower optic density than the lowest standard. After analysis, we observed that the levels of PTX3 were significantly increased in MS patients when compared to healthy controls (Controls = 0.8202 ± 0.08821, MS Patients = 1.704 ± 0.1461, $t_{(95)}$ = 4.448, p < 0.0001, Cohen's d = 0.998) (Figure 14), indicating a possible role of this protein in MS pathophysiology or simply a response to the underlying inflammation observed in MS.

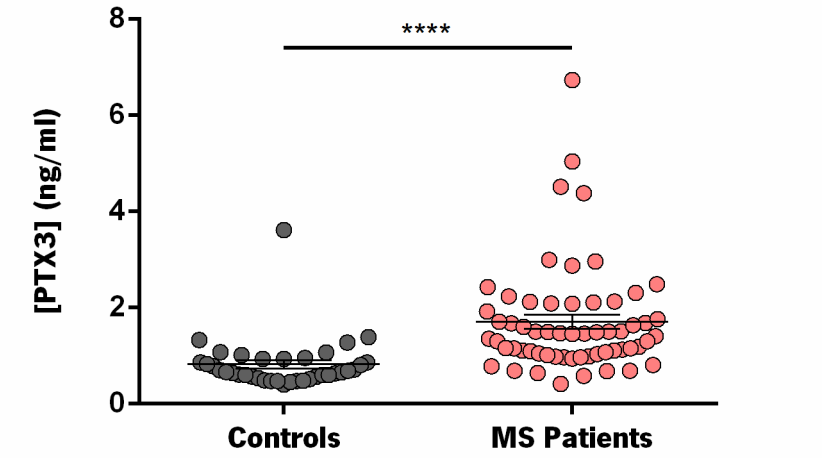

Figure 14. Circulating levels of PTX3 are increased in MS patients. Serum levels of PTX3 were measured by ELISA in both MS patients and in healthy controls. MS patients present a significantly higher level of serum PTX3 than healthy controls. $n_{controls} = 37$, $n_{MS\ Patients} = 60$. Results are presented as mean ± SEM. **** $p < 0.0001$.

4.8 PTX3 haplotypes do not influence Multiple Sclerosis susceptibility

PTX3 haplotype h2/h2, which includes variant genotypes for both the rs2305619 and rs3816527 SNPs, has been associated with a higher predisposition for diseases such as invasive aspergillosis (Cunha et al., 2014). However, there is no information regarding the role of these SNPs in neurodegenerative diseases and in particular, in MS. In this sense, we aimed at understanding if these polymorphisms were associated with MS susceptibility. For this, 48 MS patients and 215 controls of European descent were genotyped for both SNPs. The distribution of haplotypes in the study group and the results from the Chi-Square test are presented in Table 20.

Table 20. Distribution of haplotypes in MS patients and controls and results from the Chi-Square test.

Study groups (n)	Haplotypes			χ^2	*p* value
	h1/h1	h1/h2	h2/h2		
Controls (215)	45	112	58	0.6704	0.7152
MS Patients (48)	12	22	14		

After correlation of genotypes, haplotype frequencies were compared between controls and MS patients, but none of the haplotypes significantly affected disease susceptibility (Figure 15A). Next, taking into consideration that the h2/h2 haplotype includes two SNPs that have been described to impair PTX3 protein expression and/or function, we correlated the levels of this protein with the different haplotypes

in both patients and controls. Surprisingly, we did not find any differences in the serum levels of circulating PTX3 between haplotypes in either patients or controls (Figure 15B).

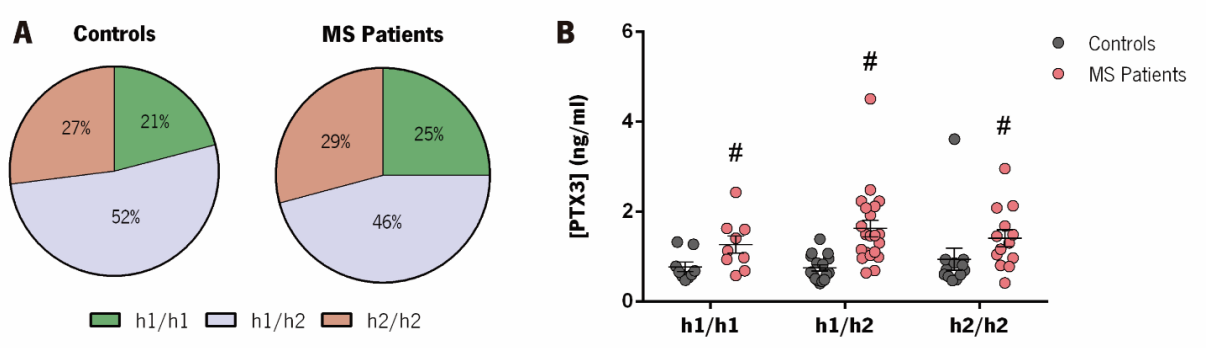

Figure 15. Frequencies of *PTX3* gene haplotypes on MS patients and their effect on serum levels of PTX3. (A) Healthy controls and MS patients present similar frequencies of haplotypes. $n_{Controls\ h1/h1} = 45$, $n_{Controls\ h1/h2} = 112$, $n_{Controls\ h2/h2} = 58$, $n_{MS\ Patients\ h1/h1} = 12$, $n_{MS\ Patients\ h1/h2} = 22$, $n_{MS\ Patients\ h2/h2} = 14$. (B) The levels of circulating PTX3 are similar between haplotypes in controls and in MS patients. However, MS patients have significantly higher levels of this protein than controls. ($n_{Controls\ h1/h1} = 9$, $n_{Controls\ h1/h2} = 16$, $n_{Controls\ h2/h2} = 12$, $n_{MS\ Patients\ h1/h1} = 9$, $n_{MS\ Patients\ h1/h2} = 21$, $n_{MS\ Patients\ h2/h2} = 13$. # $p < 0.05$ for MS Patients h1/h1 / h1/h2 / h2/h2 vs Controls h1/h1 / h1/h2 / h2/h2).

5. Discussion

MS is one of the most common chronic inflammatory diseases of the CNS, but at the moment there is no cure for it (Reich, Lucchinetti, & Calabresi, 2018). Consequently, the physical, psychological and economic burden of this disease continues to increase. Although some important discoveries have been made and some therapies can somewhat improve the quality of life of these patients, they still suffer from debilitating conditions and there are still high healthcare costs. This motivates us to study this disease and to try to uncover new players and possible therapy targets, always keeping in mind the improvement in the quality of life of MS patients. Taking this into consideration, our aim with this thesis was to better comprehend how the multifunctional protein, PTX3, could be playing a role in MS pathophysiology and potentially contribute to the better understanding of this disease.

For this, we took advantage of the most used animal model of MS, the EAE model that together with genetically altered mice that did not express PTX3 would help us explore the role of this protein in MS. Of interest, EAE had already been induced in *Ptx3*$^{-/-}$ mice. However, no differences were found in the disease course of *Ptx3*$^{-/-}$ mice compared to WT, in what concerns day of onset or time to reach maximum clinical score (Ummenthum et al., 2016). In fact, this is in line with our work, as we also did not find any differences in the clinical score of *Ptx3*$^{-/-}$ mice in comparison to their WT littermates. However, when analysing the percentage of lesioned area in the cerebellum we could observe a tendency for a lower percentage of lesions in *Ptx3*$^{-/-}$ mice in comparison to WT littermates, as assessed by Luxol Fast Blue staining. This variation was not statistically significant, but it remained present in both the onset and on the chronic phases of disease. On the contrary, Ummenthum *et al,* reports that they did not find any differences in the extent of myelin damage between *Ptx3*$^{-/-}$ and WT animals. However, this assessment was made in the spinal cord and not in the cerebellum and using a different technique to our own, which limits comparisons. Moreover, in our samples the percentage of lesioned area in the onset phase is higher than in the chronic phase, which could be explained by the partial recovery observed during that period in MOG-induced EAE mice. Indeed, differences between this lesions in acute and chronic phases of disease have already been reported (Popescu & Lucchinetti, 2012). More specifically, this increased percentage of lesioned area in the onset phase of disease when compared to the chronic phase was already observed in WT mice induced with EAE (Das Neves et al., 2018). In the future, to confirm if a decreased lesioned area is a phenotypic trait of *Ptx3*$^{-/-}$ mice we should repeat the experiments with an increased number of animals, as in this case only four animals were analysed per group. If confirmed, it could indicate a pathogenic role of PTX3 in MS, as opposed to the protective role it plays in several other

diseases, such as stroke (Rajkovic et al., 2018; Shindo et al., 2016), cancer (Bonavita et al., 2015; Presta et al., 2018) and aspergillosis (Bozza et al., 2014).

Next, to better understand if this tendency for decreased lesion percentages in *Ptx3*$^{-/-}$ mice was associated with a decreased inflammatory phenotype, we decided to analyse the gene expression of inflammatory cytokines in these mice. After this analysis, we did not see significant differences in the expression of any of the analysed cytokines, between the two genotypes during EAE disease course. However, although not significant we observed a contradictory expression of this cytokines between the onset and the chronic phases. In fact, in the onset phase, *Ptx3*$^{-/-}$ mice appeared to present lower expression levels of pro-inflammatory cytokines than WT mice, while in the chronic phase the opposite occurred. We postulate that this could be due to a more pro-inflammatory role of PTX3 in the acute phase of disease, were it would help initiate the immune response. Then, in a more chronic phase of disease, this protein could be playing an anti-inflammatory role, helping in the clearance of myelin debris and in tissue repair. This is in line with previous findings stating that *Ptx3*$^{-/-}$ mice present a deficient Th1 response, characterized by a decreased production of *Ifng* and *Il12* and have a cytokine profile more directed at a Th2 response, in the lung (Garlanda et al., 2002). Furthermore, it was shown that administration of PTX3 leads to an increased frequency of Th1 response, with increased levels of *Ifng* and decreased *Il4* producing cells in the spleen of mice with invasive aspergillosis (Gaziano et al., 2004). Again, these findings could support the idea of a pathogenic role of PTX3 in the initial steps of disease development and of a role in the maintenance of homeostasis and tissue repair afterwards. It would be of interest to repeat these experiments and try to understand if PTX3 could in fact be playing a dual role in MS pathogenesis.

Although we did not find any differences in cytokine gene expression between genotypes, we did find differences between EAE animals and non-induced controls. Interestingly, in the onset phase of disease, we found an increased expression of *Il12* and *Ifng,* important players of the Th1 response, as well as an increased Th17 response, as shown by the overexpression of *Il6* and *Il17a*, in the EAE animals. Of interest, it is described that in MS there is a deregulation of the inflammatory response skewed towards a Th1/Th17 pro-inflammatory response (Fletcher, Lalor, Sweeney, Tubridy, & Mills, 2010; Hernández-Pedro et al., 2013; Yadav et al., 2015). These pro-inflammatory cytokines seem to play an important role in both the recruitment and activation of immune cells, initiating and aggravating the inflammatory response directed at the myelin layer (Hernández-Pedro et al., 2013).

Considering this pro-inflammatory pattern of the cerebellum of EAE mice, we then decided to look into the cells producing these cytokines. In this sense, we focused on the analysis of glial cells, important

immune mediators in the brain. Initially, we decided to explore the impact of PTX3 ablation on the activation of astrocytes during EAE. Astrocytes are known to play a role in MS pathophysiology, being activated in the lesion sites, promoting inflammation and being responsible for the formation of glial scars (Lassmann, 2018; Lassmann & Bradl, 2017; Ludwin, Rao, Moore, & Antel, 2016). Indeed, studies show that inactivation of NF-KB transcription factor in astrocytes, results in a decreased disease severity and inflammatory profile, supporting the role of astrocytes as pathogenic components in MS pathophysiology (Brambilla et al., 2014). Furthermore, *Ptx3* has been described as an A2 specific gene (which are considered to be more anti-inflammatory) (Liddelow et al., 2017) and to be produced by astrocytes under the active phase of stroke (Shindo et al., 2016). Also during stroke, the lack of PTX3 was shown to reduce the expression of reactive astrocytes (Rajkovic et al., 2018), suggesting that PTX3 could be modulating astrocytic activation. Overall, herein we also saw, at the onset phase that the lack of PTX3, is leading to a decreased inflammatory response and a decreased expression of astrocytic markers. To better understand this interaction, we started by analysing the morphology of these cells, in the cerebellum. In fact, in the onset phase we observed that EAE animals present astrocytes with increased process length when compared to non-induced animals. This is in accordance with the activation of astrocytes during MS and EAE disease course. Moreover, astrocytes from EAE *Ptx3*$^{-/-}$ mice displayed an increased complexity, as assessed by the higher number of intersections, when compared to non-induced *Ptx3*$^{-/-}$ and WT mice. Taking into account that *Ptx3* is considered to be an A2 specific gene (Liddelow et al., 2017), this increased reactivity of astrocytes in *Ptx3*$^{-/-}$ mice could represent an effect of the lack of PTX3 in shifting the astrocytic phenotype into a more reactive A1 state. On the other hand, we did not find differences in either the process length nor in the complexity of astrocytes, in the chronic phase of disease. Of interest, it was shown that in chronic active lesions, astrocytes show varying degrees of reactivity (Ludwin et al., 2016), which could explain the lack of differences in the morphology of astrocytes in the chronic phase of EAE. Interestingly, we also did not find differences between NAWM and lesion sites in either time point, which was unexpected. Indeed, it has been reported that in EAE rat spinal cord and cerebellar white matter, astrocytes from active lesions are “larger and more branched” than those in the NAWM (Haindl, Köck, Zeitelhofer-Adzemovic, Fazekas, & Hochmeister, 2019).

After the morphological analysis, we still wanted to understand if the expression of these astrocyte related molecules were increased in the cerebellum of EAE animals. For that, we measured the gene expression levels of several astrocytic markers and more specifically of A1, A2 and pan-reactive specific genes. A1 astrocytes are induced by neuroinflammation and have been reported has presenting a more pro-inflammatory profile, while A2 astrocytes are induced by ischaemia and are considered to be more

anti-inflammatory, being involved in tissue repair and homeostasis. Pan-reactive astrocytes, on their turn, are induced by both neuroinflammation and ischaemia (Liddelow et al., 2017). Of interest, a significant decrease in A2 specific gene *S100a10* in *Ptx3*$^{-/-}$ mice when compared to their WT counterparts, in the onset phase of disease, was observed. Again, this decreased expression of *S100a10* could simply be a reflection of a deregulation of A2 specific molecules, caused by the lack of PTX3 in these animals. In addition, in the chronic phase of disease, an overexpression of the A1 specific gene *Fbln5* was observed in *Ptx3*$^{-/-}$ mice when compared to WT mice, again this could be correlated with a decreased A2 response and erratic A1 activation. Besides A1 and A2 response, an increase in pan-reactive genes *Gfap* and *Lcn2* was observed in the onset phase of disease, which is in accordance with the high neuroinflammatory component of this phase of disease. Of interest, *Lcn2* has already been reported as being increased in the EAE brain and in MS patients in active phases of disease. In addition, its expression was correlated with that of astrocytes (Marques et al., 2012). In the chronic phase, we saw a significantly increased expression of *Gfap*, but not of *Lcn2,* demonstrating that although astrocytes are still activated in this phase, a decreased inflammatory response could be taking place. This can also be related with the overexpression of *S100a10*, observed in this phase of disease in EAE animals, as this molecule is related with an anti-inflammatory astrocytic profile.

After evaluating the structure and activation of astrocytes in EAE mice, we thought that it would also be important to look at other glial cells. Microglia are the resident innate immune cells of the CNS and consequently serve as its first line of defence. These cells play important roles in the recruitment of inflammatory mediators and in phagocytosis, during infection/inflammation. In fact, they were already reported in the context of MS, as being present in lesioned areas, alongside astrocytes (Chu et al., 2018; O'Loughlin, Madore, Lassmann, & Butovsky, 2018) and they are thought to be the most abundant immune cells in active MS lesions (O'Loughlin et al., 2018). Interestingly, PTX3 seems to be co-expressed with activated microglia, on MS preactive lesions, indicating an intrinsic production of these molecules in the CNS during MS (Ummenthum et al., 2016). Furthermore, microglia can produce PTX3 upon inflammatory stimuli, and this protein, on its turn, can regulate the phagocytic activity of microglia (Jeon et al., 2010). Taking all this into account, we decided to explore the activation status of these cells in EAE mice lacking PTX3. For this, we measured the expression levels of microglial markers, through qRT-PCR. After analysis, we found an increased expression of reactive microglia markers, namely *iNos* and *Iba1,* in EAE mice when compared to non-induced controls, in the onset phase of disease. Interestingly, we found a decreased *Mhc2* expression in *Ptx3*$^{-/-}$ mice when compared to WT, also in the onset phase, which suggests that PTX3 could be somehow modulating the process of antigen presentation in microglia. In

the chronic phase, however, this tendency changes towards an increase of *Mhc2* expression in the *Ptx3*$^{-/-}$ mice. Although not statistically significant, this suggests once again a dual role of PTX3 in EAE disease course, which is in accordance with our results from the cytokine and astrocytic markers assessment. Also, in the chronic phase, there is an overexpression of both *Iba1* and *Mhc2* in EAE animals suggesting a perpetuation of the self-destructive environment by presentation of myelin antigens to autoreactive T cells, even in later stages of disease. Of interest, in macrophages, PTX3 appears to be a marker of the M2 phenotype (Pucci et al., 2014; Sun et al., 2015) which is in accordance with its astrocytic phenotype, in which PTX3 is characterized as an A2 specific gene (Liddelow et al., 2017). However, in what concerns microglia, no information regarding the effect of PTX3 on microglial polarization was found. In the future, it would be interesting to also evaluate the number and morphology of microglia in these animals, in both phases of disease, to better understand the role it might be playing in the modulation of the inflammatory profile of *Ptx3*$^{-/-}$ mice.

Being an acute phase protein, PTX3 is generally not expressed or is expressed at low levels in healthy individuals but upon inflammatory stimuli, its expression increases rapidly. In fact, an increase in the plasmatic levels of this protein was already reported in some CNS disorders such as Parkinson's disease (Lee, Choi, & Suk, 2011), subarachnoid haemorrhage (Zanier et al., 2011) and glioma (Locatelli et al., 2013). On what regards PTX3 levels in the context of MS, there is contradictory information. In one hand, *Wang et al.*, showed that PTX3 plasma levels were found increased in RRMS patients during the relapse phase and that during this phase, its levels correlated with higher Expanded Disability Status Scale (EDSS) scores (Wang et al., 2013). On the other hand, *Ummenthum et al.,* reports that PTX3 was only detectable in plasma samples of three MS cases and three controls (Ummenthum et al., 2016). These differences could be due to racial differences, as the first is assessed in the Asian population while the second refers to the European population. Considering this inconsistent data, we decided to measure the levels of circulating PTX3 in the serum of MS patients and in age and gender-matched healthy controls. Interestingly, we found increased levels of this protein in MS patients when compared to controls, which is in accordance to *Wang et al.* results, suggesting that the different results obtained in the two studies above referred, are probably not due to racial differences. Therefore, our data supports the idea that PTX3 could be a potential biomarker of the underlying inflammatory response occurring in MS.

It is believed that the genetic component plays an important role in the pathogenesis of MS. In fact, several genetic alterations have been related with an increased susceptibility for MS development (Didonna & Oksenberg, 2015). Also, as previously referred, given the polygenic nature of this disease, the analysis of single nucleotide polymorphisms (SNPs) of several immune-related molecules will be

important to allow an earlier treatment of MS (Hemmer et al., 2015). Besides, genetic polymorphisms of the *PTX3* gene have already been associated with increased susceptibility for several diseases. Of interest, genetic polymorphisms leading to the deficient production of PTX3 were shown to increase the risk of invasive aspergillosis in patients undergoing hematopoietic stem cell transplantation (Cunha et al., 2014). Moreover, other studies suggest that genetic variation in the *PTX3* gene affect lung colonization by *Pseudomonas aeruginosa* in patients with Cystic Fibrosis (Chiarini et al., 2010). Also in the lung, there is evidence claiming that *PTX3* gene variation modulates the risk for tuberculosis in West Africans (Olesen et al., 2007). On the other hand, when assessing the effect of these SNPs in myocardial infarction risk, no association was found between genotypes/haplotypes and the risk of developing the disease. However, an association between the haplotypes and a variation in PTX3 plasma levels was found, supporting the phenotypic importance of these SNPs (Barbati et al., 2012). Considering that in the CNS and more specifically, in MS, these SNPs have not been studied, we decided to genotype MS patients for two functional polymorphisms of the *PTX3* gene, rs2305619 and rs3816527 that have been associated and studied in the context of the pathologies referred above, to evaluate if they could serve as early markers of MS susceptibility. After genotyping, we compared the haplotype frequency between patients and controls. However, we did not find any differences between these groups. Though, we only tested this in a small number of patients. In this sense, it would be of interest to increase the sample size and to evaluate the distributions of these haplotypes in larger population groups and correlate that with the different MS disease profiles. Furthermore, the majority of the reports that showed a significant effect of these SNPs in disease susceptibility were performed on lung-related pathologies and, to our knowledge, no information exists regarding the role of these SNPs in neurodegenerative diseases, nor, in a broader sense, in pathologies associated with the CNS. Therefore, it would be of interest to continue the study of these SNPs in brain related pathologies to better comprehend their functional impact.

Finally, to evaluate if the h2/h2 haplotype was in fact related with a deficiency in PTX3 in our samples, we correlated the levels of circulating PTX3 with the different haplotypes. However, we did not find differences in the levels of PTX3 in either haplotype in the control group. We still do not know if this is an intrinsic characteristic of our control samples or if it is related with the small number of samples we have analysed, but this could explain why in our study, PTX3 is not associated with susceptibility to MS. Besides, so far, we only have analysed the levels of this protein but not its functionality. Given the fact that these SNPs are thought to alter protein function, a functional impairment could be taking place despite the absence of differences in protein levels.

6. Concluding Remarks

Overall, with this thesis we show that PTX3 could be playing a dual role in MS pathophysiology, exacerbating the pro-inflammatory Th1 response in the onset phase of disease and playing a more anti-inflammatory role in the chronic phase. Besides, we also show that in EAE mice, there is a tendency for a pro-inflammatory Th1/Th17 skewed response in both the onset and chronic phases of disease, and that glial cells, namely astrocytes and microglia, are activated during the disease course and could be playing an essential role in the maintenance of the pro-inflammatory milieu necessary for MS development. Furthermore, PTX3 could be modulating the response of these cells, by exacerbating the A1 neuroinflammatory responses of astrocytes during the active phase of disease but then shifting this phenotype to a more anti-inflammatory A2 profile in later of stages of disease. In addition, we show that there is an increase in the circulating levels of PTX3 in MS patients and suggest that this protein could serve as a biomarker of the underlying neuroinflammatory activity occurring in MS.

In the future, we believe that it would be important to repeat our experiments with an increased number of samples, in order to be able to take more substantiated conclusions. This applies to both the human studies and to the animal experiments. In addition, considering the role of PTX3 as an acute phase protein, in the animal experiments it would be of interest to study the role of PTX3 even in earlier stages of disease development, that is, in the moment of appearance of clinical symptoms. Furthermore, the role that microglia plays in MS is still not completely understood, so the study of these cells from a morphological perspective through 3D reconstruction would be relevant. Finally, considering that complement molecules are important ligands of PTX3 and also that these molecules could be somewhat modulating astrocytic reactivity, the study of the gene expression of these molecules in EAE *Ptx3*$^{-/-}$ animals, could provide some insights into the mechanisms played by PTX3 in MS/EAE.

To conclude, we show that PTX3 could in fact be playing a role in the modulation of this disease, however, the exact mechanisms underlying this effect are still unknown. Consequently, the research of these topics would be of interest and should be continued, always aiming at the improvement in the quality of life of MS patients.

7. References

Aeinehband, S., Lindblom, R. P. F., Nimer, F. Al, Vijayaraghavan, S., Sandholm, K., Khademi, M., … Piehl, F. (2015). Complement component C3 and butyrylcholinesterase activity are associated with neurodegeneration and clinical disability in Multiple Sclerosis. *PLoS ONE*, *10*(4). https://doi.org/10.1371/journal.pone.0122048

Agnello, D., Carvelli, L., Muzio, V., Villa, P., Bottazzi, B., Polentarutti, N., … Ghezzi, P. (2000). Increased peripheral benzodiazepine binding sites and pentraxin 3 expression in the spinal cord during EAE: Relation to inflammatory cytokines and modulation by dexamethasone and rolipram. *Journal of Neuroimmunology*, *109*(2), 105–111. https://doi.org/10.1016/S0165-5728(00)00279-4

Barbati, E., Specchia, C., Villella, M., Rossi, M. L., Barlera, S., Bottazzi, B., … Franzosi, M. G. (2012). Influence of pentraxin 3 (PTX3) genetic variants on myocardial infarction risk and PTX3 plasma levels. *PLoS ONE*, *7*(12). https://doi.org/10.1371/journal.pone.0053030

Bonavita, E., Gentile, S., Garlanda, C., Mantovani, A., Bonavita, E., Gentile, S., … Mantovani, A. (2015). PTX3 is an extrisinc oncosupressor regulating complement-dependent inflammation in cancer. *Cell*, *160*, 700–714. https://doi.org/10.1016/j.cell.2015.01.004

Bottazzi, B., Doni, A., Garlanda, C., & Mantovani, A. (2010). An integrated view of humoral innate immunity: Pentraxins as a paradigm. *Annual Review of Immunology*, *28*(1), 157–183. https://doi.org/10.1146/annurev-immunol-030409-101305

Bozza, S., Campo, S., Arseni, B., Inforzato, A., Ragnar, L., Bottazzi, B., … Romani, L. (2014). PTX3 binds MD-2 and promotes TRIF-Dependent immune protection in Aspergillosis. *The Journal of Immunology*, *193*(5), 2340–2348. https://doi.org/10.4049/jimmunol.1400814

Brambilla, R., Morton, P. D., Ashbaugh, J. J., Karmally, S., Lambertsen, K. L., & Bethea, J. R. (2014). Astrocytes play a key role in EAE pathophysiology by orchestrating in the CNS the inflammatory response of resident and peripheral immune cells and by suppressing remyelination. *Glia*, *62*(3), 452–467. https://doi.org/10.1002/glia.22616

Butterfield, R. J., Blankenhorn, E. P., Roper, R. J., Zachary, J. F., Doerge, R. W., Sudweeks, J., … Teuscher, C. (1999). Genetic analysis of disease subtypes and sexual dimorphisms in mouse experimental allergic encephalomyelitis (EAE): Relapsing/Remitting and monophasic remitting/nonrelapsing EAE are immunogenetically distinct. *The Journal of Immunology*, *162*, 3096–3102. https://doi.org/10.4049/jimmunol.1000583

Chiarini, M., Sabelli, C., Melotti, P., Garlanda, C., Savoldi, G., Mazza, C., … Badolato, R. (2010). PTX3 genetic variations affect the risk of Pseudomonas aeruginosa airway colonization in cystic fibrosis patients. *Genes and Immunity*, *11*(8), 665–670. https://doi.org/10.1038/gene.2010.41

Chu, F., Shi, M., Zheng, C., Shen, D., Zhu, J., Zheng, X., & Cui, L. (2018). The roles of macrophages and microglia in Multiple Sclerosis and experimental autoimmune encephalomyelitis. *Journal of Neuroimmunology*, *318*, 1–7. https://doi.org/10.1016/j.jneuroim.2018.02.015

Clos, T. W. Du. (2013). Pentraxins: Structure, function, and role in inflammation. *ISRN Inflammation*, *2013*. https://doi.org/10.1155/2013/379040

Constantinescu, C. S., Farooqi, N., O'Brien, K., & Gran, B. (2011). Experimental autoimmune encephalomyelitis (EAE) as a model for multiple sclerosis (MS). *British Journal of Pharmacology*, *164*(4), 1079–1106. https://doi.org/10.1111/j.1476-5381.2011.01302.x

Cunha, C., Aversa, F., Lacerda, J. F., Busca, A., Kurzai, O., Grube, M., … Carvalho, A. (2014). Genetic PTX3 Deficiency and Aspergillosis in Stem-Cell Transplantation. *New England Journal of Medicine*, *370*(5), 421–432. https://doi.org/10.1056/NEJMoa1211161

Cunningham, C., Wilcockson, D. C., Boche, D., & Perry, V. H. (2005). Comparison of Inflammatory and Acute-Phase Responses in the Brain and Peripheral Organs of the ME7 Model of Prion Disease.

Journal of Virology, *79*(8), 5174–5184. https://doi.org/10.1128/jvi.79.8.5174-5184.2005

Das Neves, S. P., Serre-Miranda, C., Nobrega, C., Roque, S., Cerqueira, J. J., Correia-Neves, M., & Marques, F. (2018). Immune thymic profile of the MOG-induced experimental autoimmune encephalomyelitis mouse model. *Frontiers in Immunology*, *9*(OCT), 1–11. https://doi.org/10.3389/fimmu.2018.02335

Deban, L., Bottazzi, B., Garlanda, C., Martinez, Y., Torre, D., & Mantovani, A. (2009). Pentraxins: Multifunctional proteins at the interface of innate immunity and inflammation. *Biofactors*, *35*(2), 138–145. https://doi.org/10.1002/biof.21

Deban, L., Russo, R. C., Sironi, M., Moalli, F., Scanziani, M., Zambelli, V., … Mantovani, A. (2010). Regulation of leukocyte recruitment by the long pentraxin PTX3. *Nature Publishing Group*, *11*(4), 328–334. https://doi.org/10.1038/ni.1854

Didonna, A., & Oksenberg, J. R. (2015). Genetic determinants of risk and progression in multiple sclerosis. *Clinica Chimica Acta*, *449*, 16–22. https://doi.org/10.1002/cncr.27633.Percutaneous

Dobson, R., & Giovannoni, G. (2018). Multiple Sclerosis - a review. *European Journal of Neurology*. https://doi.org/10.1111/ene.13819

Fayyaz, M., & Jaffery, S. S. (2018). Natalizumab-associated Progressive Multifocal Leukoencephalopathy in patients with Multiple Sclerosis: A mini review. *Cureus*, *10*(8), 8–11. https://doi.org/10.7759/cureus.3093

Fletcher, J. M., Lalor, S. J., Sweeney, C. M., Tubridy, N., & Mills, K. H. G. (2010). T cells in multiple sclerosis and experimental autoimmune encephalomyelitis. *Clinical and Experimental Immunology*, *162*(1), 1–11. https://doi.org/10.1111/j.1365-2249.2010.04143.x

Fornai, F., Carrizzo, A., Ferrucci, M., Damato, A., Biagioni, F., Gaglione, A., … Vecchione, C. (2015). Brain diseases and tumorigenesis: The good and bad cops of pentraxin3. *International Journal of Biochemistry and Cell Biology*, *69*, 70–74. https://doi.org/10.1016/j.biocel.2015.10.017

Fossati, G., Pozzi, D., Canzi, A., Mirabella, F., Valentino, S., Morini, R., … Menna, E. (2019). Pentraxin 3 regulates synaptic function by inducing AMPA receptor clustering via ECM remodeling and β1-integrin. *The EMBO Journal*, *38*(1), e99529. https://doi.org/10.15252/embj.201899529

Freund, J., & McDermott, K. (1942). Sensitization to horse serum by means of adjuvants. *Experimental Biology and Medicine*, *49*(4), 548–553. https://doi.org/10.3181/00379727-49-13625

Gandhi, R., Laroni, A., & Weiner, H. L. (2010). Role of the innate immune system in the pathogenesis of Multiple Sclerosis. *Journal of Neuro-Oncology*, *221*(1–2), 7–14. https://doi.org/10.1016/j.jneuroim.2009.10.015.Role

Garlanda, C., Hirsch, E., Bozza, S., Salustri, A., De Acetis, M., Nota, R., … Mantovani, A. (2002). Non-redundant role of the long pentraxin PTX3 in anti-fungal innate immune response. *Nature*, *420*(6912), 182–186. https://doi.org/10.1038/nature01195

Gaziano, R., Bozza, S., Bellocchio, S., Perruccio, K., Montagnoli, C., Pitzurra, L., … Romani, L. (2004). Anti-Aspergillus fumigatus efficacy of pentraxin 3 alone and in combination with antifungals. *Antimicrobial Agents and Chemotherapy*, *48*(11), 4414–4421. https://doi.org/10.1128/AAC.48.11.4414-4421.2004

Gelfand, J. M. (2014). Multiple sclerosis: Diagnosis, differential diagnosis, and clinical presentation. In D. S. Goodin (Ed.), *Handbook of Clinical Neurology* (3rd ed., Vol. 122, pp. 269–290). Elsevier B.V. https://doi.org/10.1016/B978-0-444-52001-2.00011-X

Goodman, A. R., Cardozo, T., Abagyan, R., Altmeyer, A., Wisniewski, H., & Vilekt, J. (1996). Long pentraxins: an emerging group of proteins with diverse functions. *Cytokine and Growth Factor Reviews*, *7*(2), 191–202.

Haindl, M. T., Köck, U., Zeitelhofer-Adzemovic, M., Fazekas, F., & Hochmeister, S. (2019). The formation of a glial scar does not prohibit remyelination in an animal model of multiple sclerosis. *Glia*, *67*(3), 467–481. https://doi.org/10.1002/glia.23556

Hauser, S. L., & Goodin, D. S. (2015). Multiple Sclerosis and other demyelinating diseases. In D. L. Kasper, A. S. Fauci, S. L. Hauser, D. L. Longo, J. L. Jameson, & J. Loscalzo (Eds.), *Harrison's Principles of Internal Medicine* (19th ed., pp. 2661–2674). McGraw-Hill Education.

Hedström, A. K. (2018). Smoking and its interaction with genetics in MS etiology. *Multiple Sclerosis Journal*, *00*(0), 135245851880172. https://doi.org/10.1177/1352458518801727

Hemmer, B., Archelos, J. J., & Hartung, H. P. (2002). New concepts in the immunopathogenesis of Multiple Sclerosis. *Nature Reviews Neuroscience*, *3*(4), 291–301. https://doi.org/10.1038/nrn784

Hemmer, B., Kerschensteiner, M., & Korn, T. (2015). Role of the innate and adaptive immune responses in the course of multiple sclerosis. *The Lancet Neurology*, *14*(4), 406–419. https://doi.org/10.1016/S1474-4422(14)70305-9

Hernández-Pedro, N. Y., Espinosa-Ramirez, G., De La Cruz, V. P., Pineda, B., & Sotelo, J. (2013). Initial immunopathogenesis of multiple sclerosis: Innate immune response. *Clinical and Developmental Immunology*, *2013*. https://doi.org/10.1155/2013/413465

Hutchinson, M. (2007). Natalizumab: A new treatment for relapsing remitting multiple sclerosis. *Therapeutics and Clinical Risk Management*, *3*(2), 259–268. https://doi.org/10.2147/tcrm.2007.3.2.259

Inforzato, A., Doni, A., Barajon, I., Leone, R., Garlanda, C., Bottazzi, B., & Mantovani, A. (2013). PTX3 as a paradigm for the interaction of pentraxins with the Complement system. *Seminars in Immunology*, *25*(1), 79–85. https://doi.org/10.1016/j.smim.2013.05.002

Ingram, G., Loveless, S., Howell, O. W., Hakobyan, S., Dancey, B., Harris, C. L., … Morgan, B. P. (2014). Complement activation in multiple sclerosis plaques: an immunohistochemical analysis. *Acta Neuropathologica Communications*, *2*(53). https://doi.org/10.1186/2051-5960-2-53

Introna, M., Alles, V. V, Castellano, M., Picardi, G., De Gioia, L., Bottazzai, B., … Mantovani, A. (2014). Cloning of mouse ptx3, a new member of the pentraxin gene family expressed at extrahepatic sites. *Blood*, *87*(5), 1862–1872. https://doi.org/10.1016/1043-4666(94)90299-2

Jeon, H., Lee, S., Lee, W. H., & Suk, K. (2010). Analysis of glial secretome: The long pentraxin PTX3 modulates phagocytic activity of microglia. *Journal of Neuroimmunology*, *229*(1–2), 63–72. https://doi.org/10.1016/j.jneuroim.2010.07.001

Kipp, M., Van Der Star, B., Vogel, D. Y. S., Puentes, F., Van Der Valk, P., Baker, D., & Amor, S. (2012). Experimental in vivo and in vitro models of Multiple Sclerosis: EAE and beyond. *Multiple Sclerosis and Related Disorders*, *1*(1), 15–28. https://doi.org/10.1016/j.msard.2011.09.002

Kuerten, S., Kostova-Bales, D. A., Frenzel, L. P., Tigno, J. T., Tary-Lehmann, M., Angelov, D. N., & Lehmann, P. V. (2007). MP4- and MOG35-55-induced EAE in C57BL/6 mice differentially target brain, spinal cord and cerebellum. *Journal of Neuroimmunology*, *189*(1–2), 31–40. https://doi.org/10.1063/1.5002341

Lassmann, H. (2018). Multiple sclerosis pathology. *Cold Spring Harbor Perspectives in Medicine*, *8*(3), 1–16. https://doi.org/10.1101/cshperspect.a028936

Lassmann, H., & Bradl, M. (2017). Multiple sclerosis: experimental models and reality. *Acta Neuropathologica*, *133*(2), 223–244. https://doi.org/10.1007/s00401-016-1631-4

Lee, H.-W., Choi, J., & Suk, K. (2011). Increases of pentraxin 3 plasma levels in patients with Parkinson's disease. *Movement Disorders*, *26*(13), 2364–2370. https://doi.org/10.1002/mds.23871

Liddelow, S. A., Guttenplan, K. A., Clarke, L. E., Bennett, F. C., Bohlen, C. J., Schirmer, L., … Barres, B. A. (2017). Neurotoxic reactive astrocytes are induced by activated microglia. *Nature*, *541*(7638), 481–487. https://doi.org/10.1038/nature21029

Lindblom, R. P. F., Aeinehband, S., Ström, M., Al, F., Sandholm, K., Khademi, M., … Ekdahl, K. N. (2016). Complement Receptor 2 is increased in cerebrospinal fluid of multiple sclerosis patients and regulates C3 function. *Clinical Immunology*, *166–167*, 89–95.

https://doi.org/10.1016/j.clim.2016.04.003
Liu, B., Ai, P., Zheng, D., Jiang, Y., Liu, X., Pan, S., & Wang, H. (2018). Cerebrospinal fluid pentraxin 3 and CD40 ligand in anti-N-menthyl-D-aspartate receptor encephalitis. *Journal of Neuroimmunology*, *315*(April 2017), 40–44. https://doi.org/10.1016/j.jneuroim.2017.11.016
Locatelli, M., Ferrero, S., Martinelli, F., Boiocchi, L., Zavanone, M., Maria, S., … Garlanda, C. (2013). The long pentraxin PTX3 as a correlate of cancer-related inflammation and prognosis of malignancy in gliomas. *Journal of Neuroimmunology*, *260*(1–2), 99–106. https://doi.org/10.1016/j.jneuroim.2013.04.009
Lucas, R. M., Byrne, S. N., Correale, J., Ilschner, S., & Hart, P. H. (2015). Ultraviolet radiation, vitamin D and multiple sclerosis. *Neurodegenerative Disease Management*, *5*(5), 413–424. https://doi.org/10.2217/nmt.15.33
Ludwin, S. K., Rao, V. T. S., Moore, C. S., & Antel, J. P. (2016). Astrocytes in multiple sclerosis. *Multiple Sclerosis*, *22*(9), 1114–1124. https://doi.org/10.1177/1352458516643396
Luzzio, C., & Dangond, F. (2018). Multiple Sclerosis: Clinical Presentation. Retrieved October 25, 2018, from https://emedicine.medscape.com/article/1146199-clinical
Mantovani, A., Garlanda, C., & Doni, A. (2008). Pentraxins in innate immunity: From C-reactive protein to the long pentraxin PTX3. *Journal of Clinical Immunology*, *28*, 1–13. https://doi.org/10.1007/s10875-007-9126-7
Marques, F., Mesquita, S. D., Sousa, J. C., Coppola, G., Gao, F., Geschwind, D. H., … Palha, J. A. (2012). Lipocalin 2 is present in the EAE brain and is modulated by natalizumab. *Frontiers in Cellular Neuroscience*, *6*(33). https://doi.org/10.3389/fncel.2012.00033
May, L., Kuningas, M., van Bodegom, D., Meij, H. J., Frolich, M., Slagboom, P. E., … Westendorp, R. G. J. (2010). Genetic variation in pentraxin (PTX) 3 gene associates with PTX3 production and fertility in women. *Biology of Reproduction*, *82*(2), 299–304. https://doi.org/10.1095/biolreprod.109.079111
Mckay, K. A., Kwan, V., Duggan, T., & Tremlett, H. (2015). Risk factors associated with the onset of relapsing-remitting and primary progressive Multiple Sclerosis: A systematic review. *BioMed Research International*, *2015*. https://doi.org/10.1155/2015/817238
Miller, R. H., Fyffe-Maricich, S., & Caprariello, A. C. (2017). Animal models for the study of Multiple Sclerosis. In P. M. Conn (Ed.), *Animal Models for the Study of Human Disease* (2nd ed., pp. 967–988). Academic Press.
Mouhieddine, T. H., Darwish, H., Fawaz, L., Yamout, B., Tamim, H., & Khoury, S. J. (2015). Risk factors for multiple sclerosis and associations with anti-EBV antibody titers. *Clinical Immunology*, *158*(1), 59–66. https://doi.org/10.1016/j.clim.2015.03.011
Munoz, J. J., Bernard, C. C. A., & Mackay, I. R. (1984). Elicitation of experimental allergic encephalomyelitis (EAE) in mice with the aid of pertussigen. *Cellular Immunology*, *83*, 92–100. https://doi.org/10.1111/j.1467-9701.1992.tb00539.x
Nejati, A., Shoja, Z., Shahmahmoodi, S., Tafakhori, A., Mollaei-Kandelous, Y., Rezaei, F., … Marashi, S. M. (2016). EBV and vitamin D status in relapsing-remitting multiple sclerosis patients with a unique cytokine signature. *Medical Microbiology and Immunology*, *205*(2), 143–154. https://doi.org/10.1007/s00430-015-0437-7
Niculescu, T., Weerth, S., Soane, L., Niculescu, F., Rus, V., Raine, C. S., … Rus, H. (2004). Effects of complement C5 on apoptosis in experimental autoimmune encephalomyelitis. *The Journal of Immunology*, *172*, 5702–5706. https://doi.org/10.4049/jimmunol.172.9.5702
O'Loughlin, E., Madore, C., Lassmann, H., & Butovsky, O. (2018). Microglial phenotypes and functions in multiple sclerosis. *Cold Spring Harbor Perspectives in Medicine*, *8*(2), 1–22. https://doi.org/10.1101/cshperspect.a028993
Oh, J., Vidal-Jordana, A., & Montalban, X. (2018). Multiple sclerosis: Clinical aspects. *Current Opinion in*

Neurology, *31*. https://doi.org/10.1097/WCO.0000000000000622

Olesen, R., Wejse, C., Velez, D. R., Bisseye, C., Sodemann, M., Aaby, P., … Sirugo, G. (2007). DC-SIGN (CD209), pentraxin 3 and vitamin D receptor gene variants associate with pulmonary tuberculosis risk in West Africans. *Genes and Immunity*, *8*(6), 456–467. https://doi.org/10.1038/sj.gene.6364410

Orihuela, R., Mcpherson, C. A., & Harry, G. J. (2016). Microglial M1/M2 polarization and metabolic states. *British Journal of Pharmacology*, *173*, 649–665. https://doi.org/10.1111/bph.13139

Owen, J. A., Punt, J., & Stranford, S. A. (2013). *Kuby Immunology* (7th ed.). New York: W.H.Freeman and Company. https://doi.org/10.1007/s13398-014-0173-7.2

Parmar, K., Stadelmann, C., Rocca, M. A., Langdon, D., D'Angelo, E., D'Souza, M., … Sprenger, T. (2018). The Role of the Cerebellum in Multiple Sclerosis. *Neuroscience & Biobehavioral Reviews*, *89*, 85–98. https://doi.org/10.1016/j.neubiorev.2018.02.012

Polentarutti, N., Bottazzi, B., Di, E., Blasi, E., Agnello, D., Ghezzi, P., … Mantovani, A. (2000). Inducible expression of the long pentraxin PTX3 in the central nervous system. *Journal of Neuroimmune Pharmacology*, *106*, 87–94. Retrieved from papers2://publication/uuid/E6933B30-56A5-41E9-A8CD-42F5FC80CBB0

Popescu, B. F. G., & Lucchinetti, C. F. (2012). Pathology of Demyelinating Diseases. *Annual Review of Pathology: Mechanisms of Disease*, *7*(1), 185–217. https://doi.org/10.1146/annurev-pathol-011811-132443

Presta, M., Camozzi, M., Salvatori, G., & Rusnati, M. (2007). Role of the soluble pattern recognition receptor PTX3 in vascular biology. *Journal of Cellular and Molecular Medicine*, *11*(4), 723–738. https://doi.org/10.1111/j.1582-4934.2007.00061.x

Presta, M., Foglio, E., Churruca Schuind, A., & Ronca, R. (2018). Long pentraxin-3 modulates the angiogenic activity of fibroblast growth factor-2. *Frontiers in Immunology*, *9*(2327). https://doi.org/10.3389/fimmu.2018.02327

Procaccini, C., De Rosa, V., Pucino, V., Formisano, L., & Matarese, G. (2015). Animal models of Multiple Sclerosis. *European Journal of Pharmacology*, *759*, 182–191. https://doi.org/10.1016/j.ejphar.2015.03.042

Pucci, S., Fisco, T., Zonetti, M. J., Bonanno, E., Mazzarelli, P., & Mauriello, A. (2014). PTX3: A modulator of human coronary plaque vulnerability acting by macrophages type 2. *International Journal of Cardiology*, *176*(3), 710–717. https://doi.org/10.1016/j.ijcard.2014.07.109

Rajkovic, I., Denes, A., Allan, S. M., & Pinteaux, E. (2016). Emerging roles of the acute phase protein pentraxin-3 during central nervous system disorders. *Journal of Neuroimmunology*, *292*, 27–33. https://doi.org/10.1016/j.jneuroim.2015.12.007

Rajkovic, I., Wong, R., Lemarchand, E., Rivers-Auty, J., Rajkovic, O., Garlanda, C., … Pinteaux, E. (2018). Pentraxin 3 promotes long-term cerebral blood flow recovery, angiogenesis, and neuronal survival after stroke. *Journal of Molecular Medicine*, *96*(12), 1319–1332. https://doi.org/10.1007/s00109-018-1698-6

Ransohoff, R. M. (2012). Animal models of multiple sclerosis: The good, the bad and the bottom line. *Nature Neuroscience*, *15*(8), 1074–1077. https://doi.org/10.1038/nn.3168

Ravizza, T., Moneta, D., Bottazzi, B., Peri, G., Garlanda, C., Hirsch, E., … Vezzani, A. (2001). Dynamic induction of the long pentraxin PTX3 in the CNS after limbic seizures: Evidence for a protective role in seizure-induced neurodegeneration. *Neuroscience*, *105*(1), 43–53. https://doi.org/10.1016/S0306-4522(01)00177-4

Reich, D. S., Lucchinetti, C. F., & Calabresi, P. A. (2018). Multiple sclerosis. *The New England Journal of Medicine*, *378*(2), 169–180. https://doi.org/10.1007/978-1-4939-7880-9_8

Rivers, T. M., Sprunt, D. H., & Berry, G. P. (1933). Observations on attempts to produce acute disseminated encephalomyelitis in monkeys. *Journal of Experimental Medicine*, *58*(1), 39–53.

Robinson, A. P., Harp, C. T., Noronha, A., & Miller, S. D. (2014). The experimental autoimmune encephalomyeltis (EAE) model of MS: Utility for understanding disease pathophysiology and treatment. *Handbook of Clinical Neurology*, *122*, 173–189. https://doi.org/10.1016/B978-0-444-52001-2.00008-X

Salustri, A., Garlanda, C., Hirsch, E., Acetis, M. De, Maccagno, A., Bottazzi, B., ... Mantovani, A. (2004). PTX3 plays a key role in the organization of the cumulus oophrus extracellular matrix and in in vivo fertilization. *Development*, *131*, 1577–1586. https://doi.org/10.1242/dev.01056

Saresella, M., Gatti, A., Tortorella, P., Marventano, I., Piancone, F., La Rosa, F., ... Clerici, M. (2014). Toll-like receptor 3 differently modulates inflammation in progressive or benign multiple sclerosis. *Clinical Immunology*, *150*(1), 109–120. https://doi.org/10.1016/j.clim.2013.10.012

Shindo, A., Maki, T., Mandeville, E. T., Liang, A. C., Egawa, N., Itoh, K., ... Arai, K. (2016). Astrocyte-derived pentraxin 3 supports blood-brain barrier integrity under acute phase of stroke. *Stroke*, *47*(4), 39–46. https://doi.org/10.1161/STROKEAHA.115.012133.

Sokolov, A. A., Grivaz, P., & Bove, R. (2018). Cognitive deficits in Multiple Sclerosis: Recent advances in treatment and neurorehabilitation. *Current Treatment Options in Neurology*, *20*(53). https://doi.org/10.1007/s11940-018-0538-x

Steinman, L. (2001). Multiple sclerosis : a two-stage disease. *Nature Immunology*, *2*(9), 762–764. https://doi.org/10.1038/ni0901-762

Steinman, L. (2012). The discovery of Natalizumab, a potent therapeutic for Multiple Sclerosis. *Journal of Cell Biology*, *199*(3), 413–416. https://doi.org/10.1083/jcb.201207175

Stuart, G., & Krikorian, K. S. (1928). The neuro-paralytic accidents of anti-rabies treatment. *Annals of Tropical Medicine and Parasitology*, *22*(3), 327–377. https://doi.org/10.1080/00034983.1928.11684582

Sun, H., Tian, J., Xian, W., Xie, T., & Yang, X. (2015). Pentraxin-3 Attenuates Renal Damage in Diabetic Nephropathy by Promoting M2 Macrophage Differentiation. *Inflammation*, *38*(5), 1739–1747. https://doi.org/10.1007/s10753-015-0151-z

Tavares, G., Martins, M., Correia, J. S., Sardinha, V. M., Gomes, S. G., Neves, S. P. das, ... Oliveira, J. F. (2017). Employing an open-source tool to assess astrocyte tridimensional structure. *Brain Structure and Function*, *222*, 1989–1999. https://doi.org/10.1007/s00429-016-1316-8

Tillett, W. S., & Jr., T. F. (1930). Serological reactions in pneumonia with a non-protein somatic fraction of pneumococcus. *Journal of Experimental Medicine*, *52*(4), 561–571.

Tornes, L., Conway, B., & Sheremata, W. (2014). Multiple Sclerosis and the cerebellum. *Neurologic Clinics*, *32*(4), 957–977. https://doi.org/10.1016/j.ncl.2014.08.001

Ummenthum, K., Peferoen, L. A. N., Finardi, A., Baker, D., Pryce, G., Mantovani, A., ... Amor, S. (2016). Pentraxin-3 is upregulated in the central nervous system during MS and EAE, but does not modulate experimental neurological disease. *European Journal of Immunology*, *46*(3), 701–711. https://doi.org/10.1002/eji.201545950

Varani, S., Elvin, J. A., Yan, C., Mayo, J. D. E., Mayo, F. J. D. E., Horton, H. F., ... Matzuk, M. M. (2002). Knockout of pentraxin 3, a downstream target of female subfertility. *Molecular Endocrinology*, *16*(6), 1154–1167. https://doi.org/10.1210/mend.16.6.0859

Wang, H., Wang, K., Wang, C., Zhong, X., Qiu, W., & Hu, X. (2013). Increased plasma levels of pentraxin 3 in patients with multiple sclerosis and neuromyelitis optica. *Multiple Sclerosis Journal*, *19*(7), 926–931. https://doi.org/10.1177/1352458512457845

Weissert, R. (2013). The immune pathogenesis of multiple sclerosis. *Journal of Neuroimmune Pharmacology*, *8*(4), 857–866. https://doi.org/10.1007/s11481-013-9467-3

Wilkins, A. (2017). Cerebellar dysfunction in Multiple Sclerosis. *Frontiers in Neurology*, *8*(312). https://doi.org/10.3389/fneur.2017.00312

Yadav, S. K., Mindur, J. E., Ito, K., & Dhib-Jalbut, S. (2015). Advances in the immunopathogenesis of

Multiple Sclerosis. *Current Opinion in Neurology*, *28*(3), 206–219. https://doi.org/10.1097/WCO.0000000000000205

Zanier, E. R., Brandi, G., Peri, G., Longhi, L., Zoerle, T., Tettamanti, M., … Stocchetti, N. (2011). Cerebrospinal fluid pentraxin 3 early after subarachnoid hemorrhage is associated with vasospasm. *Intensive Care Medicine*, *37*(2), 302–309. https://doi.org/10.1007/s00134-010-2075-2

Zhang, P., Wang, R., Li, Z., Wang, Y., Gao, C., Lv, X., … Li, B. (2016). The risk of smoking on multiple sclerosis: a meta-analysis based on 20,626 cases from case-control and cohort studies. *Peer Journal*, *4*. https://doi.org/10.7717/peerj.1797